1213928

[0092873]

RPP-RPT-50758, Rev. 0

Three-Dimensional Surface Geophysical Exploration of the Eastern Portion of the BY Tank Farm

Author Name: N. Crook, G. Noonan, hydroGEOPHYSICS, Inc.
Columbia Energy and Environmental Services, Inc.
Washington River Protection Solutions, LLC
Richland, WA 99352
U.S. Department of Energy Contract DE-AC27-08RV14800

RECEIVED
MAY 15 2012
EDMC

EDT/ECN:	DRF	UC:	
Cost Center:		Charge Code:	
B&R Code:		Total Pages:	82

Key Words: Surface Geophysical Exploration, SGE, Survey Report, BY tank farm

Abstract: A surface geophysical exploration survey that included direct current electrical resistivity was conducted within the BY tank farm on the Hanford Site near Richland, Washington. This survey formed Stage 2 of a two-part survey and focused on the eastern area of the tank farm, covering the area around storage tanks BY-101 through BY-106 and portions of storage tanks BY-107 through BY-109.

TRADEMARK DISCLAIMER. Reference herein to any specific commercial product, process, or service by trade name, trademark, manufacturer, or otherwise, does not necessarily constitute or imply its endorsement, recommendation, or favoring by the United States Government or any agency thereof or its contractors or subcontractors.

OCT 24 2011
DATE:
STA: 15
HANFORD RELEASE
ID:
65

Nancy A Fouad 10/24/2011

Release Approval Date Release Stamp

Approved For Public Release

EXECUTIVE SUMMARY

A surface geophysical exploration survey using a direct current electrical resistivity method was conducted within the BY tank farm on the Hanford Site near Richland, Washington. This survey formed Stage 2 of a two-part survey and focused on the northeastern area of the tank farm, covering the area around single shell storage tanks BY-101 through BY-106 and portions of storage tanks BY-107 through BY-109. The survey included electrical current transmission and voltage measurements on 185 surface electrodes within a grid layout, 57 depth electrodes in seven boreholes, and 33 wells acting as long electrodes. Data collection took place between July 6 and 10, 2011.

A prior survey was performed that focused on the southwest corner of the farm. The prior survey is documented in RPP-RPT-49129, *Three-Dimensional Surface Geophysical Exploration of the BY Tank Farm*, and served as Stage 1 of the two-part survey.

The surface electrode and depth electrode data from the Stage 1 and Stage 2 surveys were combined to produce a joint inversion model for the majority of BY tank farm. The results indicate low resistivity targets to the north and northeast of storage tank BY-108, in between and to the east of storage tanks BY-107 and BY-108, and in between storage tanks BY-102 and BY-103. A secondary target of apparently higher concentration (lower resistivity) was observed between tanks BY-107, BY-108, BY-110, and BY-111. Figure ES-1 displays the distribution of resistivity in a three dimensional representation of the tank farm. Two contours of low resistivity values are highlighted:

- Opaque value (blue) representing 0.5 ohm-meter
- Transparent value (green) representing 0.7 ohm-meter.

The success of the project likely came from the extensive network of depth electrodes installed in the twelve boreholes within the survey areas. Approximately 35 percent of the data came from the depth electrodes. Their locations below the infrastructure provided a means to separate the electrolytic targets (assumed to be ionic waste plumes) from the electronic targets (metal) and increase resolution at depth in the model.

Combined Stage 1 and Stage 2 modeling of the well to well data for BY tank farm showed a low resistivity target to the east of storage tanks BY-107 and BY-108, trending towards the north east (Figure ES-2). The footprint of the low resistivity target coincided with expectations based on knowledge of past releases in the tank farm. These results correspond well to similar target locations observed in the 2006 SGE of the entire BY tank farm and the truncated 2010 survey of the western half of the tank farm, although different resistivity ranges are observed between the full and truncated data sets. Additional smaller low resistivity targets are observed around storage tank BY-111 and between and to the east of storage tanks BY-102 and BY-103.

Figure ES-1. Low Resistivity Targets Within the BY Tank Farm; Surface Electrode and Depth Electrode Modeling Results (Isometric View From The Southwest).

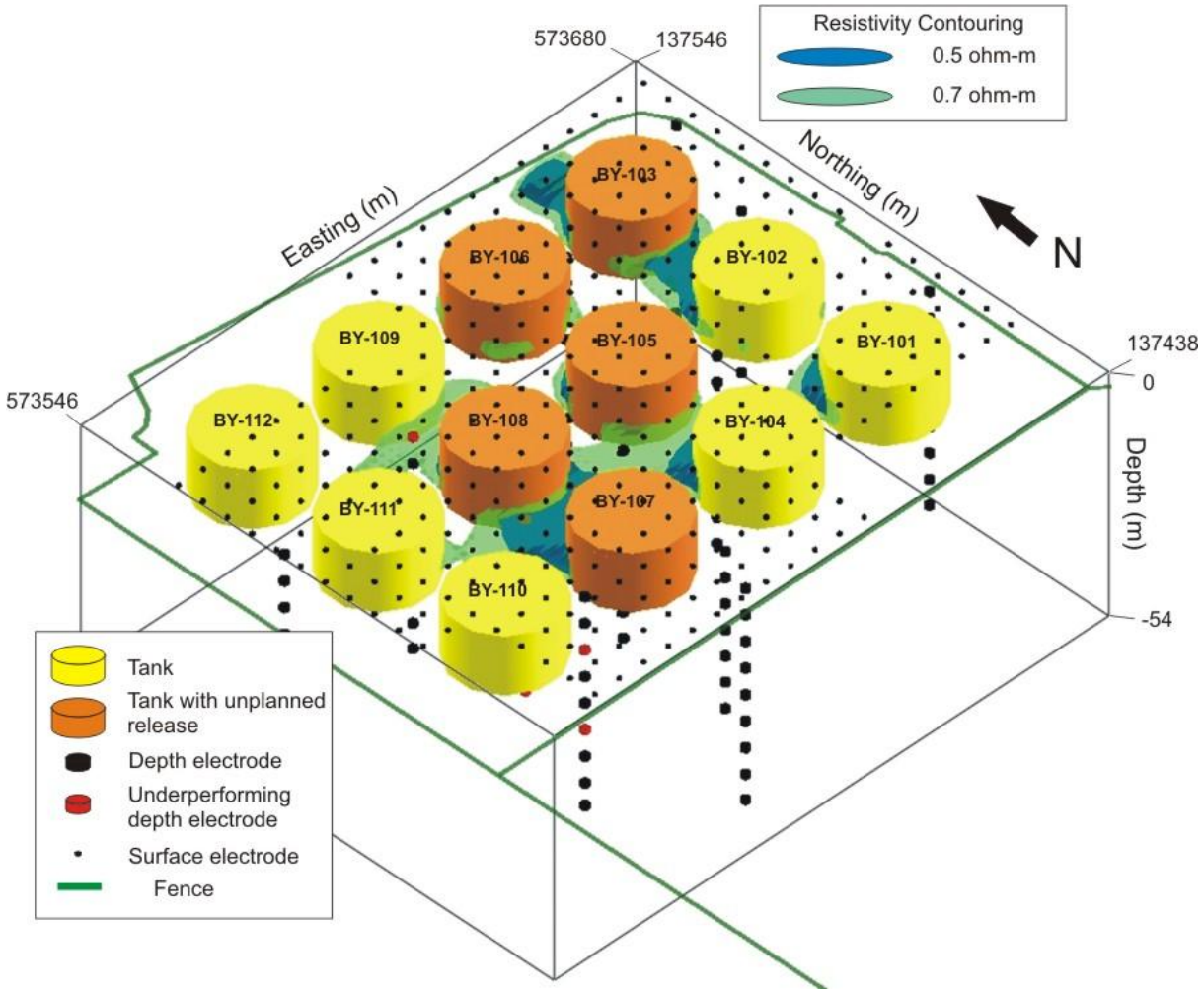

Figure ES-2. Low Resistivity Targets Within the BY Tank Farm; Well to Well Modeling Results (Resistivity Units: ohm-m).

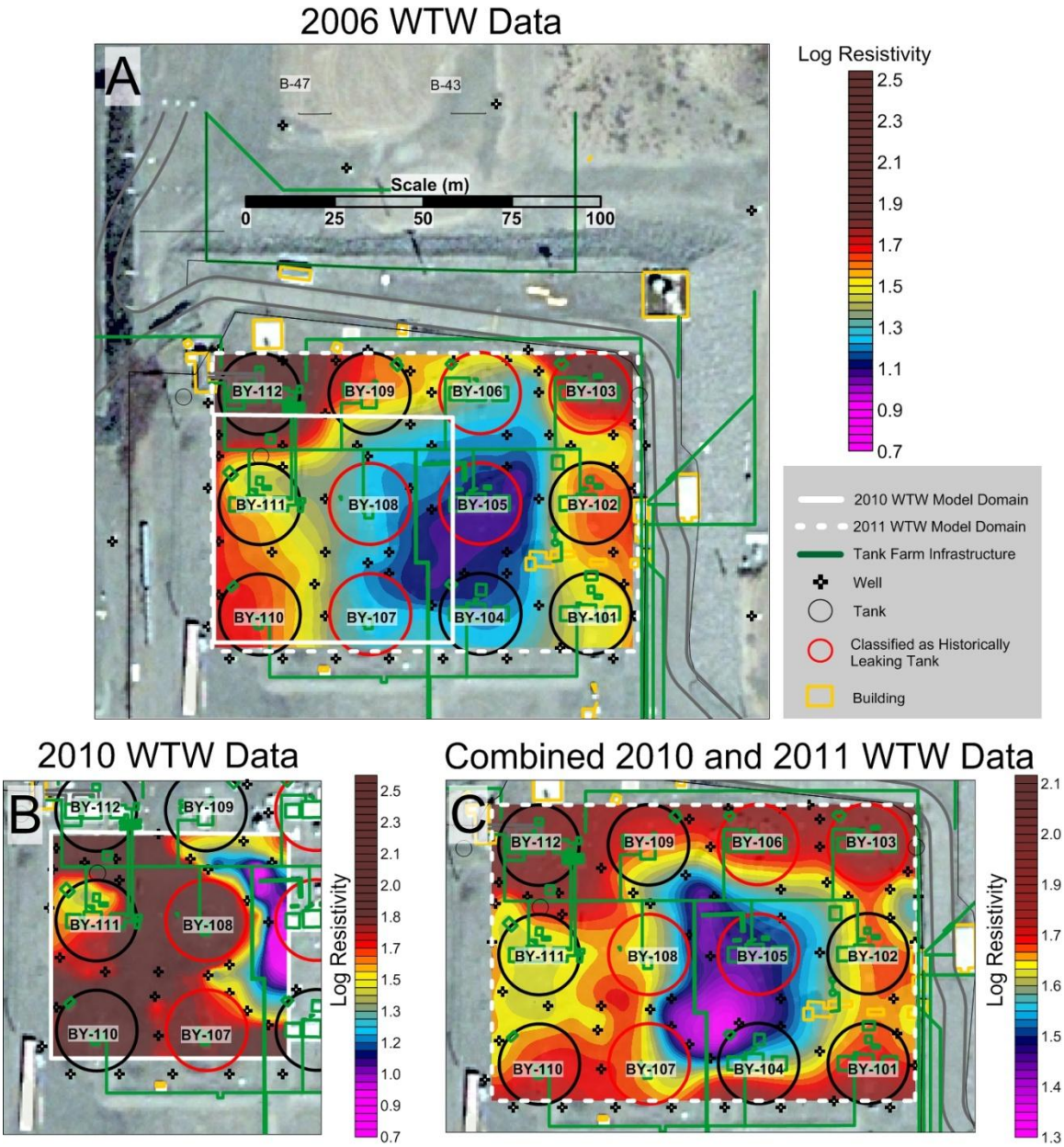

TABLE OF CONTENTS

1.0 INTRODUCTION 1
1.1 SCOPE 1
1.2 OBJECTIVES 1
1.3 REPORT LAYOUT 1

2.0 BACKGROUND 3
2.1 SITE DESCRIPTION 3
2.2 OPERATIONAL HISTORY 7
2.2.1 Liquid Waste Releases at B Complex 8
2.3 ENVIRONMENTAL SETTING 21
2.4 HISTORICAL CHARACTERIZATION EFFORTS 21
2.5 RECENT CHARACTERIZATION EFFORTS IN BY TANK FARM 28

3.0 DATA ACQUISITION AND PROCESSING METHODOLOGY 31
3.1 SURVEY DESIGN 31
3.2 EQUIPMENT 37
3.2.1 Electrode and Cable Layout 37
3.2.2 Resistivity Meter 38
3.3 ACQUISITION METHODOLOGY 39
3.4 DATA PROCESSING 40
3.4.1 Data Reduction 40
3.4.2 Depth Electrode Performance 43
3.4.3 Time Lapse Performance of Well-To-Well Data 48
3.4.4 3D Inverse Modeling 49

4.0 MODELING RESULTS 49
4.1 POINT ELECTRODE MODELING 50
4.2 LONG ELECTRODE MODELING (WELL-TO-WELL INVERSION) 60

5.0 CONCLUSIONS 63

6.0 REFERENCES 64

LIST OF APPENDICES

A QUALITY ASSURANCE ..... A-i

LIST OF FIGURES

1. Color Contoured Results from 2006 Well-to-Well SGE Efforts at the BY Farm Indicating the Limits of the Stage 1 Survey and the Current Stage 2 Survey 2
2. Location of the BY Tank Farm within the 200 East Area of the Hanford Site 5
3. B, BX, and BY Tank Farm and Surrounding Facilities.....6
4. General Configuration of Tank Construction in Waste Management Area B-BX-BY 7
5. Visual Based on Drywell Logging Activity at 4 Feet in 241-BY Tank Farm 11
6. Visual Based on Drywell Logging Activity at 9 Feet in 241-BY Tank Farm 12
7. Visual Based on Drywell Logging Activity at 35, 55, and 69 Feet in 241-BY Tank Farm. 13
8. Liquid Waste Volumes Discharged Around B Complex Area.....16
9. Major Cations Discharged Around B Complex Area 17
10. Major Anions Discharged Around B Complex Area.....18
11. Major Radionuclides Discharged Around B Complex Area 19
12. Infrastructure Map for BY Farm.....20
13. Vertical Distribution of Moisture Content in Monitoring Wells Surrounding the B Complex.....26
14. Vertical Distribution of Nitrate (Red Line) and Sulfate (Blue Line) from Select B Complex Monitoring Wells 27
15. Uranium Plume Distribution in the Unconfined Aquifer Underlying Waste Management Area B-BX-BY in 2000, 2003, 2006, and 2009 (Measured and Contoured Uranium Values, Units μg/L).....28
16. Neutron Moisture Content Within the Northwestern Area of the BY Tank Farm 30
17. 2010 (BY West) and 2011 (BY East) BY Tank Farm Electrical Resistivity Survey Areas 32
18. Electrode Layout for the BY East Tank Farm Survey Area 33
19. Resistivity Cable and Surface Electrode Layout 38
20. Remote Locations Used for the Pole-Pole Array.....39
21. Forward and Reverse Data Sets (Raw Data).....41
22. Forward and Reverse Data Sets after Data Editing 42
23. Performance Measure for Each of the Depth Electrodes.....47
24. Transfer Resistance Comparison for 2006 and 2011 WTW Data 48
25. Size And Position of the Inverse Model Grid Used To Model the BY3D Point Electrode Data.....51
26. *A Priori* Model Blocks Added to the Inverse Modeling Domain (Isometric View From The Southwest).....52
27. Plan View Depth Slices of Calculated Resistivity for Point Electrode Dataset 55
28. Three-Dimensional Rendered Bodies of the Low Resistivity Targets in the BY Tank Farm (Isometric View From The Southwest) 58

29. Three-Dimensional Rendered Bodies Of The Low Resistivity Targets in the BY Tank Farm (Isometric View From The Northeast) 59
30. Three-Dimensional Rendered Bodies of the Low Resistivity Targets in the BY Tank Farm, View From the East 60

LIST OF TABLES

1. Potential Pipeline Failures and Other Unplanned Waste Releases at BY Farm 9
2. Liquid Waste Disposal Facilities and Discharge Volumes near B Complex.....14
3. Depth Electrode Locations.....34
4. Well Locations 36
5. Number of Data Points Retained During Data Editing Steps 42
6. Construction Details for BY East Depth Electrodes.....43
7. Construction Details for BY Depth Electrodes.....44
8. Depth Electrode Statistics for BY East 44
9. Inverse Modeling Data Statistics 50

LIST OF TERMS

°F	degrees Fahrenheit
µg/L	micrograms per liter
1C	first cycle
2D	two-dimensional
3D	three-dimensional
AGI®	Advanced Geosciences, Inc.
Columbia Energy	Columbia Energy and Environmental Services, Inc.
dpm	disintegration per minute
ft^2	square feet
FY	fiscal year
GE®	General Electric
GPS	global positioning system
HGI	hydroGEOPHYSICS, Inc.
hr	hour
ITS	in-tank solidification
m	meters
mg/L	milligrams per liter
pCi/L	picocurie per liter
RCRA	*Resource Conservation and Recovery Act of 1976*
RMS	root-mean-square
SGE	surface geophysical exploration
SIM	Hanford Soil Inventory Model
SST	single-shell tank
TBP	tributyl phosphate
UPR	unplanned release
WIDS	Waste Information Data System
WMA	waste management area
WRPS	Washington River Protection Solutions, LLC
WTW	well-to-well

® AGI is a registered trademark of Advanced Geosciences, Inc.
® GE is a registered trademark of the General Electric Company.

1.0 INTRODUCTION

This report documents the results of the second stage of a two-part surface geophysical exploration (SGE) survey completed within the 241-BY tank farm at the U.S. Department of Energy Hanford Site in Washington State in fiscal years (FY) 2010 and 2011. The first stage focused on the six western tanks and this second stage focuses on the six eastern tanks of BY tank farm. hydroGEOPHYSICS, Inc. (HGI) and Columbia Energy and Environmental Services, Inc. (Columbia Energy), with support from technical staff of Washington River Protection Solutions, LLC (WRPS), conducted a three-dimensional (3D) geophysical survey of the subsurface using electrical resistivity to complete both stages. Data acquisition and analysis were performed in accordance with RPP-PLAN-47487, *Work Plan for Supplemental Surface Geophysical Exploration in the 241-BY Tank Farm.* Electrical resistivity data were acquired using 185 surface electrodes (located at the ground surface), seven boreholes containing depth electrode arrays (total of 57 depth electrodes), and 33 wells completed within the BY tank farm region.

1.1 SCOPE

The scope of this electrical resistivity characterization survey included:

- Data acquisition on surface electrodes, depth electrodes, and wells,
- Statistical evaluation of depth electrodes to ensure quality in data acquisition,
- Compilations of 3D electrical resistivity images of the BY tank farm.

1.2 OBJECTIVES

The main objective for this geophysical investigation was to collect and analyze electrical resistivity data to identify and map low resistivity regions around the BY tank farm.
Low resistivity is indicative of increased moisture or increased concentration of electrolytes compared to background conditions. An earlier two-dimensional (2D) electrical resistivity survey in this region indicated potential low resistivity regions as shown in Figure 1.
The objective of this survey is to further assess the presence, and if present, extent and depth of the low resistivity regions.

1.3 REPORT LAYOUT

The overall scope and content of this report is divided into several main sections as follows:

- **Section 1.0, Introduction** – Describes the scope and objectives of the investigation.
- **Section 2.0, Background** – Describes the geologic and hydrologic setting and information regarding the disposal activities in and around 241-BY tank farm.
- **Section 3.0, Data Acquisition and Processing Methodology** – Presents general layout of the data acquisition and processing, with the methods and controls used to ensure the quality and control of data collection, reduction, and processing used in this study.

- **Section 4.0, Modeling Results** – Presents the preliminary modeling results from the electrical resistivity surveying effort.
- **Section 5.0, Conclusions** – Provides a summary and conclusions drawn from the results and interpretations.
- **Section 6.0, References** – Provides a listing of references cited in the report.
- **Appendix A, Quality Assurance** – Presents general methods and controls used to ensure the quality and control of data collection, reduction, and processing and configuration control of software and database changes used in this study.

Figure 1. Color Contoured Results from 2006 Well-to-Well SGE Efforts at the BY Farm Indicating the Limits of the Stage 1 Survey and the Current Stage 2 Survey.

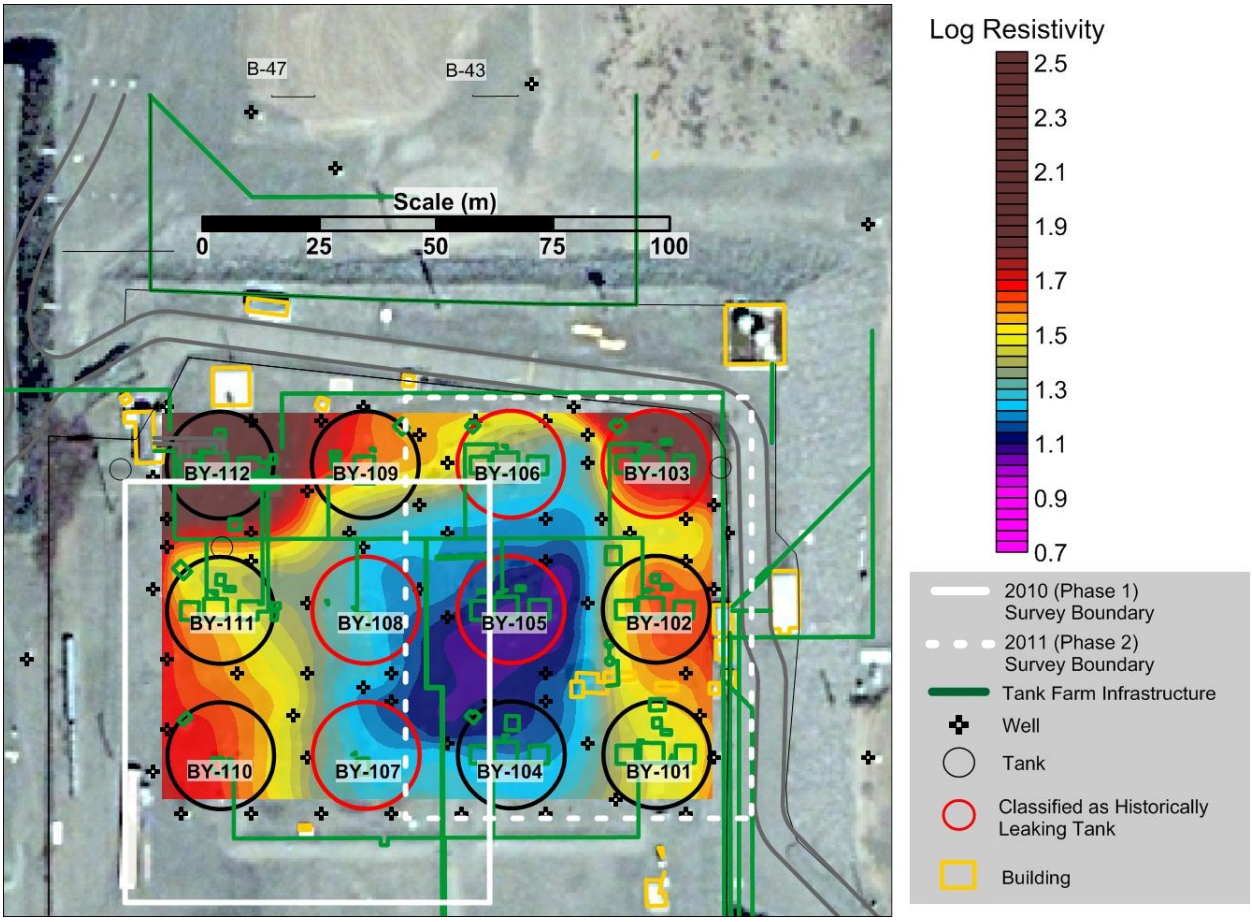

NOTE: Stage 1 survey boundary identified by solid white line. Stage 2 survey boundary identified by dotted white line. The 2006 well-to-well (WTW) modeling included groundwater wells surrounding BY Farm but the model has been clipped to the limits of the 2010/2011 domain.

2.0 BACKGROUND

2.1 SITE DESCRIPTION

The B, BX, and BY tank farms are three single-shell tank (SST) farms on the Hanford Site that form waste management area (WMA) B-BX-BY (referred to as B Complex). The B Complex is located in the northern portion of the 200 East Area (Figure 2), and includes a number of cribs and trenches on the west, north, and northeast sides (Figure 3). The majority of the cribs and trenches received waste directly from the B and U Plants (WHC-SD-WM-ER-575, *Liquid Radioactive Waste Discharges from B-Plant to Crib*).

The B Complex consists of the following tank farm facilities:

- B tank farm
  - Twelve 100-series SSTs of 530,000-gallon capacity
  - Four 200-series SSTs of 55,000-gallon capacity
- BX tank farm
  - Twelve 100-series SSTs of 530,000-gallon capacity
- BY tank farm
  - Twelve 100-series SSTs of 758,000-gallon capacity
- Leak detection systems
- Tank ancillary equipment.

The 100-series SSTs are 75 feet (23 meters) in diameter. The four 200-series SSTs in B tank farm are 20 feet (6.1 meters) in diameter. The B and BX SSTs are approximately 30 feet (9 meters) tall from base to dome. The smaller SSTs are approximately 26 feet (8 meters) tall. The general configuration of tanks in the B Complex is shown in Figure 4. As noted in Figure 3, 20 of the 40 SSTs in the B Complex are currently designated as assumed to have leaked tanks in HNF-EP-0182, *Waste Tank Summary for the Month Ending July 31, 2011*. However, the most recent assessment reports, including RPP-RPT-43704, *Hanford BY-Farm Leak Assessments Report*, and RPP-RPT-47562, *Hanford BX-Farm Leak Assessments Report*, suggest that the actual number of leaking tanks may be much lower due to the leaks originating from unplanned releases (UPRs) associated with pipeline failures or from surface spills or In-Tank Stabilization (ITS) operations. Re-evaluation of the current tank integrity classification was recommended for all of the tanks in BY farm except BY-103 and for all 5 of the tanks currently classified as "assumed leakers" in BX farm plus BX-107, currently classified as "sound."

Information on the B Complex construction, operations, and tank leak histories can be found in HNF-5231, *Historical Vadose Zone Contamination from B, BX, and BY Tank Farm Operations*. An understanding of contaminant occurrences and environmental conditions at the B Complex is presented in HNF-5507, *Subsurface Conditions Description of the B-BX-BY Waste Management*

Area. Enhanced understanding of B Complex subsurface contamination based on field characterization activities conducted in 2000 and 2001 is provided in RPP-10098, *Field Investigation Report for Waste Management Area B-BX-BY*. Additional shallow vadose zone characterization sampling was conducted in the BX tank farm during fiscal year 2006 and in BY tank farm in fiscal years 2010 and 2011. The samples from BY tank farm are currently being analyzed.

Figure 2. Location of the BY Tank Farm within the 200 East Area of the Hanford Site.

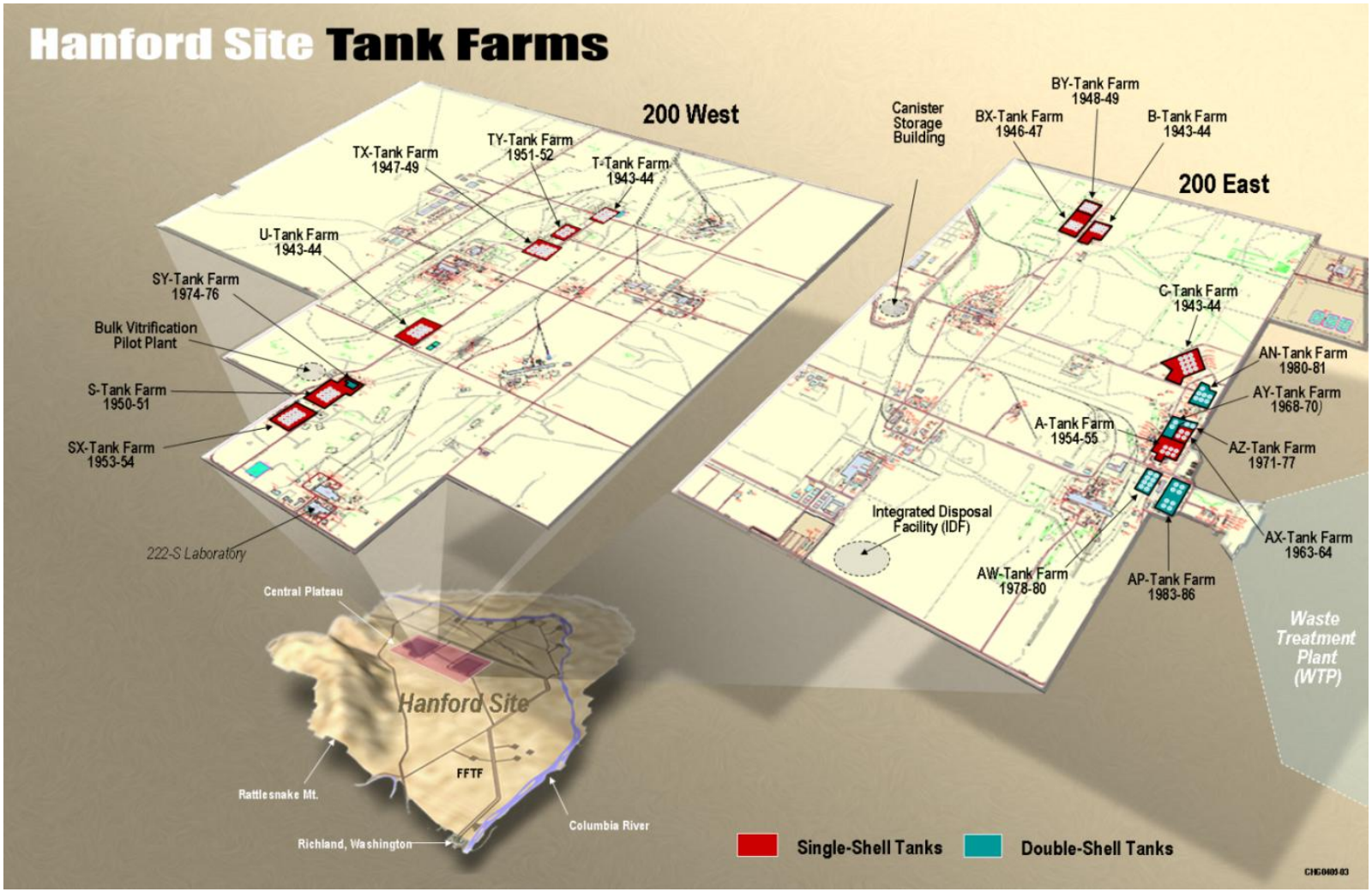

Figure 3. B, BX, and BY Tank Farm and Surrounding Facilities.

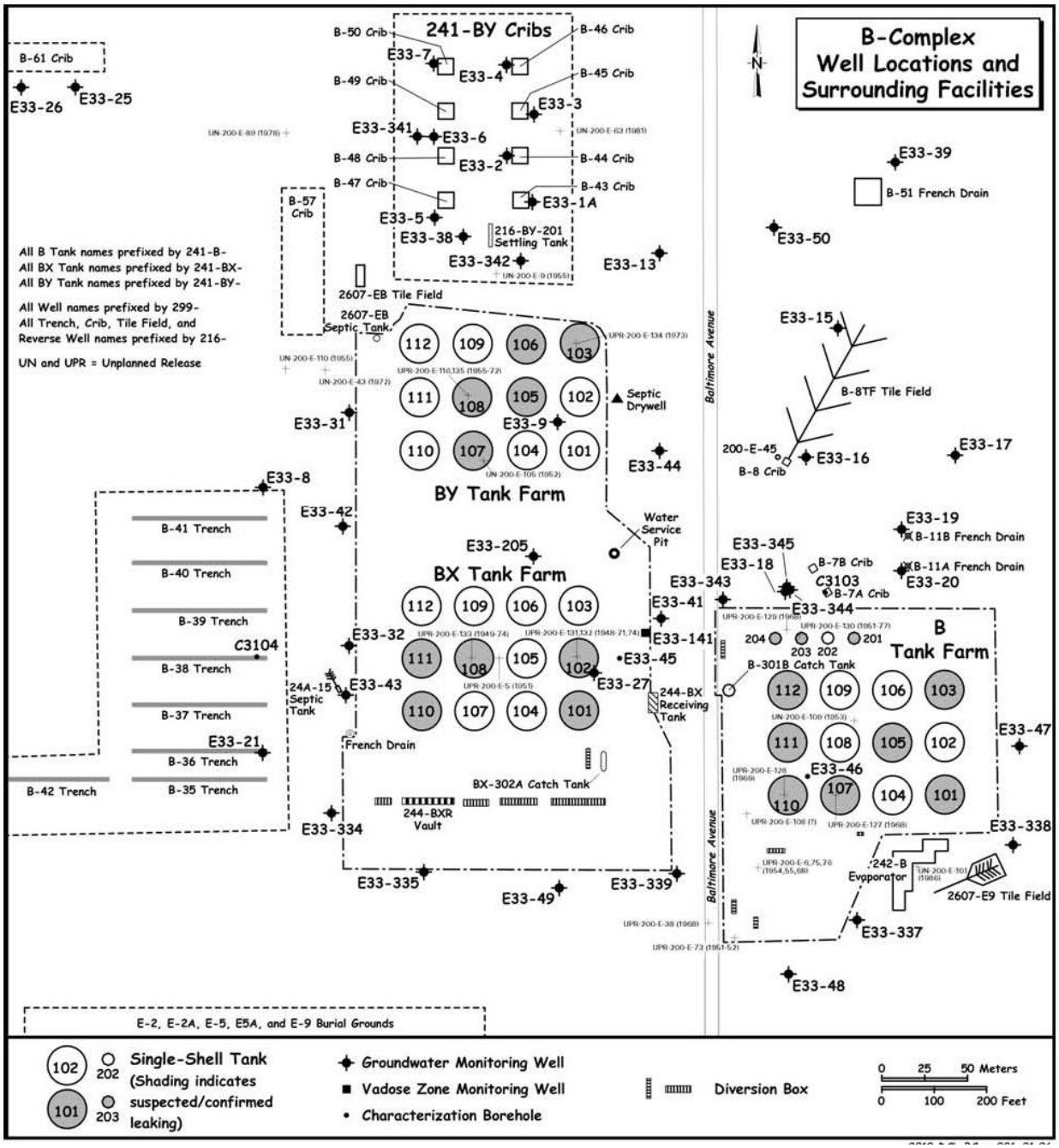

NOTE: Shaded tanks are designated as assumed to have leaked tanks according to HNF-EP-0182, 2011, *Waste Tank Summary Report for Month Ending July 31, 2011*, Revision 280, Washington River Protection Solutions, LLC, Richland, Washington. Three out of four of the B tank farm 200-series tanks are thought to have leaked. Source: RPP-RPT-43704, 2011, *Hanford BY-Farm Leak Assessments Report*, Revision 0, Washington River Protection Solutions LLC, Richland, Washington.

Figure 4. General Configuration of Tank Construction in Waste Management Area B-BX-BY.

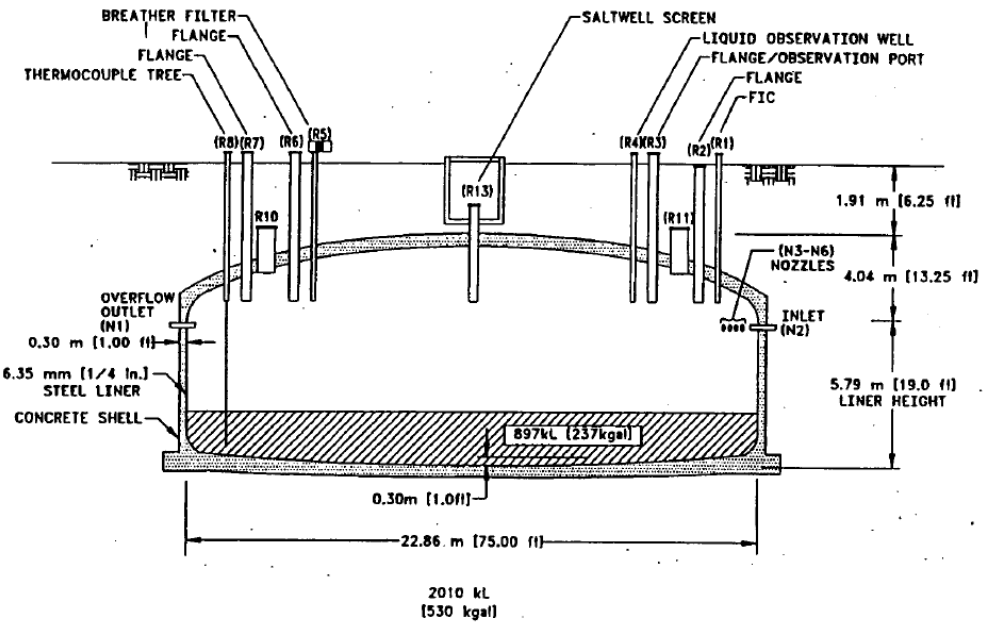

Source: HNF-5507, 2000, *Subsurface Conditions Description of the B-BX-BY Waste Management Area*, Revision 0, CH2M HILL Hanford Group, Inc., Richland, Washington.

2.2 OPERATIONAL HISTORY

The BY tank farm is a second-generation tank farm constructed at the Hanford Site to store high-level radioactive waste generated from chemical processing of irradiated uranium fuel. Located in the north-central part of the 200 East Area, north of B Plant, BY tank farm was constructed in 1948 and 1949 by General Electric (GE), the Hanford Site operations contractor at that time. BY tank farm consists of twelve 758,000-gallon underground waste storage tanks. Figure 3 shows the relative positions of these tanks and the groundwater monitoring wells around them. In addition, a number of drywells surround each tank within the perimeter of the BY tank farm. The drywells were drilled to roughly 100 feet below ground surface; the water table is currently approximately 247 feet below ground surface beneath the BY tank farm.

The tanks in BY tank farm are a modified 241-B tank farm design, a second generation design or Type III tank. They are domed tanks 75 feet in diameter, with a maximum operational height (maximum waste level) of approximately 23 feet above the tank bottom (Figure 4). The tops of the tanks are covered with approximately 6 feet of fill material, and the bottoms of the tanks are dished down. The tanks have a steel-reinforced concrete shell that is 1 foot thick and a mild carbon steel inner liner that covers the bottom and sides of the shell. The steel liner on the tank sides extends approximately 1 foot above the cascade-line connections. The tanks were designed for a maximum fluid temperature of 220 degrees Fahrenheit (°F).

The BY tank farm storage tanks are sited at slightly different elevations, creating a gradient from south to north that allows fluids to flow from one tank to another as they are filled. The tanks are

arranged in four cascades, each consisting of a three-tank cascade series with the receiving tank 1 foot lower than the feed tank. The cascade inlet and overflow connections to the tank are approximately 23 feet above the tank bottom. The inlet and overflow line connections are sleeved through the concrete shell and welded to the steel tank liner. The domes of the BY tank farm tanks were modified from previous designs to accommodate additional tank risers, which allowed more uniform access to the tank interior. The BY tank farm tanks are connected to the end tanks of the 241-BX tank farm in the following configurations:

- Tank BX-103 to tank BY-101
- BX-106 to BY-104
- BX-109 to BY-107
- BX-112 to BY-110.

Tanks BY-103 and BY-108 are assumed to have leaked and tanks BY-105, BY-106, and BY-107 were questionable integrity tanks and are currently classified assumed to have leaked (HNF-EP-0182). Also, tank BY-102 was classified in 1972 as a dormant leaker. This interim classification described a tank where initial elevated radiation levels in drywells or an initial drop in liquid level stabilized. Occasionally, a tank that had shown liquid level losses or an increasing radiation level has been stabilized by lowering the operating level in that tank.

Recently, the tanks have been reevaluated for the potential of past leaks (RPP-RPT-43704). Tank BY-103 was thought to have leaked <5,000 gallons based on uncertainty in manual tape recordings for liquid level monitoring. The tank remains in the assumed leaker status. The status of tanks BY-105 and BY-106 as assumed leakers was based on gamma logging in a nearby drywell showing hits. The reevaluation suggests that available data indicate that these tanks may not have leaked. Tank BY-107 was thought to have leaked approximately 15,000 gallons based on liquid level monitoring. New evidence suggests that the use of the monitoring tape may have been flawed or that the leak observed in nearby drywells was actually the result of a UPR in proximity to tank BY-107 of approximately 23,000 gallons. Lastly, the status of BY-108 as an assumed leaker is in question because of the number of potential sources of contamination, including a leaking tank, a leak through a spare inlet valve, or piping.

The BY tank farm was initially operated as a backup to the BX tank farm. Tanks BY-101 through BY-106 received B Plant metal wastes in cascade after the BX tank farm tanks were filled. Tanks BY-107 through BY-110 received B Plant first-cycle and tributyl phosphate (TBP) waste, while tanks BY-111 and BY-112 provided temporary storage of metal waste. A series of aggressive evaporation campaigns used several BY tank farm tanks for feed staging and evaporator bottoms receiving. A sluicing operations program for uranium recovery operated between January 1954 and August 1955 to remove waste from the tanks.

2.2.1 Liquid Waste Releases at B Complex

Over their operating history, facilities in and around the B Complex have unintentionally and intentionally released liquid wastes to the vadose zone. The list of unintentional releases, in the form of unplanned releases, is contained in DOE/RL-88-30, *Hanford Site Waste Management Units Report*. Unplanned releases, pipeline failures, and near-surface releases, summarized in

Table 1, were identified through review of operational histories for the BY tank farm (RPP-RPT-43704). Some of these releases are not currently included in the Waste Information Data System (WIDS) as UPRs. UPR-200-E-134 and UPR-200-E-135 are associated with tank leaks from BY-103 and BY-108, respectively. UPR-200-E-110 and UPR-200-E-116 were established for a valve pit and piping leak at tank BY-112.

Table 1. Potential Pipeline Failures and Other Unplanned Waste Releases at BY Farm. (2 sheets)

Date	Event	Reference	Comments
1952	About 23,000 gallons of first cycle waste leaked from a manifold header at tank BY-107. The leak covered 300 ft^2 of ground surface. Radiation surveys recorded a maximum dose rate of 150 rad/hr 2 inches from the surface of the release.	UPR-105; HWR-28471, p.5	After evaluating the spill, it was deemed impractical to decontaminate the area and was instead covered with concrete.
1955	Liquid contaminants spread through the soil from the BY-112 valve pit. A crescent-shaped soil mass around the pit, a fire hose and workers gloves were contaminated. The release covered approximately 25,000 ft^2 with radioactivity levels up to 22 rad/hr.	UPR-110; BHI-00179	Probably metal waste based on the time of the leak. UPR-200-E-110 states that it was 1C waste, but BY-110 never received 1C waste. SIM estimates 5,100 gallons, assuming 1-inch depth.
1955	Approximately 11,000 gallons of scavenged TBP overflowed the 216-BY flush tank associated with the 216-B-43 through 216-B-50 Cribs.	UPR-9; BHI-00179	Most of the contaminated soil was excavated and placed in a shallow pit south of the 216-B-43 Crib and covered with 2 feet of clean topsoil. The remaining contaminated area near the flush tank was reported to be covered with 10 feet of clean soil.
1969	When placing the ITS heater into a 42-inch riser on tank BY-112, a "cloud" was released and blown in a westerly direction. 4 pickups, 3 employees outside the zone, the control shack, transformer area, the crane, and ground area were contaminated to up to 100,000 dpm.	Historical Radiation Reports	Perimeter roads were clean, contaminated areas were marked and hosed down to prevent further spread. Cleanup begun. Not in WIDS/SIM.
1970	Leak in encased process line between the BY-111 and BY-112 tanks. Operators decontaminating the trench with steam and water were exposed to 2.5 rads/hr.	Historical Radiation Reports	No volume estimate for leak.
1972	BY-102 pump, sleeved in plastic for burial, broke while loading onto trailer permitting liquid to run from the sleeving. Contamination to 100 mrads/hr by riser.	UPR-43; BHI-00179	Not in SIM.
1972	Gasket failure while backflushing a pump at tank BY-112. 1 to 3 rad/hr in pit.	UPR-116	The pit was covered with dirt.

Table 1. Potential Pipeline Failures and Other Unplanned Waste Releases at BY Farm. (2 sheets)

Date	Event	Reference	Comments
1975	During overground transfer from BY-105 to BY-109, a flange leaked contaminating the ground under the flange over a 5 by 6 feet area to 5 rad/hr at 6 inches.	East tank farm Historical Occurrence Reports	Pump secured and 1 foot of dirt placed over contaminated area, which was then covered with plastic.

dpm	=	disintegration per minute	SIM	=	Hanford Soil Inventory Model
ft^2	=	square feet	TBP	=	tributyl phosphate
hr	=	hour	UPR	=	unplanned release
1C	=	first cycle (waste)	WIDS	=	Waste Information Data System.
ITS	=	in-tank solidification			

Sources:

RPP-RPT-43704, 2011, *Hanford BY-Farm Leak Assessments Report*, Revision 0, Washington River Protection Solutions, LLC, Richland, Washington.

WHC-SD-WM-ER-575, 1996, *Liquid Radioactive Waste Discharges from B-Plant to Crib*, Revision 0, Westinghouse Hanford Company, Richland, Washington.

Figures 5, 6, and 7 are cross-section visualizations based on spectral gamma drywell measurements. The green anomalies presented in Figures 5 and 6 are addressed in RPP-RPT-43704, and are not included for the purposes of this study. The figures illustrate the impact of the near-surface UPR at tank BY-112, and show that low levels of cesium-137 activity are widely distributed across the farm in the top 9 feet below ground surface. At 35 feet, except for the UPR at tank BY-112, the highest activity for cesium-137 is observed near tank BY-103. In addition, at this and subsequent depths cobalt-60 plumes begin to be observed in the similar locations to the near-surface cesium-137 activity highs. At 64 feet below ground surface, cobalt-60 activity is seen on the east side of tanks BY-107 and BY-108, extending to the northeast towards tank BY-106. This correlates well with the assumed leaking tanks.

Figure 5. Visual Based on Drywell Logging Activity at 4 Feet in 241-BY Tank Farm.

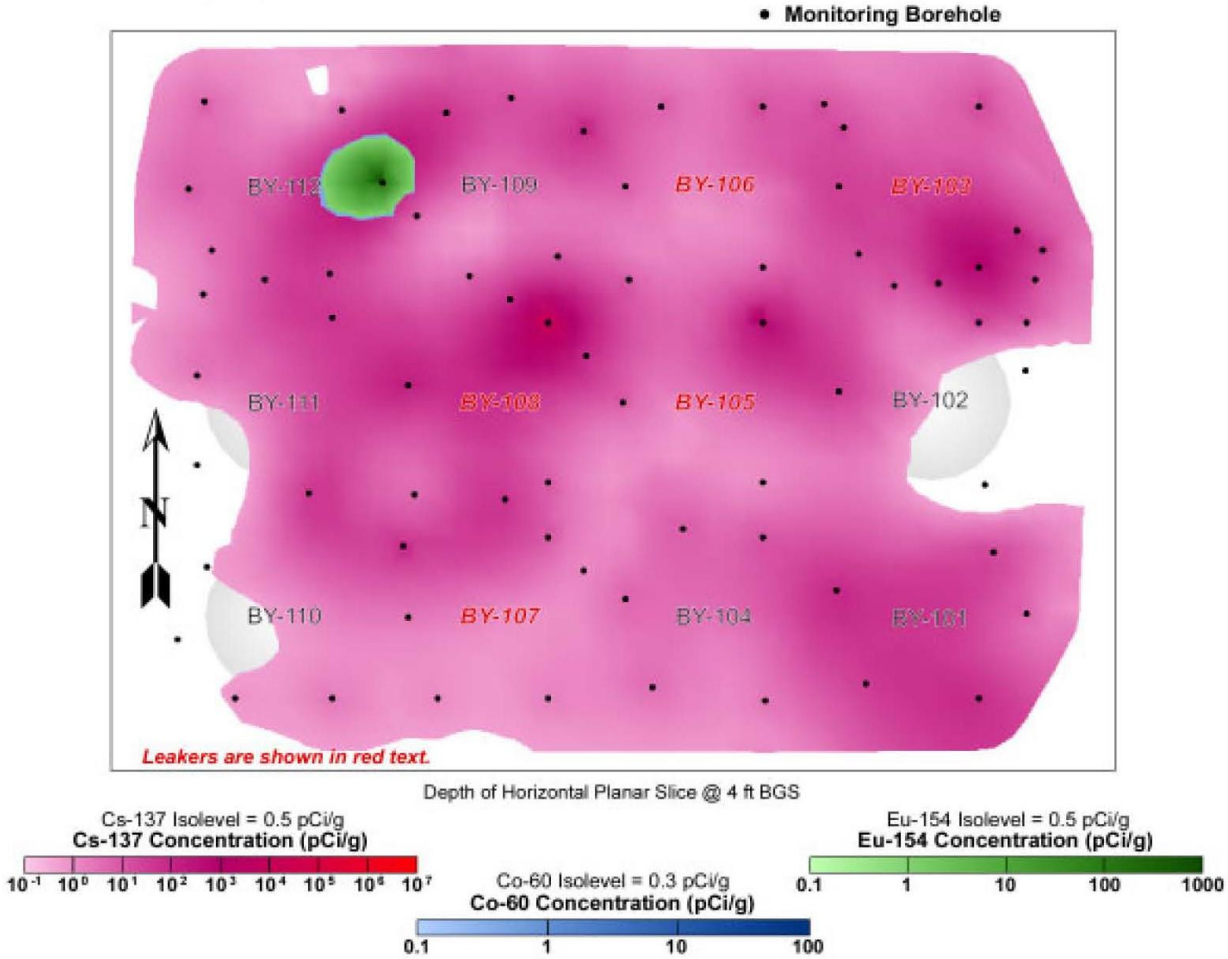

Source: RPP-RPT-43704, 2011, *Hanford BY-Farm Leak Assessments Report*, Revision 0, Washington River Protection Solutions, LLC. Richland, Washington.

Figure 6. Visual Based on Drywell Logging Activity at 9 Feet in 241-BY Tank Farm.

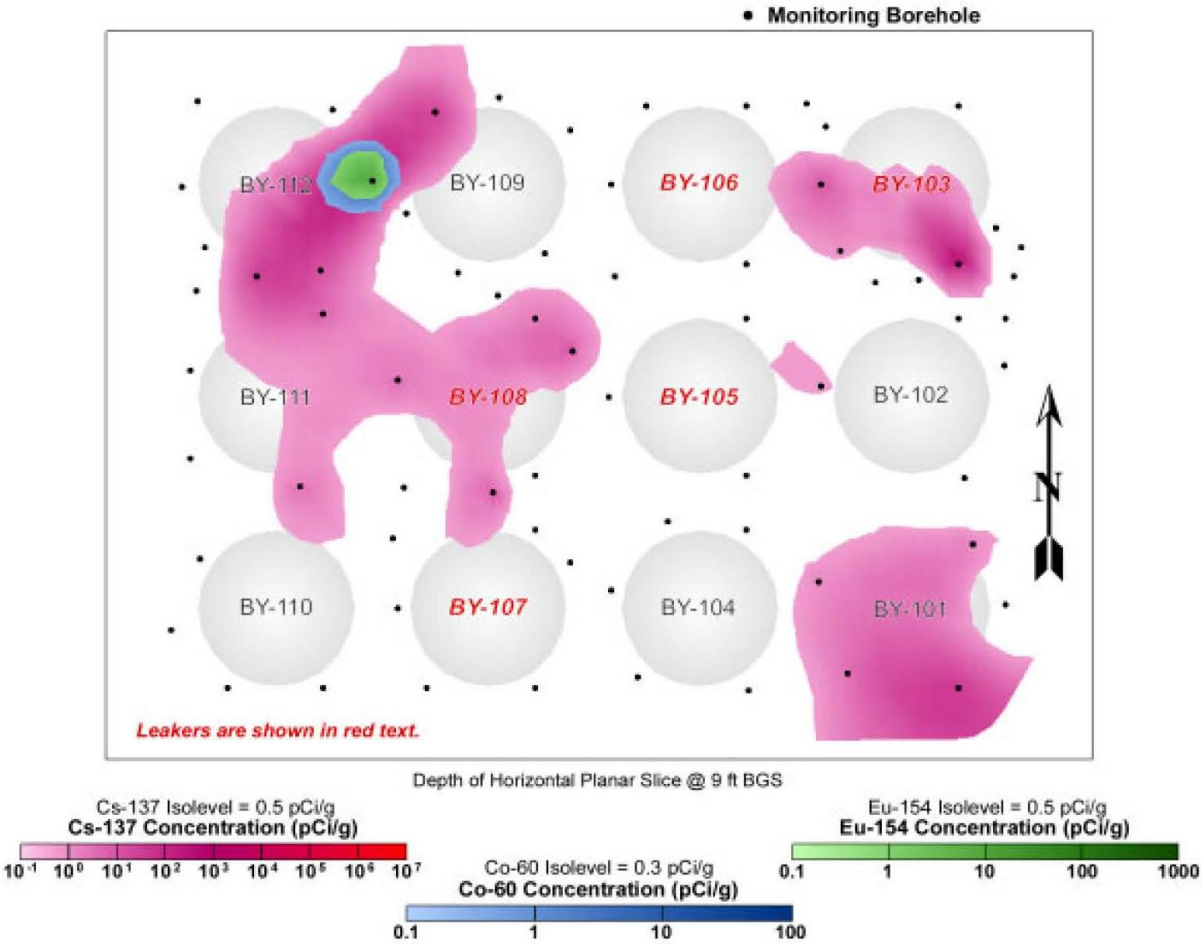

Source: RPP-RPT-43704, 2011, *Hanford BY-Farm Leak Assessments Report*, Revision 0, Washington River Protection Solutions, LLC, Richland, Washington.

Figure 7. Visual Based on Drywell Logging Activity at 35, 55, and 69 Feet in 241-BY Tank Farm.

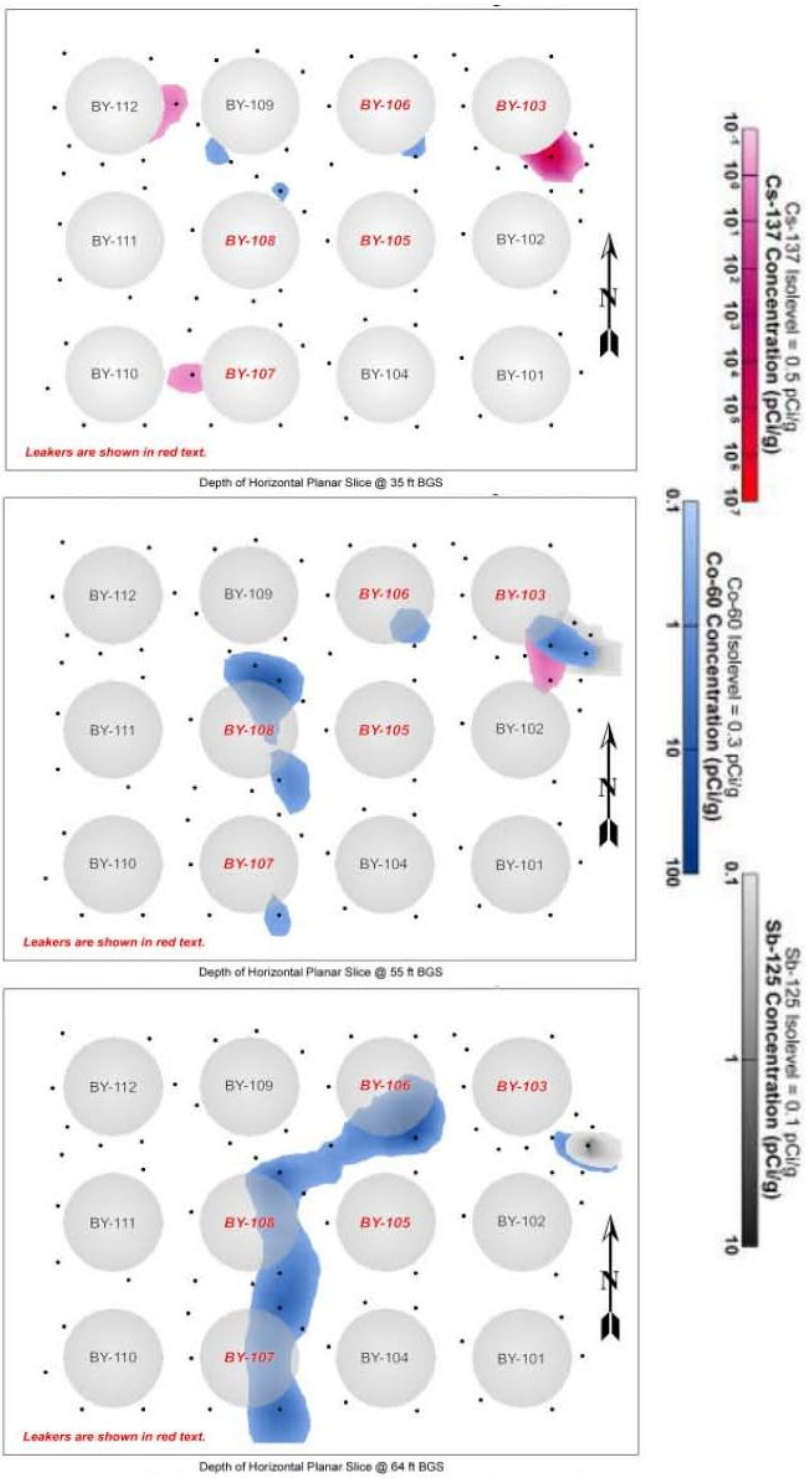

Source: RPP-RPT-43704, 2011, *Hanford BY-Farm Leak Assessments Report*, Revision 0, Washington River Protection Solutions, LLC, Richland, Washington.

The adjacent waste management facilities (216-B trenches and 216-B cribs) intentionally discharged liquid waste to the vadose zone while some of the SSTs, along with some of their associated ancillary equipment, are known or suspected to have unintentionally released waste to the vadose zone. These discharges have led to contaminant plumes distributed in the vadose zone (and possibly to the water table) within and around the tank farm.

During waste management operations, substantial volumes of liquid waste were discharged to the cribs and trenches near the B Complex as shown in Table 2. These occurred during three large-scale operation periods. The first was the bismuth phosphate processing period mentioned previously (1945 to 1954). The second period of B Complex operations occurred from 1952 to 1955 for uranium recovery activities. Since the tank waste still contained a large and convenient source of uranium, their contents were sluiced for extraction. B Complex was activated once again for isotope recovery and storage from 1967 to 1979. In-tank stabilization activities began after uranium extraction events in 1952. Predominantly, this occurred with the in-tank solidification operations program that occurred from 1965 to 1974. Subsequently, the in-tank solidification program was replaced by a more efficient method referred to as saltwell pumping. Removal of pumpable liquids has been completed at all B Complex SSTs and the tanks are all listed as interim stabilized in HNF-EP-0182.

Table 2. Liquid Waste Disposal Facilities and Discharge Volumes near B Complex. (2 sheets)

Facility/Component	Liquid Waste Discharge Volume (gallons)	Operational Period
B-7A&B cribs	11,334,214	1946–1967
B-8 crib	7,186,262	1948–1952
B-11 A&B reverse wells	7,825,902	1951–1954
B-35 trench	280,053	1954
B-36 trench	512,549	1954
B-37 trench	1,141,348	1954
B-38 trench	377,807	1954
B-39 trench	406,869	1953–1954
B-40 trench	433,289	1954
B-41 trench	380,449	1954
B-42 trench	396,301	1955
B-43 crib	560,106	1954
B-44 crib	1,479,524	1954–1955
B-45 crib	1,299,868	1955
B-46 crib	1,770,145	1955
B-47 crib	972,259	1955
B-48 crib	1,080,581	1955–1957
B-49 crib	1,770,145	1955
B-50 crib	14,462,322	1965–1974

Table 2. Liquid Waste Disposal Facilities and Discharge Volumes near B Complex. (2 sheets)

Facility/Component	Liquid Waste Discharge Volume (gallons)	Operational Period
B-51	264	1956–1958
B-57 trench	22,280,318	1968–1973

Source: WHC-SD-WM-ER-575, 1996, *Liquid Radioactive Waste Discharges from B-Plant to Crib*, Revision 0, Westinghouse Hanford Company, Richland, Washington.

The volumetric distribution of discharged waste around the B Complex varies. Figure 8 shows the disposal volumes and tank leak volumes graphically, depicted as circles with the diameter relative to the amount of discharge (the smaller the diameter of the circle, the smaller the discharged volume). The figure shows that a significant volume of liquid has been discharged to the subsurface, equating to almost 79 million gallons. Most of the liquid has been discharged to the 216-B cribs, with approximately 60 percent of the waste volume disposed in the northern and northeastern portion of the site. The tanks discharged a total of <200,000 gallons to the subsurface.

Figures 9 through 11 show the distribution of electrolytes (anions and cations) and major radionuclides.

Figure 8. Liquid Waste Volumes Discharged Around B Complex Area.

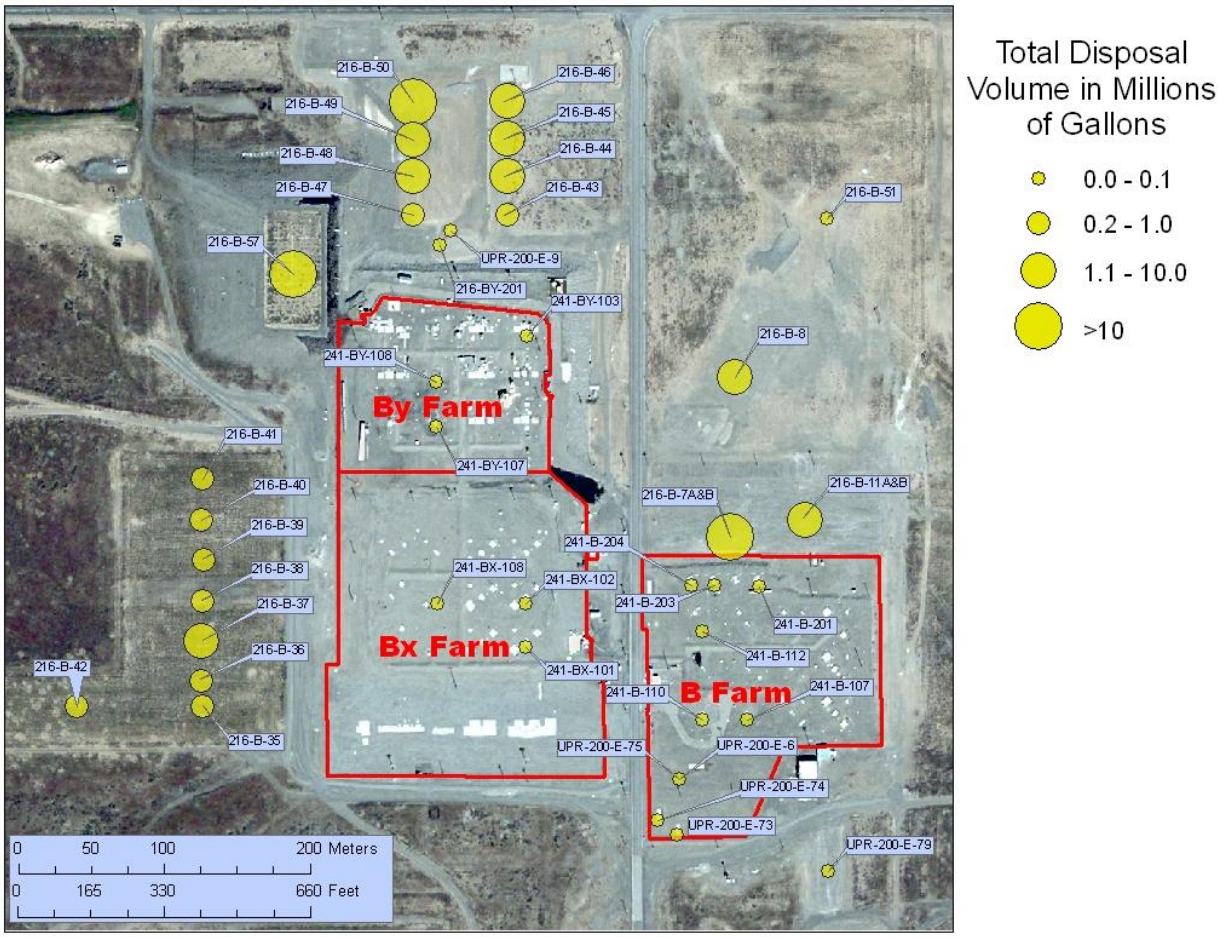

Figure 9. Major Cations Discharged Around B Complex Area.

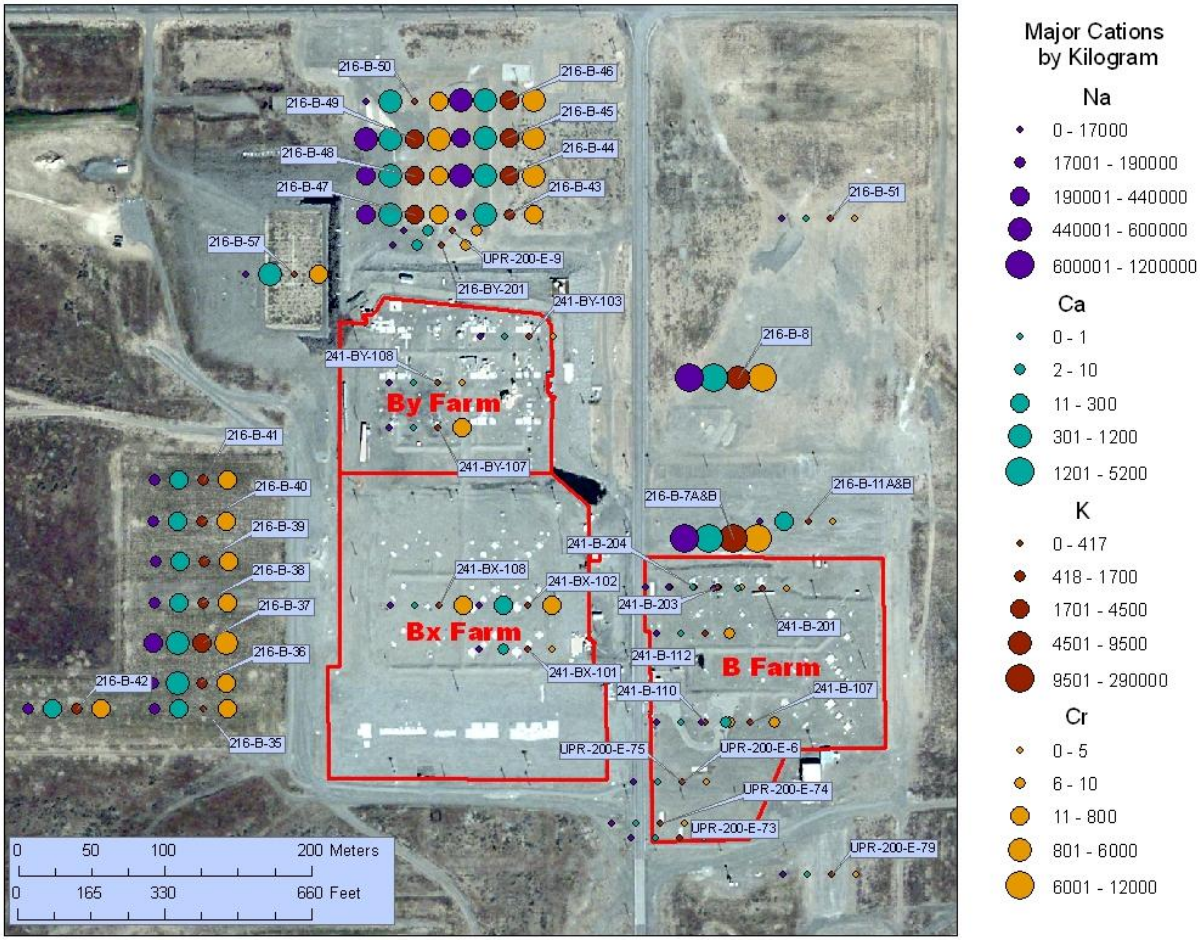

Figure 10. Major Anions Discharged Around B Complex Area.

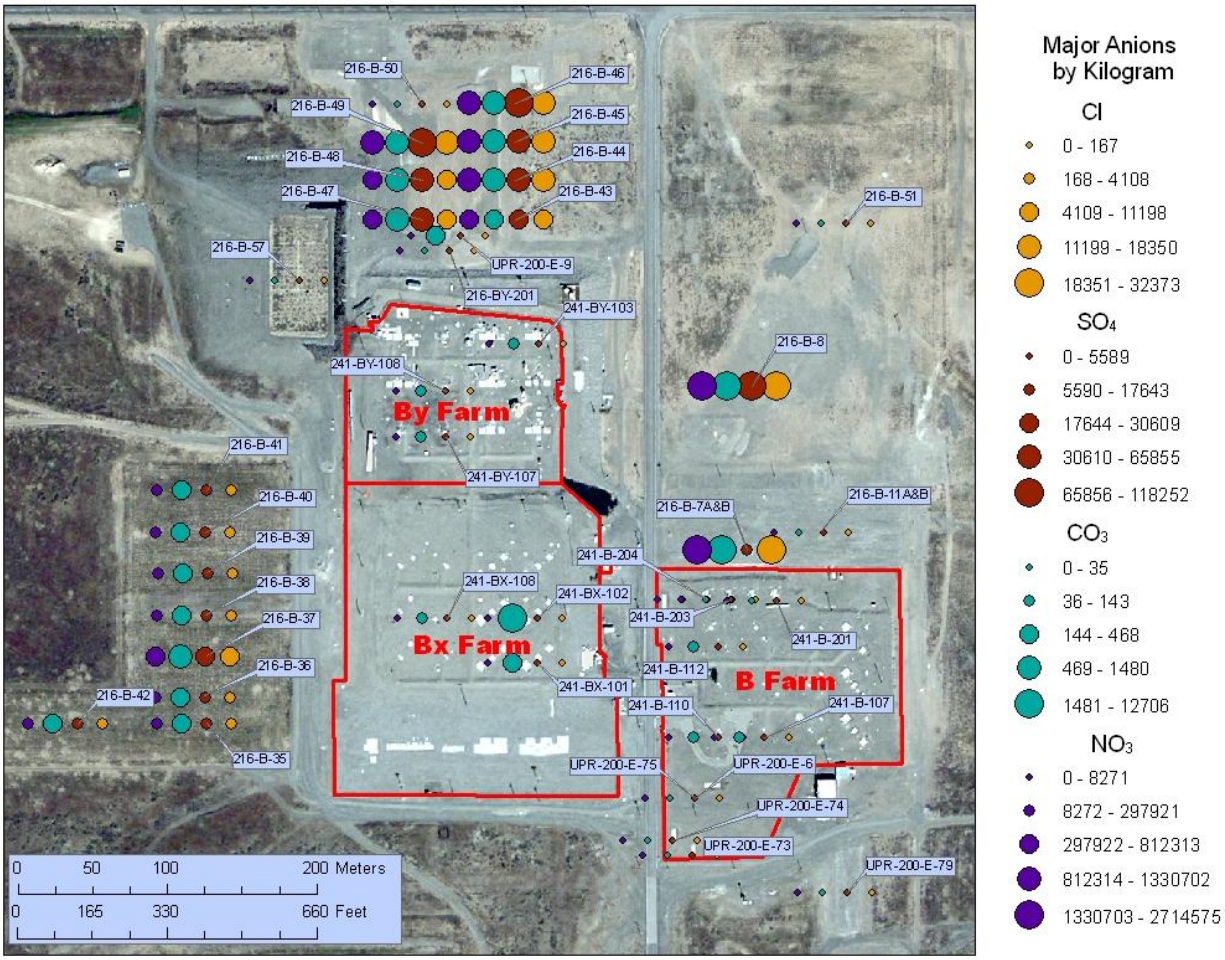

Figure 11. Major Radionuclides Discharged Around B Complex Area.

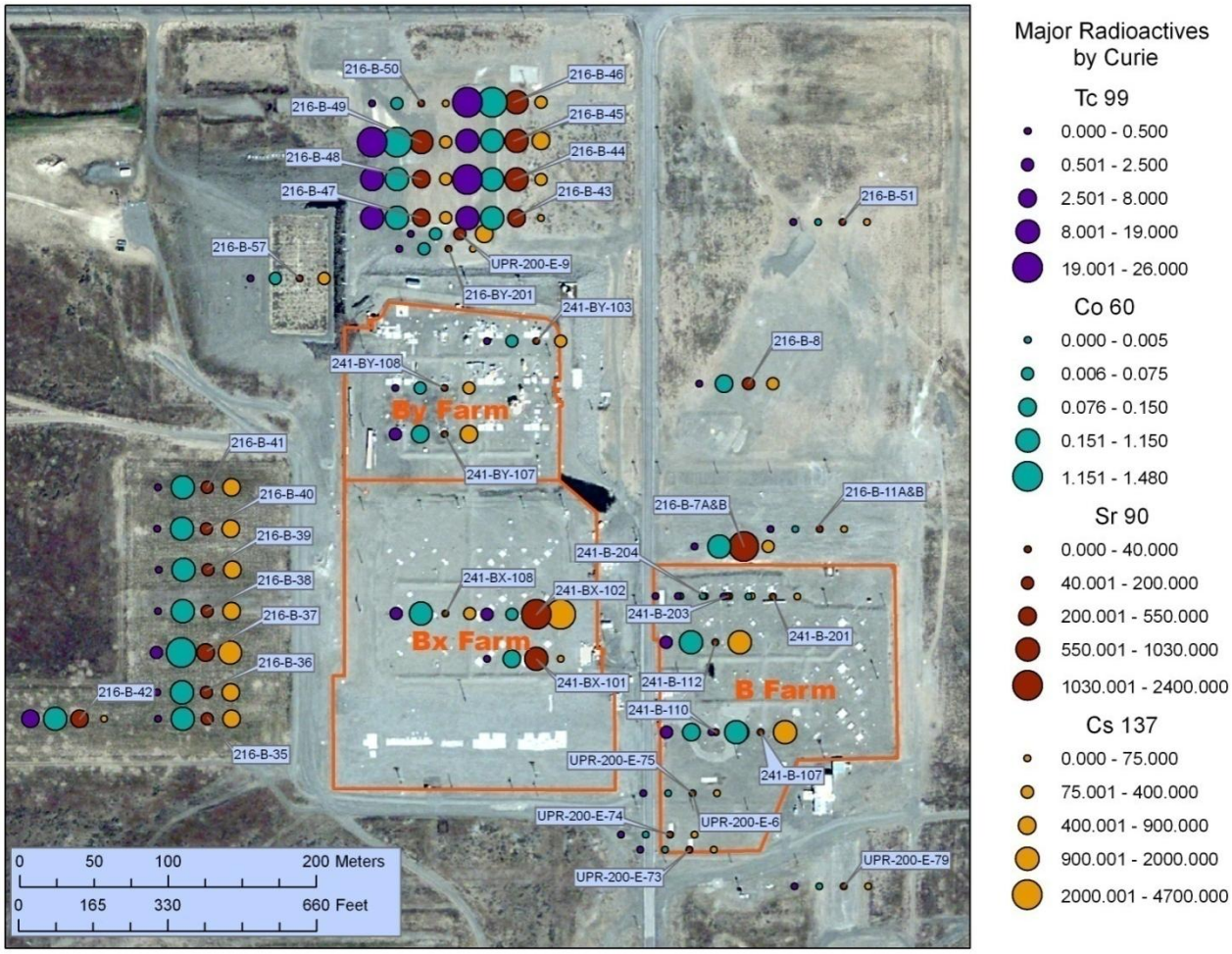

Within the BX series of trenches, trench 216-B-42 is the only trench in the subgroup that received uranium waste stream product. All other trenches received first cycle waste. Although large volumes of liquid were discharged to the northern trenches, the liquid was "highly diluted compared to the uranium recovery wastes discharged to the BY cribs" (RPP-10098). Within the BY cribs, technetium-99 values of 12,000 picocurie per liter (pCi/L) were measured in 2001. Previous studies have indicated that strong lateral migration of subsurface contamination exists within the B-BX-BY area and is caused by complex hydrogeologic conditions (RPP-10098).

As previously noted, 20 of the 40 SSTs in the B Complex are currently designated as assumed leakers (HNF-EP-0182), including five tanks in the BY tank farm. Seventeen of the 20 tanks are 100-series tanks and three are 200-series tanks. Reported leak volumes for the 100-series tanks range from approximately 140,000 gallons (tank BX-102) to 2,000 gallons (tank B-112). Reported leak volumes for 200-series tanks range from 1,200 gallons (B-201) to 300 gallons (B-203). Some of the waste loss events (e.g., BX-102) are well documented (RPP-RPT-47562), while others are questionable and have minimal data available to support a leak volume estimate. HNF-EP-0182 provides leak volumes for 11 of the 20 designated leakers in the B Complex.

Leak assessments are currently being reevaluated to determine the leak location and volume estimates. B tank farm is currently in progress, soon to be released for peer review (as report number RPP-RPT-49089). The reassessment for the tanks in BX tank farm is RPP-RPT-47562, Revision 0, and the reassessment for the tanks in BY tank farm is RPP-RPT-43704, Revision 0A.

2.2.2 Infrastructure and Waste Delivery to B Complex

In addition to the intentional liquid waste discharges to the cribs and unplanned waste releases, leaks from water distribution lines in and around the tank farm and known meteorological events may have contributed significantly to waste migration in the vadose zone (RPP-10098). Figure 12 shows the infrastructure, including pipes, tanks, and diversion boxes, used to transfer waste and supply water to the BY tank farm. The infrastructure is divided among groupings of years, based on the work by HNF-5231.

Figure 12. Infrastructure Map for BY Farm.

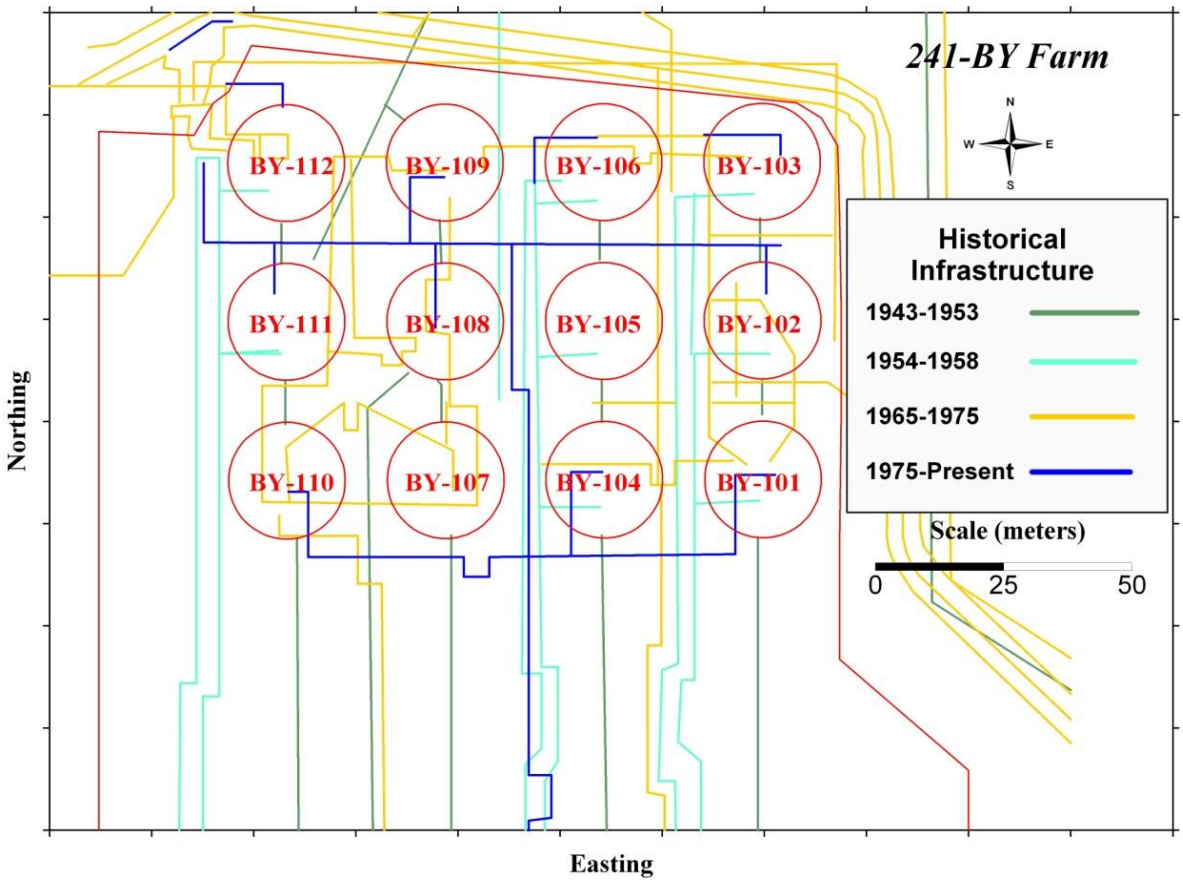

Adapted from HNF-5231, 1999, *Historical Vadose Zone Contamination from B, BX, and BY Tank Farm Operations*, Revision 0, Fluor Hanford, Inc., Richland, Washington.

2.3 ENVIRONMENTAL SETTING

The geology of the B Complex and immediate vicinity is well understood as a result of several decades of site characterization activities. Sedimentary and stratigraphic conditions have been described in numerous reports, including the following publications:

- RPP-10098, *Field Investigation Report for Waste Management Area B-BX-BY*
- HNF-5507, *Subsurface Conditions Description for the B-BX-BY Waste Management Area*
- PNNL-14119, *Characterization of Vadose Zone Sediment: Borehole 299-E33-46 Near B 110 in the B-BX-BY Waste Management Area*
- PNNL-14128, *Characterization of Vadose Zone Sediment: Borehole C3103 Located in the 216-B-7A Crib and Selected Samples from Borehole C3104 Located in the 216-B-38 Trench Near the BX Tank Farm*
- PNNL-12128, *Borehole Data Package for Well 299-E33-44 at Single-Shell Tank Waste Management Area B-BX-BY*
- PNNL-14121, *Characterization of Vadose Zone Sediment: RCRA Borehole 299-E33-338 Located Near the B-BX-BY Waste Management Area*
- RHO-ST-23, *Geology of the Separations Areas, Hanford Site, South Central Washington*
- RPP-23748, *Geology, Hydrogeology, Geochemistry, and Mineralogy Data Package for the Single-Shell Tank Waste Management Areas at the Hanford Site*.

Four major stratigraphic units underlie the B Complex. In ascending order they include:

1. Miocene-age igneous Columbia River Basalt Group (three sedimentary units).
2. Cold Creek Units (Hf/CCU).
3. Sand-dominated sequence of the Hanford formation (H2).
4. Gravel-dominated sequence of the Hanford formation (H1 Unit).

In addition, backfill materials consist of poorly sorted cobbles, pebbles, and coarse to medium sand are distributed around the tanks and tank infrastructure.

The backfill and Hanford formation (H1, H2, Hf/CCU) make up the vadose zone. The Hanford formation ranges from approximately 141 feet to 275 feet (43 meters to 83 meters) and thins to the north. A perched water zone is typically encountered within the upper CCU unit and the regional aquifer occurs in the lower CCUg (gravel) sequence at an approximate depth of 249 feet (76 meters) below ground surface. All major stratigraphic units are inferred to be continuous in this area, although unit thicknesses vary.

2.4 HISTORICAL CHARACTERIZATION EFFORTS

The SSTs are regulated under various U.S. Department of Energy orders and policies in addition to the Washington State RCW 70.105, *Hazardous Waste Management Act* and its implementing requirements in *Washington Administrative Code* 173-303, “Dangerous Waste Regulations.”

The SSTs are operating under interim status permit pending closure. For regulatory compliance purposes, the SST farms are grouped into WMAs.

Each 100-series tank in the B Complex is surrounded by a group of monitoring boreholes (drywells) in which radiometric instruments are used to detect changes in activity levels in the sediments surrounding the borehole. From 1944 to 1974, 50 to 75 of these drywells were installed in each of the B Complex tank farms. The depth ranges for most of the drywells are between 60 and 150 feet (18 and 46 meters) below ground surface.

During active waste management operations, the drywells serve as both primary and secondary leak detection devices. Gross gamma logging of the drywells took place over several decades allowing evaluation of the time-dependent behavior of the gamma-emitting radionuclides. From 1995 to 1999, high-resolution spectral gamma logging of the B Complex drywells was conducted as part of the baseline vadose zone characterization for the B Complex. Results are documented in tank farm summary reports issued by the U.S. Department of Energy Grand Junction, Colorado office:

- GJO-96-2-TAR , *Vadose Zone Characterization Project at the Hanford Tank Farms: BY Tank Farm Report*
- GJO-98-40-TAR, *Hanford Tank Farms Vadose Zone: BX Tank Farm Report*
- GJO-99-113-TAR, *Hanford Tank Farms Vadose Zone: B Tank Farm Report*.

From 2000 to 2001, field characterization activities were conducted at the B Complex in support of *Resource Conservation and Recovery Act of 1976* (RCRA) corrective action process requirements. The major investigative activities for this effort included borehole installation, soil sampling, and analysis at locations east of tank BX-102, northeast of tank B-110, near trench 216-B-38 (west of BX tank farm), and near cribs 216-B-7A and 216-B-7B (north of B tank farm). Investigation results are documented in RPP-10098.

Chemicals and radionuclides have been tracked in unconfined aquifer samples collected from monitoring wells in and around the B Complex for about the past 15 years (RPP-10098). Waste Management Area B-BX-BY was placed in assessment groundwater monitoring in 1996 due to elevated specific conductance (a measure of electrical conductivity of water), in down gradient monitoring wells (PNNL-13032, *RCRA Assessment Plan for Single-Shell Tank Waste Management Area B-BX-BY at the Hanford Site*). Technetium-99, uranium, chromium, cyanide, and nitrate are constituents that have historically exceeded Title 40 *Code of Federal Regulations*, Part 141, “National Primary Drinking Water Regulations," (40 CFR 141) at the B Complex.

Contaminants currently present in groundwater at the B Complex along with potential contamination sources are discussed in DOE/RL-2011-01, Hanford Site Groundwater Monitoring Report for 2010. In fiscal year 2010, a network of 26 monitoring wells was used to monitor the groundwater at WMA B-BX-BY (DOE/RL-2011-01). Sampling was conducted quarterly in most wells. Monitoring is conducted under the requirements of RCRA, CERCLA, and the *Atomic Energy Act of 1954*. Groundwater monitoring wells have been developed both inside WMA B-BX-BY and in the nearby cribs and trenches to evaluate contaminant occurrence in the unconfined aquifer resulting from the unintentional and intentional discharges in these locations.

2.4.1 Vadose Zone

The major gamma-emitting contaminants associated with the B Complex vadose zone are cesium-137, cobalt-60, europium-154, ruthenium-106, and antimony-125 (HNF-5507). Spectral gamma logging data indicate that higher contaminant concentration zones are located mostly in and around areas of suspected tank and pipeline leaks. The data also indicate that generalized near-surface contamination at lower concentrations is widespread across the three tank farm areas. The evaluation of time-dependent behavior indicates that in certain areas the more mobile radionuclides, such as cobalt-60, have migrated downward from their locations of emplacement (HNF-5507).

The most extensive region of vadose zone contamination in the B Complex is found adjacent to and east of tank BX-102. The contamination is related to a 1951 metal waste overfill event at tank BX-102 that led to a significant uranium plume in the subsurface east of that tank. Nineteen new drywells were installed in the area east of tanks BX-101 and BX-102 during investigations conducted in the early 1970s (Womack and Larkin 1971). These investigations also led to the discovery of a leaking pump pit on the dome of tank BX-101. Spectral gamma logging data from drywells in this region show a uranium plume extending from about 70 feet (21 meters) to 150 feet (46 meters) below ground surface. The data also show a second plume containing a variety of radionuclides that overlies the uranium plume. The second plume is attributed to a cesium recovery waste loss event between 1968 and 1972 from the pump pit on top of tank BX-101.

At borehole 299-E33-45, installed about 100 feet (30 meters) east of tank BX-102 during the 2001 field characterization activities, elevated concentrations of several constituents attributed to tank fluid leakage were detected in borehole soil samples; including technetium-99, uranium isotopes, nitrate, and sodium (RPP-10098). Elevated concentrations were observed primarily between about 75 and 170 feet (23 and 52 meters) below ground surface. Technetium-99 was observed between about 120 to 170 feet (37 to 52 meters) below ground surface. Uranium was observed between about 70 to 170 feet (21 meters to 52 meters) below ground surface, with a peak concentration higher in the formation at approximately 130 feet (40 meters) below ground surface. Field data indicate that extensive lateral migration of contaminants occurred in the vadose zone east of tanks BX-101 and BX-102 in response to stratigraphic controls (RPP-10098).

Spectral gamma logging data indicate another region of extensive B Complex vadose zone contamination is located near tank B-110. Borehole 299-E33-46 was drilled to the northeast of tank B-110 during the 2001 field characterization activities to investigate a suspected strontium-90 plume in this area (RPP-10098). Elevated concentrations of several constituents attributed to tank fluid leakage were detected in borehole soil samples; including strontium-90, carbonate, fluoride, nitrate, and sodium (RPP-10098). Elevated concentration levels were observed at different depth intervals for various constituents. Carbonate, fluoride, and sodium were concentrated in the upper soil column between 50 and 150 feet (15 to 46 meters) below ground surface. Elevated strontium-90 concentrations were observed between 46 and 83 feet (14 and 25 meters) below ground surface. Nitrate concentrations were highest between 84 and 200 feet (26 and 61 meters) below ground surface (RPP-10098).

The 2001 field characterization activities also included installation of boreholes near the 216-B-7A Crib north of the B tank farm (borehole C3103) and the 216-B-38 Trench west of the BX tank farm (borehole C3104). Soil analysis data from the 216-B-7A Crib indicate that minimal contamination remains in the vadose zone at this location (RPP-10098). Elevated cesium-137 and uranium concentrations were detected near the bottom of the crib between 22 and 48 feet (7 and 15 meters) below ground surface. Mobile contaminants, initially in the effluents discharged to the crib, appear to have been flushed to the unconfined aquifer (RPP-10098). Soil analysis data from the 216-B-38 Trench indicate mobile contaminants discharged to this specific retention trench still reside in the vadose zone between 35 and 150 feet (11 and 46 meters) below ground surface, although the concentrations of technetium-99 and nitrate were minimal.

Spectral gamma logging data also show gamma activity indicative of waste loss events at tanks B-107, B-112, BX-108, BY-103, BY-107, and BY-108 (RPP-23405, *Tank Farm Vadose Contamination Volume Estimates*). The activity at tank B-107 is detected at the level of the tank base and supports a tank leak origin for the contamination. RPP-23405 reports an estimated leak volume of 14,000 gallons for tank B-107. Reported leak volumes for the other tanks are smaller (2,500 gallons or less), and much of the gamma activity is detected closer to the ground surface.

The vertical distribution of moisture content in the subsurface for selected monitoring wells is shown in Figure 13. The moisture content was taken from direct measurements of soil samples using a thermogravimetric method and converted to volumetric moisture using a constant bulk density of 1.6 grams/cm^3, or from neutron moisture logs. The vertical distribution of nitrate and sulfate from recent sampling and analysis efforts are summarized in Figure 14.

2.4.2 Unconfined Aquifer

In fiscal year 2010, multiple contaminants were detected at concentrations above the drinking water standard in groundwater beneath the B Complex; including technetium-99, tritium, cobalt-60, uranium, nitrate, sulfate, chromium, and cyanide (DOE/RL-2011-01). As discussed in DOE/RL-2011-01, assessment studies have identified the following distinct suites of contaminants with possibly different sources in this area:

- **Nitrate, technetium-99, sulfate, uranium, and nitrite.** These contaminants are located under and southeast of the BY tank farm. Technetium-99, nitrate, and uranium are found in concentrations above the drinking water standards of 900 pCi/L, 45 milligrams per liter (mg/L), and 30 micrograms per liter (µg/L), respectively. The uranium concentration in well 299-E33-343 of 3,670 µg/L is the highest in the 200 East Area.
- **Tritium and nitrate.** This contaminant suite is found on the southwest corner and along the south border of the B Complex. Sharply rising trends in contaminant concentrations in this area may be related to contaminants moving through the vadose zone from a perched water table, with elevated concentrations under the BX tank farm.
- **Technetium-99, nitrate, uranium, sulfate, tritium, cobalt-60, and cyanide.** This contaminant suite, found under and around the BY Cribs, comprises the highest levels of contamination in the groundwater at the B Complex, except for the maximum uranium concentration under the BY tank farm. Fiscal year 2010 maximum concentrations were; technetium-99 at 31,000 pCi/L; nitrate at 1,540 mg/L; uranium at 3,670 µg/L; sulfate at 264

mg/L; tritium average at 10,000 pCi/L; cobalt-60 at 290 pCi/L; and cyanide at 61.4 μg/L; all of which exceeded the drinking water standards. This suite is associated with past waste releases to the BY Cribs.

- **Nitrate, nitrite, technetium-99, and uranium.** This grouping of contaminants is located under the 216-B-8 Crib. Until recently, this area lacked the high levels of nitrite and uranium associated with the contamination under the BY tank farm. The fiscal year 2006 sampling showed sharp increases in contaminant concentrations, suggesting influences from the tank farms may be affecting groundwater conditions at the 216-B-8 Crib. Further evidence of changing groundwater conditions was seen in the sharp increases in nitrate, from 664 to 881 mg/L, and in technetium-99, from 3,360 to 11,800 pCi/L, during fiscal year 2006.

The hydraulic gradient is nearly flat across the 200 East Area and there are large uncertainties associated with the groundwater flow direction and rate beneath the B Complex. Historical discharges of effluent to the ground in and around this area have resulted in complex patterns of groundwater contamination. Evidence suggests that multiple vadose zone sources may be contributing to groundwater contamination in multiple areas (PNNL-16346). Although the first two contaminant groups are attributed to waste sources associated with the tank farms, contamination from the BY Cribs is affecting groundwater in the northern part of the B Complex (DOE/RL-2011-01). Uranium contamination extends to the northwest from beneath the B Complex and surrounding cribs (Figure 15). In addition, based on the changing conditions at the 216-B-8 Crib and areas farther south, groundwater contamination possibly associated with the tank farms has been noted in the areas east and south of the farms (DOE/RL-2011-01).

Figure 13. Vertical Distribution of Moisture Content in Monitoring Wells Surrounding the B Complex.

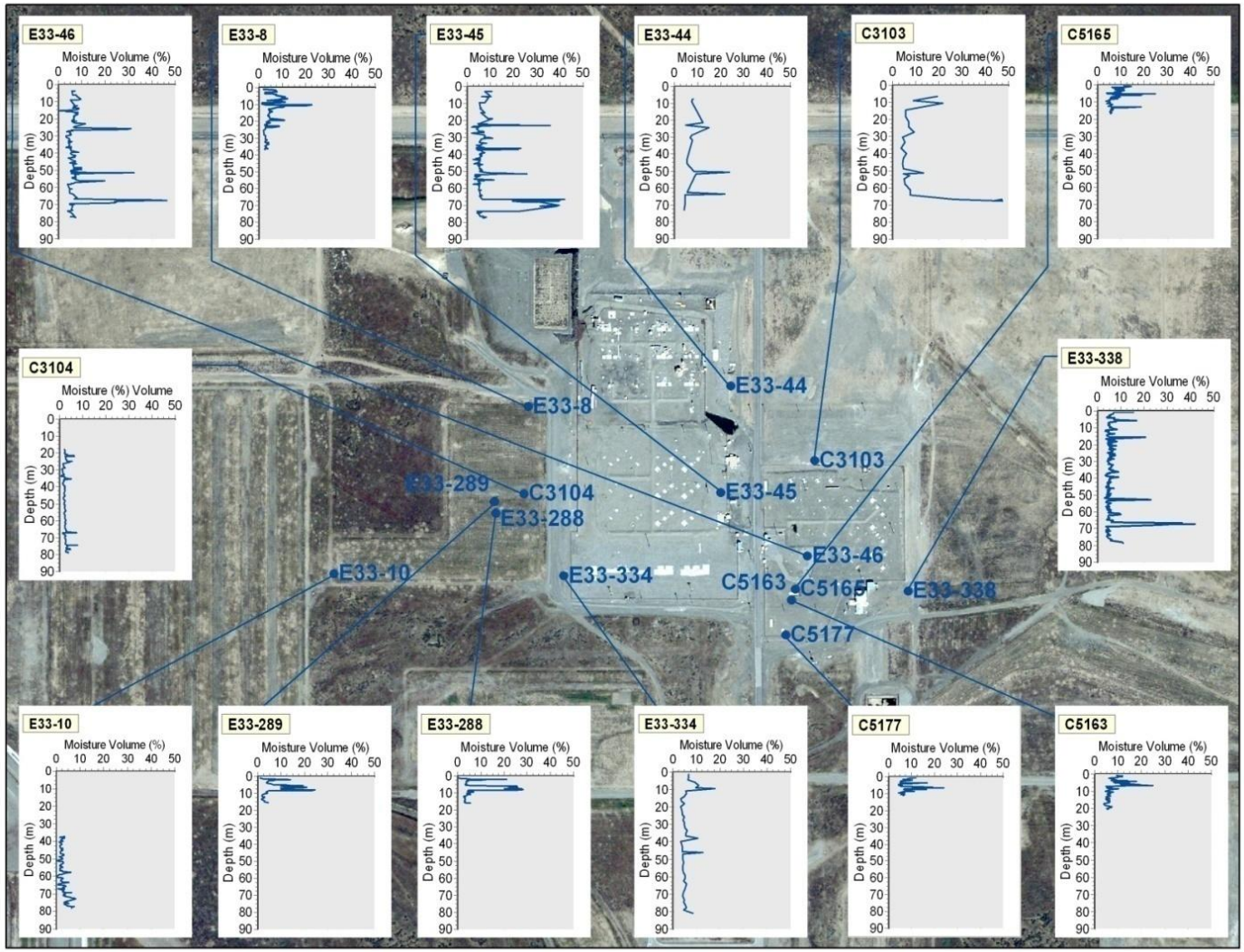

Figure 14. Vertical Distribution of Nitrate (Red Line) and Sulfate (Blue Line) from Select B Complex Monitoring Wells.

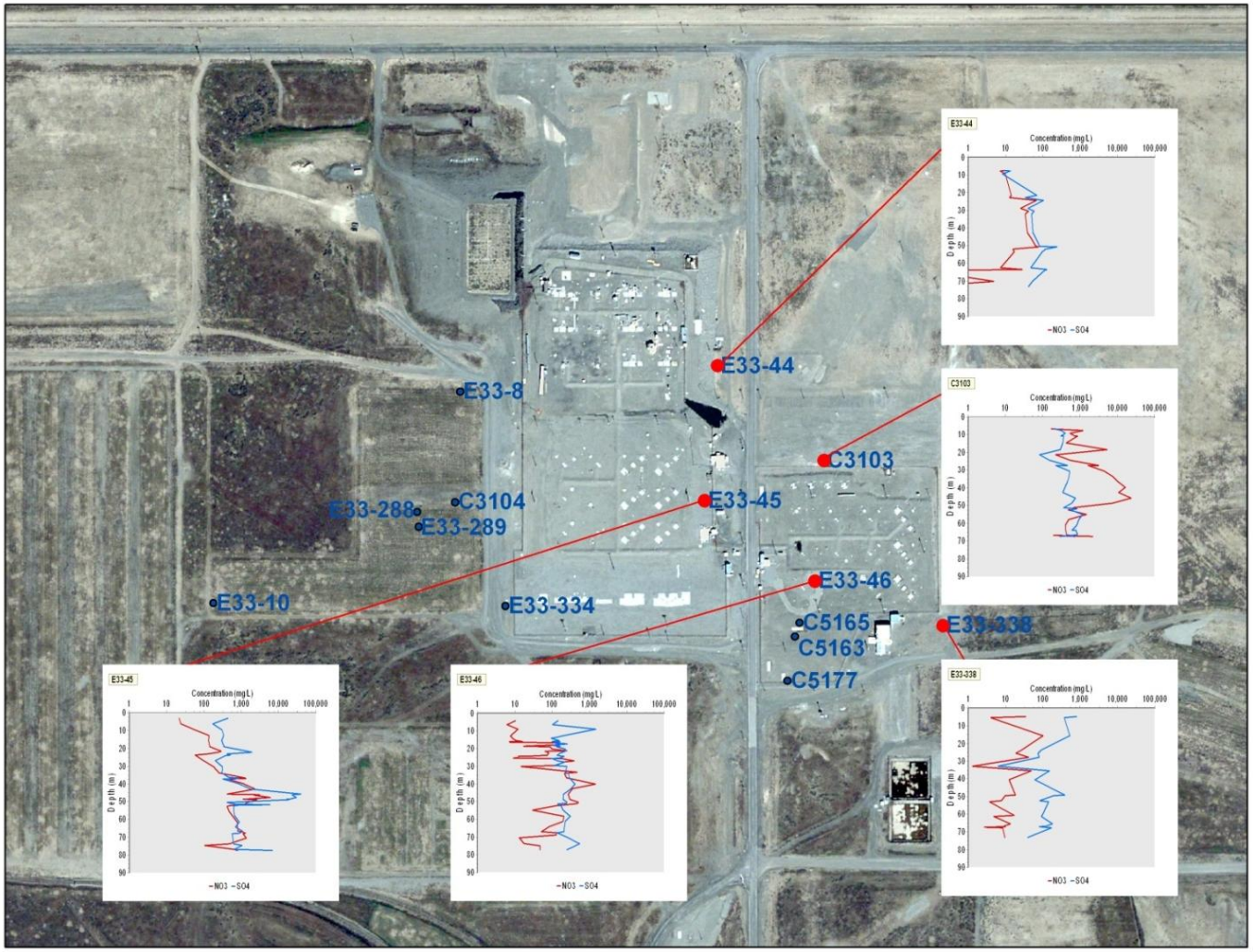

Figure 15. Uranium Plume Distribution in the Unconfined Aquifer Underlying Waste Management Area B-BX-BY in 2000, 2003, 2006, and 2009 (Measured and Contoured Uranium Values, Units µg/L).

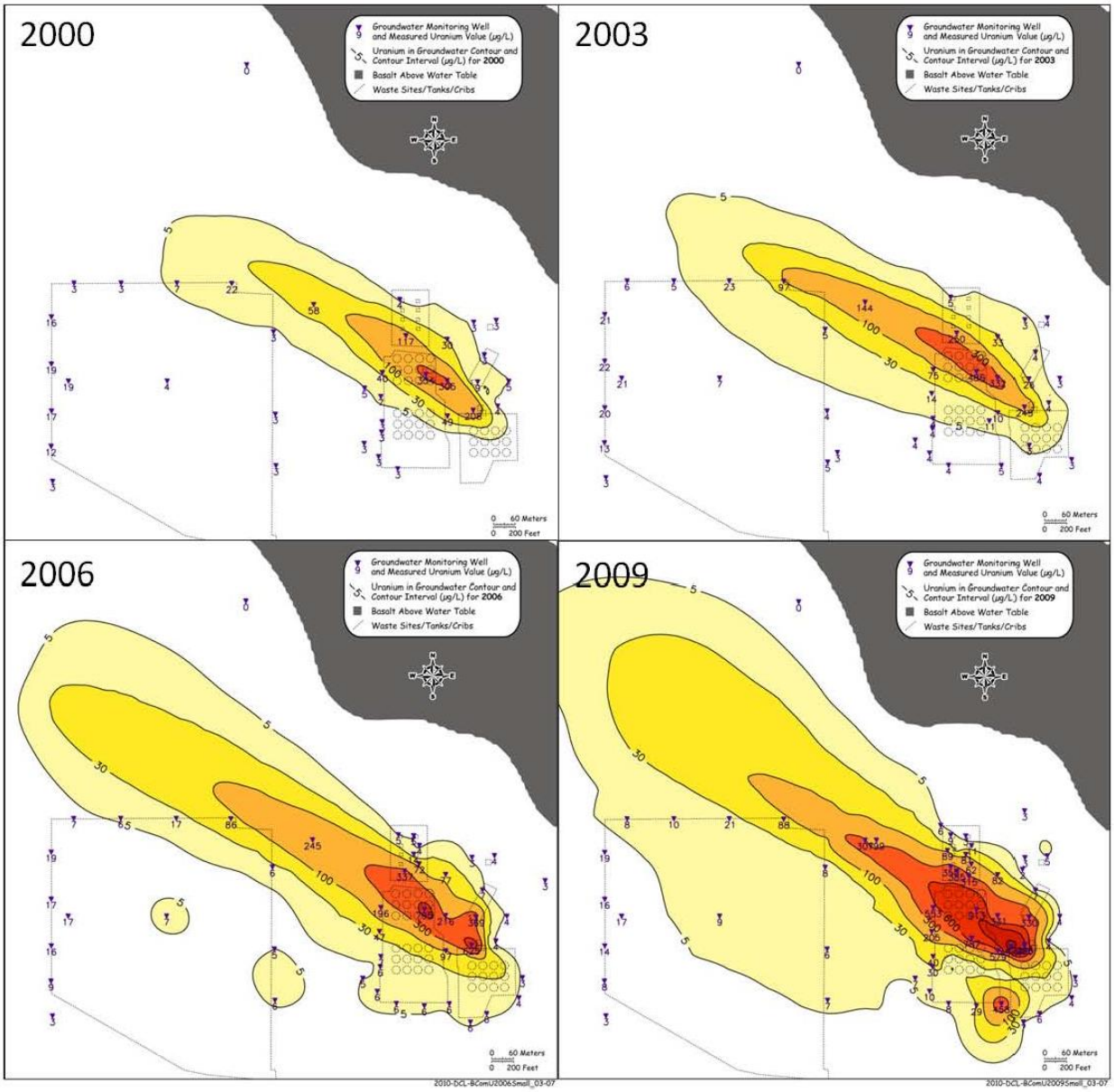

Source: PNNL-19277, 2010, *Conceptual Models for Migration of Key Groundwater Contaminants Through the Vadose Zone and into the Unconfined Aquifer Below the B-Complex*, Pacific Northwest National Laboratory, Richland, Washington.

2.5 RECENT CHARACTERIZATION EFFORTS IN BY TANK FARM

Recent sampling events have taken place (fiscal year 2010) in the southwestern corner or BY tank farm and included eight boreholes: C7811, C7813, C7815, C7817, C7819, C7821, C7823, and C7825. The locations of the boreholes are shown in Figure 16, and cross sections of

volumetric moisture content from neutron logging are shown below the figure. Distinct moisture zones can be seen in the figure, and efforts were made to connect related lithological layers that have high moisture. These high moisture zones are likely attributed to finer grained soil lenses, which could potentially contribute to some amount of lateral migration of leaked waste in the farm. Perched water was identified north of B-farm and southeast of BY-Farm during the installation of well 29-9-E33-345 further attesting to the presence of finer grained soil lenses in the vicinity (PNNL-19277).

Seven of the eight boreholes were outfitted with vertical electrode arrays for SGE imaging. The only borehole without electrodes was C7815. More information regarding the placement of the electrodes is presented in Section 3.0.

Figure 16. Neutron Moisture Content Within the Northwestern Area of the BY Tank Farm.

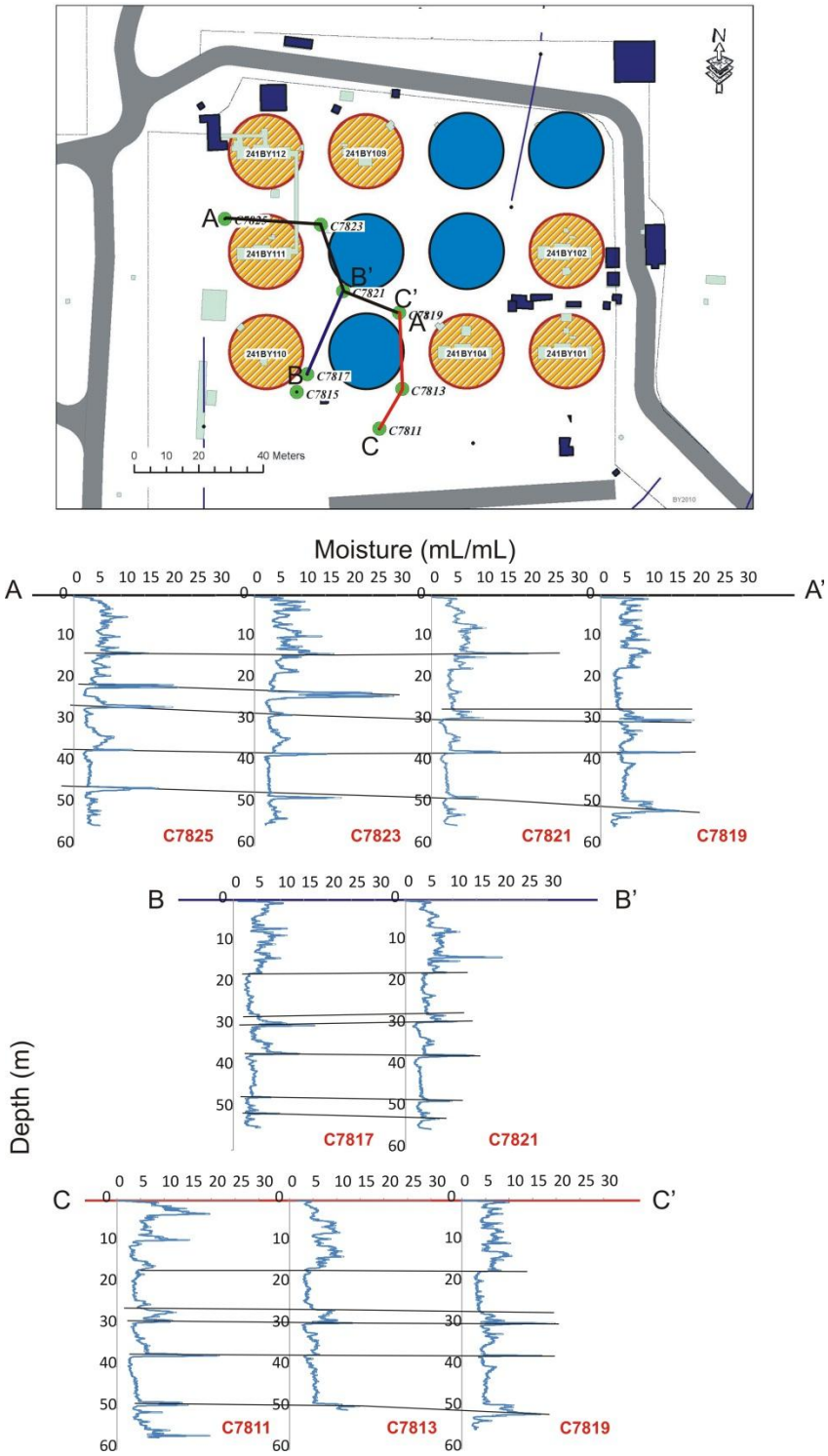

3.0 DATA ACQUISITION AND PROCESSING METHODOLOGY

Data acquisition for a 3D electrical resistivity survey at the BY tank farm began on July 6, 2011 and was completed on July 10, 2011. The geophysical survey was initiated to collect data on surface electrodes, electrode strings buried beneath the surface (i.e., depth electrodes), and wells (i.e., long electrodes). The 3D methodology is in contrast to most previous SGE surveys, where data acquisition was relegated to sets of parallel and orthogonal 2D profiles collected along individual lines, which when grouped together produce a 3D image. A 3D survey is superior to a 2D survey because considerably more data are collected to define the electrical properties of the subsurface. However, 3D surveys usually take longer to acquire and require more resistivity equipment.

Data collection activities, along with the basis and selection of data collection equipment, and data processing are described in the following sections.

3.1 SURVEY DESIGN

In FY2010 an SGE survey was completed in the western side of the BY tank farm (BY West). The current survey (BY East) was focused on the eastern side BY tank farm (BY East), although there were a number of electrodes and wells common to both surveys. In total, 52 surface electrodes, 2 depth electrodes, and 7 wells were shared. Figure 17 highlights the BY West and BY East survey areas.

Figure 17. 2010 (BY West) and 2011 (BY East) BY Tank Farm Electrical Resistivity Survey Areas.

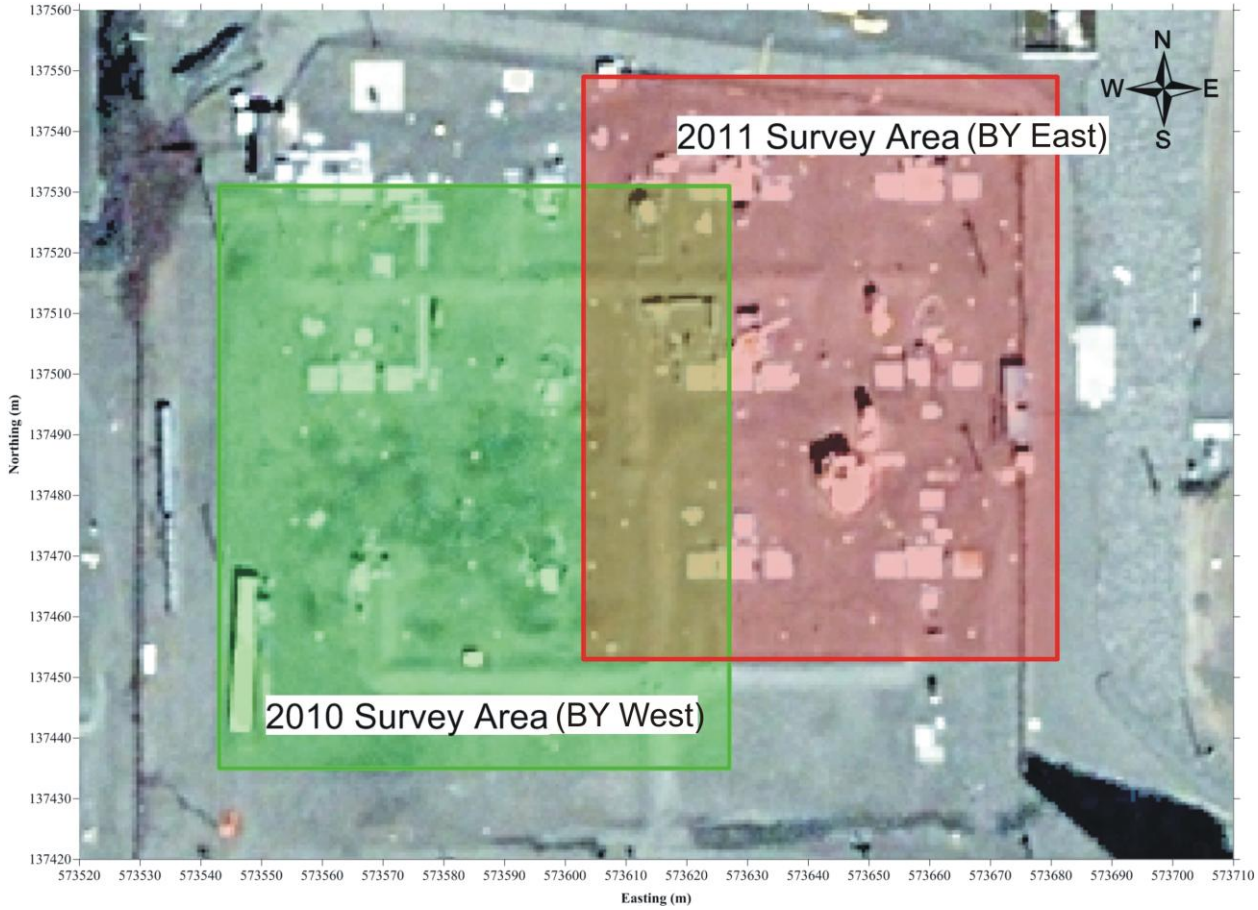

Resistivity data were collected based on a 3D data acquisition method that utilized numerous different electrode arrangements. The surface electrodes were distributed across a uniform grid to optimize the numerical inversion models used in the data analysis and interpretation. The significantly larger amounts of data associated with a 3D survey, relative to a 2D survey, makes an optimized geometry crucial to reduce modeling run times and analysis. For the current BY East tank farm survey, 185 surface electrodes were distributed across a site 72 meters by 90 meters, with electrodes spaced nominally every 6 meters in the east-west and north-south directions. Some positions within this grid were skipped based on proximity to buried near-surface infrastructure or surface obstructions. Infrastructure mapping, using ground penetrating radar, was conducted in 2006 as part of the 2D resistivity mapping of B Complex and is discussed in Appendix D of report RPP-34690, *Surface Geophysical Exploration of the B, BX, and BY Tank Farms at the Hanford Site*.

Further resolution improvements are possible by adding depth electrodes to a surface electrode geometry, whereby electrical current and voltage measurements can be made near or within a target in the subsurface. Depth electrodes have the added benefit of being further from near-surface infrastructure and the associated electrical interference and noise. For the BY east tank farm survey, five new boreholes with nested depth electrodes, labeled C-8131, C-8133,

C-8135, C-8137, and C-8139, were placed opportunistically, that is, in areas devoid of surface infrastructure and in locations to best support geophysical and sampling characterization efforts (RPP-RPT-48253, *Completion Report for 241-BY West Tank Farm Direct Push Characterization*). The existing borehole arrays at C-7813 and C-7819 were also incorporated into this survey (RPP-RPT-49650, *Completion Report for 241-BY East Tank Farm Direct Push Characterization*). The location of the depth electrode strings did not necessarily align to the surface electrode grid. Table 3 displays the locations and depths associated with each depth electrode for the current survey.

Additionally, thirty-three vadose zone wells were used as long electrodes to complement the surface and depth electrode data sets. The well data sets provide a direct comparison to historic BY resistivity data (RPP-34690, *Surface Geophysical Exploration of the B, BX, and BY Tank Farms at the Hanford Site*). Table 4 lists the specific wells used in the survey.

Figure 18. Electrode Layout for the BY East Tank Farm Survey Area.

Source: RPP-RPT-48253, 2010, *Completion Report for 241-BY West Tank Farm Direct Push Characterization*, Revision 0, Washington Rover Protection Solutions, LLC, Richland, Washington.

Source: RPP-RPT-49650, 2011, *Completion Report for 241-BY East Tank Farm Direct Push Characterization*, Revision 0, Washington Rover Protection Solutions, LLC, Richland, Washington.

Table 3. Depth Electrode Locations. (2 sheets)

Probe Hole #	Electrode #	Northing (m)	Easting (m)	Electrode Depth (m)	Electrode Depth (ft)
C-8131	C-8131-27	573680	137478	8.23	27
-	C-8131-47	-	-	14.33	47
-	C-8131-67	-	-	20.42	67
-	C-8131-107	-	-	32.61	107
-	C-8131-127	-	-	38.71	127
-	C-8131-147	-	-	44.81	147
-	C-8131-167	-	-	50.90	167
-	C-8131-186	-	-	56.69	186
C-8133	C-8133-27	573642	137492	8.23	27
-	C-8133-47	-	-	14.33	47
-	C-8133-67	-	-	20.42	67
-	C-8133-87	-	-	26.52	87
-	C-8133-107	-	-	32.61	107
-	C-8133-127	-	-	38.71	127
-	C-8133-147	-	-	44.81	147
-	C-8133-167	-	-	50.90	167
C-8135	C-8135-27	573672	137516	8.23	27
-	C-8135-47	-	-	14.33	47
-	C-8135-67	-	-	20.42	67
-	C-8135-87	-	-	26.52	87
-	C-8135-107	-	-	32.61	107
-	C-8135-127	-	-	38.71	127
-	C-8135-147	-	-	44.81	147
-	C-8135-167	-	-	50.90	167
-	C-8135-186.5	-	-	56.85	186.5
C-8137	C-8137-27	573642	137529	8.23	27
-	C-8137-47	-	-	14.33	47
-	C-8137-67	-	-	20.42	67
-	C-8137-87	-	-	26.52	87
-	C-8137-127	-	-	38.71	127
-	C-8137-147	-	-	44.81	147
-	C-8137-167	-	-	50.90	167
-	C-8137-186	-	-	56.69	186
C-8139	C-8139-27	573680	137540	8.23	27
-	C-8139-47	-	-	14.33	47

Table 3. Depth Electrode Locations. (2 sheets)

Probe Hole #	Electrode #	Northing (m)	Easting (m)	Electrode Depth (m)	Electrode Depth (ft)
-	C-8139-67	-	-	20.42	67
-	C-8139-87	-	-	26.52	87
-	C-8139-107	-	-	32.61	107
-	C-8139-127	-	-	38.71	127
-	C-8139-147	-	-	44.81	147
-	C-8139-167	-	-	50.90	167
-	C-8139-186	-	-	56.69	186
C-7813	C-7813-36	573609	137457	10.97	36
-	C-7813-56	-	-	17.07	56
-	C-7813-76	-	-	23.16	76
-	C-7813-96	-	-	29.26	96
-	C-7813-116	-	-	35.36	116
-	C-7813-136	-	-	41.45	136
-	C-7813-155	-	-	47.24	155
C-7819	C-7819-7	573608	137481	2.13	7
-	C-7819-27	-	-	8.23	27
-	C-7819-47	-	-	14.33	47
-	C-7819-67	-	-	20.42	67
-	C-7819-87	-	-	26.52	87
-	C-7819-107	-	-	32.61	107
-	C-7819-127	-	-	38.71	127
-	C-7819-147	-	-	44.81	147

Source: RPP-RPT-48253, 2010, *Completion Report for 241-BY West Tank Farm Direct Push Characterization*, Revision 0, Washington Rover Protection Solutions, LLC, Richland, Washington.

Source: RPP-RPT-49650, 2011, *Completion Report for 241-BY East Tank Farm Direct Push Characterization*, Revision 0, Washington Rover Protection Solutions, LLC, Richland, Washington.

Table 4. Well Locations.

Well Name	Tank Farm	Easting (m)	Northing (m)	Casing Length (m)
22-00-01	BY	573643	137543	46
22-00-03	BY	573674	137517	46
22-01-01	BY	573668	137478	30
22-01-03	BY	573673	137469	30
22-01-04	BY	573666	137457	30
22-01-07	BY	573650	137459	30
22-01-10	BY	573646	137473	30
22-02-01	BY	573666	137511	30
22-02-02	BY	573673	137504	30
22-02-05	BY	573667	137488	30
22-02-09	BY	573646	137501	30
22-03-04	BY	573671	137524	30
22-03-05	BY	573666	137519	30
22-03-07	BY	573654	137517	30
22-03-08	BY	573648	137521	30
22-03-09	BY	573646	137531	30
22-03-10	BY	573646	137539	30
22-04-01	BY	573635	137480	30
22-04-05	BY	573635	137457	30
22-04-07	BY	573619	137457	30
22-04-09	BY	573615	137471	30
22-04-11	BY	573623	137481	30
22-05-01	BY	573635	137511	30
22-05-05	BY	573635	137488	30
22-05-09	BY	573615	137500	30
22-06-01	BY	573635	137542	30
22-06-05	BY	573635	137519	30
22-06-07	BY	573616	137517	46
22-06-09	BY	573615	137531	30
22-06-11	BY	573620	137542	30
22-08-02	BY	573609	137506	30
22-09-02	BY	573609	137539	30
22-09-05	BY	573608	137523	30

3.2 EQUIPMENT

3.2.1 Electrode and Cable Layout

The first stage of the project assembled all available infrastructure maps for the BY tank farm area. The resulting maps were combined into an AutoCAD® drawing and subsequently used to define the coordinates for electrode placement. The maps containing infrastructure locations, including subsurface pipes/structures and surface structures, were digitized and combined with the electrode locations. Electrode locations were placed to avoid being directly over infrastructure where possible. Electrode placement was limited by a uniform 6-meter grid layout to support data processing procedures. The final electrode layout was then uploaded into a Leica® 1200 Global Positioning System (GPS) which was used to mark electrode locations on the ground surface. The Leica system has sub-centimeter accuracy, assuring the survey geometry is retained.

The electrodes are connected to the resistivity acquisition meter by way of multi-conductor cables and multiplexers. For the BY East survey, a total of three cables were deployed; each cable allowing up to 84 electrodes to be connected. The cables were placed optimally with jumpers connecting the stainless steel probe to the electrode cable. The specific location of the cable was modified to accommodate site infrastructure. Figure 19 shows the electrode cable and surface electrode layout used for this project.

Various “gender” switching cables and connectors were used to tie the three 84 electrode cables into the six 56-electrode switch boxes (multiplexers), manufactured by Advanced Geosciences, Inc. (AGI). The multiplexers provided a 336 electrode capability, of which 185 were used for surface electrodes, 57 for depth electrodes, and 33 wells. A separate patch panel was used to connect between the depth electrodes and the multiplexer.

® AutoCAD is a registered trademark of AutoDesk, Inc.
® Leica is a registered trademark of Leica Technology.

Figure 19. Resistivity Cable and Surface Electrode Layout.

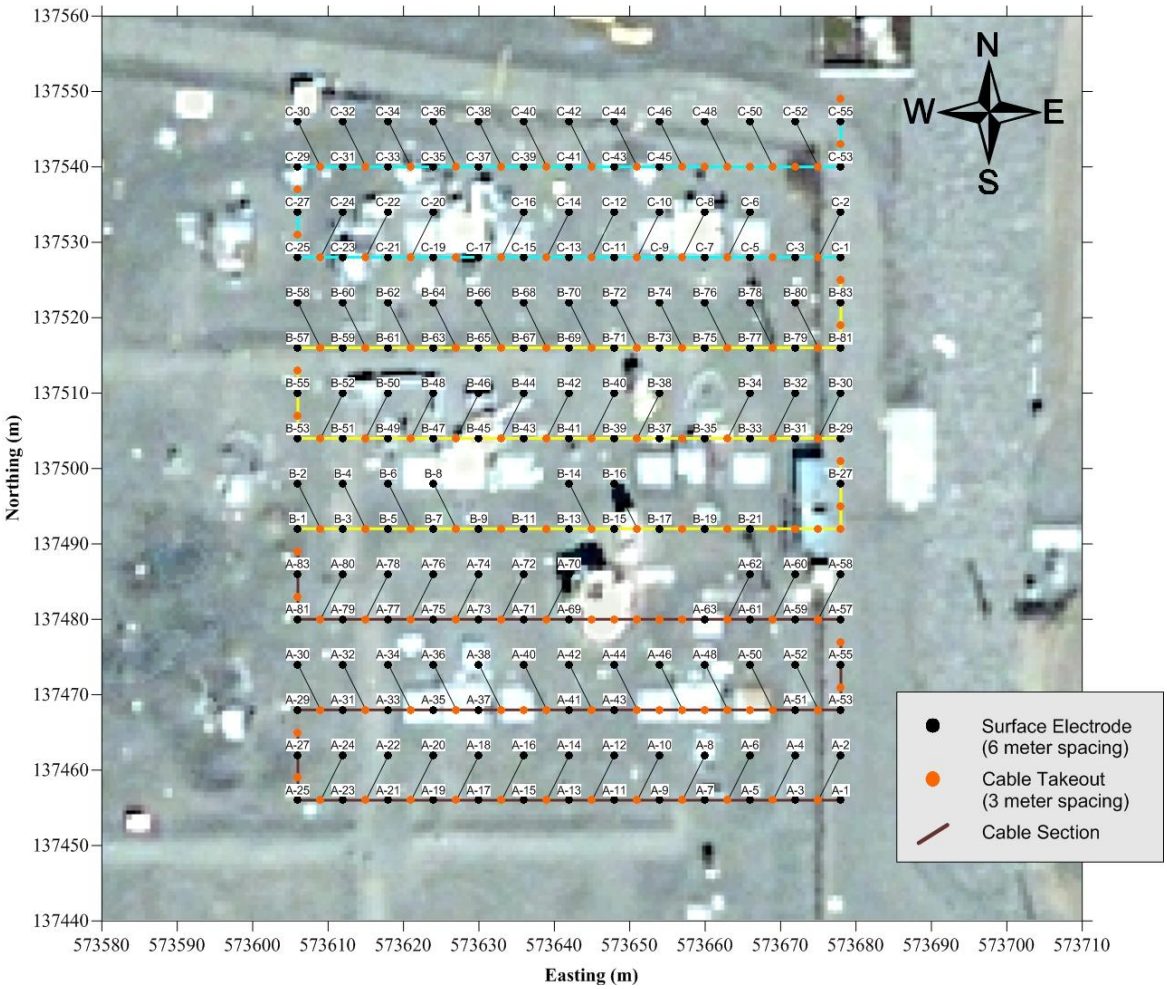

3.2.2 Resistivity Meter

A (SuperSting R8®) resistivity meter, manufactured by AGI, was used for resistivity data acquisition. The meter is capable of full 8-channel acquisition, whereby eight simultaneous measurements of voltage can be made during a single electrical current transmission. The R8 meter has been used for many SGE projects and has proven itself to be reliable for long-term, continuous acquisition campaigns.

Intensive quality assurance was completed before and after the survey to ensure the equipment was functioning appropriately as well as the quality of data was acceptable.
Calibration requirements are described for hardware used to collect geophysical data in CEES-0360, *Surface Geophysical Exploration System Design Description*. As an example, the manufacturer (AGI) of the resistivity data acquisition instrument recommends a yearly calibration of internal calibration resistors. The calibration is performed at the manufacturer's

® SuperSting R8 is a registered trademark of Advanced Geosciences, Inc.

facility and a certificate of calibration is provided. A copy of the calibration documentation, serial numbers, and expiration dates are maintained in project files.

Daily inspection of the receiver calibration was also performed onsite using the manufacturer-supplied calibration resistor test box. The supplied test box is connected to the SuperSting R8 before commencing the daily survey. A specific calibration test firmware is provided within the SuperSting and provides the operator with a pass/fail indication for each of the eight receiver channels. If any of the channels fail, a recalibration or repair is completed.

Some deficiencies with the manufacturer supplied calibration test box were found on previous SGE data collection campaigns. In response, HGI fabricated a purpose-built calibration resistor network test box to further evaluate performance of the SuperSting R8, Switch Boxes and even cable wiring. This test box was used prior, during, and after this survey to ensure data quality.

3.3 ACQUISITION METHODOLOGY

The resistivity data acquisition included a pole-pole array, where one electrode from each of the transmitting and receiving electrode pairs were placed effectively at infinity. Practically, these poles are placed remotely, at least 4 to 5 times the maximum internal electrode distance away from the site in opposite directions. Figure 20 shows the locations of the remotes used in the 2010/2011 SGE campaign, which was different than those used for the 2006 campaign.
The 2011 Stage 2 BY East survey used the same remotes as the 2010 Stage 1 effort. The survey area for 2006 was considerably larger, necessitating the larger remote electrode spacing.

Figure 20. Remote Locations Used for the Pole-Pole Array.

Data collection was initialized on July 6, 2011 and completed July 10, 2011. Data were collected approximately 16 hours a day to minimize impacts to tank farm operations. Continuous data collection was used to minimize the influence of changing moisture conditions over longer periods of time. Personnel were onsite at all times during acquisition to monitor data

collection and to keep the area clear of vehicles and equipment that could damage cables and impact data quality.

Both forward and reverse data sets were collected during data acquisition in order to increase the resolution of the resistivity survey and evaluate data quality. Forward and reverse measurements are acquired by switching the transmitting and receiving electrode pairs to produce a reciprocal dataset. The two sets of data ensured that each electrode pair acted as both transmitter and receiver; both are needed for quality control. The theory of reciprocity implies that a homogeneous earth should allow for consistent measurements in both forward and reverse measurement conditions. Thus, by varying selected reciprocal percent difference thresholds, the ratio between data quality and quantity can be assessed. For this survey effort, data measurements with a relative percent difference greater than 5 percent were considered unacceptable and removed from the dataset before commencing numerical inverse modeling.

3.4 DATA PROCESSING

3.4.1 Data Reduction

All raw data collected at the site were compiled into a relational database. Raw data included both electrical resistivity data and GPS positional data to geo-reference the resistivity data. A set of queries was designed to segregate reciprocal pair data points and assign each data point distinguishing characteristics not retained in the raw SuperSting file. This information included electrode type (surface, depth, well) and a sequential electrode number (as designated in the survey design). Additional data fields were added for the calculated distance between electrodes and percent error between reciprocal data. The data were then exported from the database for graphical filtering and plotting in a spreadsheet.

Four important diagnostic data parameters from the raw data include voltage/current (V/I; resistance), repeat error, reciprocal error, and electrical current output. The repeat error is a calculated percent error between cycled/repeated measurements. A plot of these data can provide information with regards to the statistical variation of the data population.

The process of data editing identifies and eliminates data points, but no data modification (rounding, averaging, smoothing, or splining) is permitted. The rationale is to seek out and remove spurious points that do not conform to the data population or points that violate potential theory. The first step in this editing process was to remove data outside of the statistical population; negative V/I values, noise, high instrument error, low current, low voltage, etc. Figure 21 displays the raw data distribution for the forward and reverse data, while Figure 22 displays the same data sets after filtering. The next step in data reduction was to apply a data quality filter based on reciprocity. All data with a reciprocal percent difference greater than 5 percent was removed.

Table 5 displays the percentages of data retained during steps of the editing process.

Figure 21. Forward and Reverse Data Sets (Raw Data).

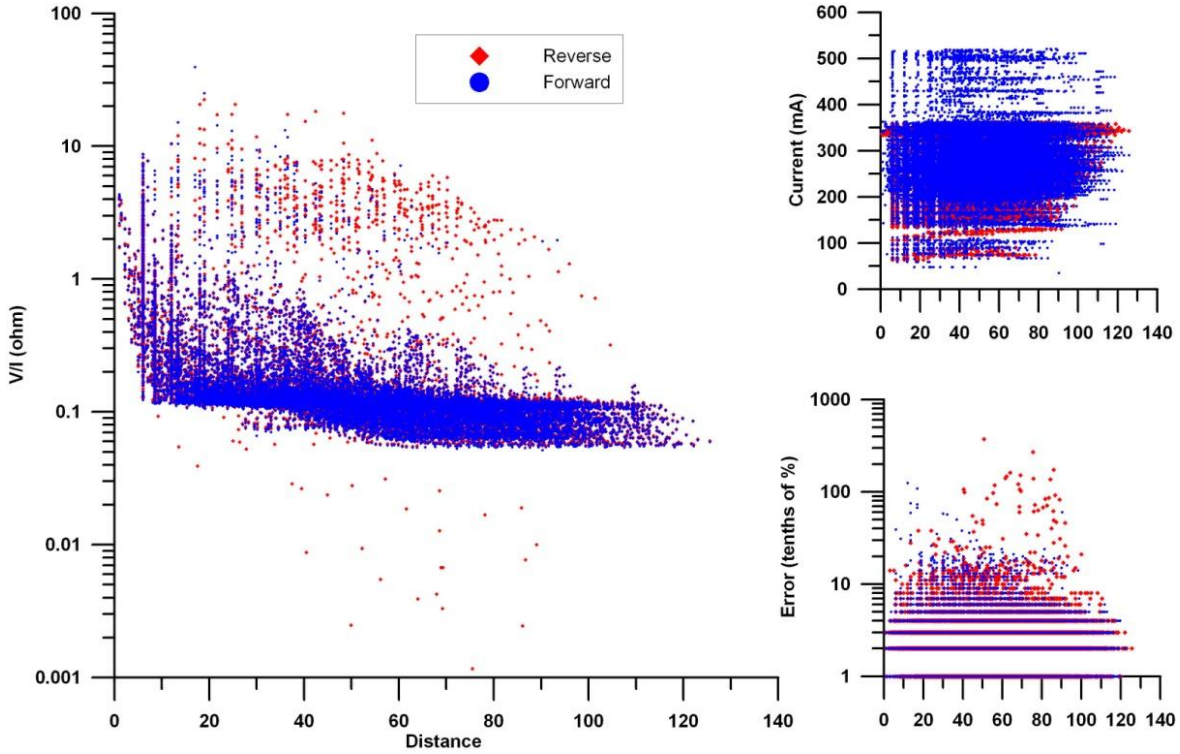

Raw data distribution for (1) V/I (left), (2) Error, and (3) Current (lower right).
All are plotted against the distance between transmitting/receiving electrode pairs.

Figure 22. Forward and Reverse Data Sets after Data Editing.

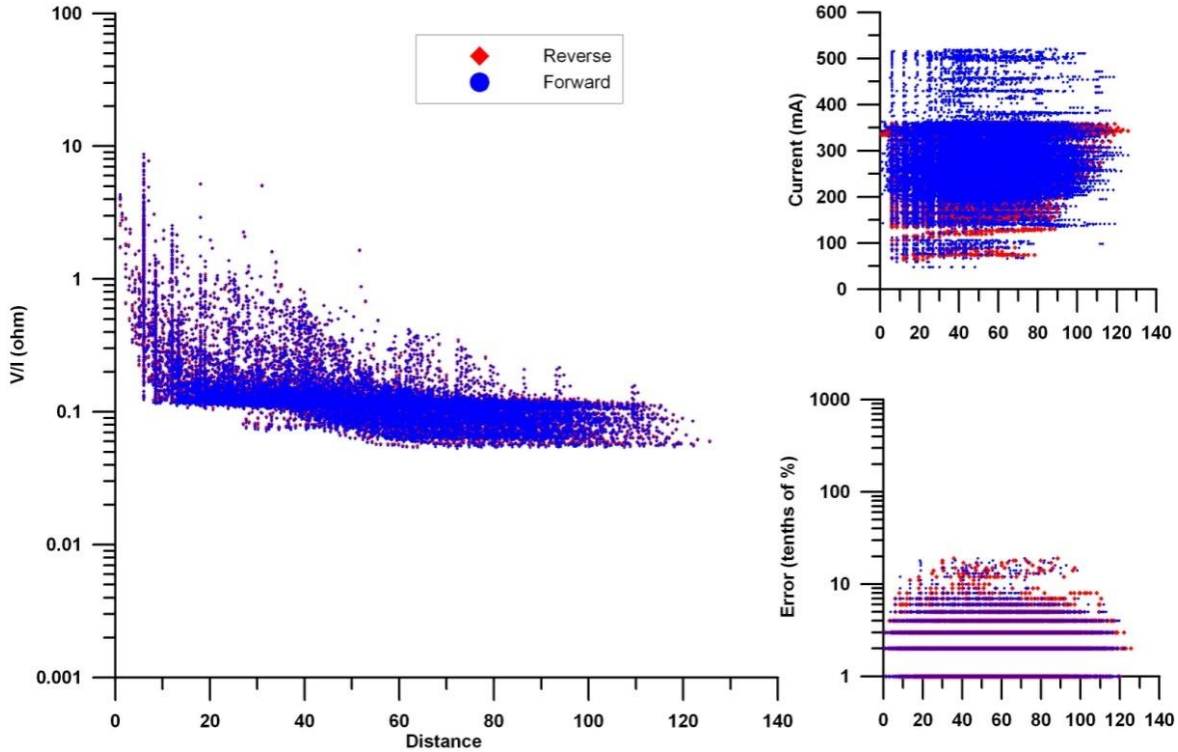

Data distribution after editing for (1) V/I (left), (2) Error, and (3) Current (lower right).
All are plotted against the distance between transmitting/receiving electrode pairs.

Table 5. Number of Data Points Retained During Data Editing Steps.

	Forward	Reverse	Sum	Percent of Total
Total Raw	36,475	37,277	73,752	100
Total Combined Reciprocal	36,391	36,391	72,782	98.7
Total Edited (<5% Reciprocal Error)	35,628	35,628	71,256	96.6

3.4.2 Depth Electrode Performance

Given the low density of depth electrodes, when compared to the hundreds of electrodes on the surface, it is important to have maximum performance from all depth electrodes. A statistical performance analysis is performed on all depth electrode data to assure only high quality data are included in the numerical inversion modeling. Tables 6 and 7 list the construction and completion details for the depth electrodes.

Table 6. Construction Details for BY East Depth Electrodes.

Electrode Name	***C8131***	***C8133***	***C8135***	***C8137***	***C8139***
Construction Type	Multi-Probe	Multi-Probe	Multi-Probe	Multi-Probe	Multi-Probe
Date of Construction	12/10	12/10	12/10	12/10	12/10
Depth of Probes (ft)	27, 47, 67, 107, 127, 147, 167, 186	27, 47, 67, 87, 107, 127, 147, 167	27, 47, 67, 87, 107, 127, 147, 167, 187	27, 47, 67, 87, 127, 147, 167, 186	27, 47, 67, 87, 107, 127, 147, 167, 186
Construction Details	Stainless steel braids encircling the main cable and exposed at selected depths along the electrode string. An old WRPS rod electrode was used at the bottom of the string.	Stainless steel braids encircling the main cable and exposed at selected depths along the electrode string. An old WRPS rod electrode was used at the bottom of the string.	Stainless steel braids encircling the main cable and exposed at selected depths along the electrode string. An old WRPS rod electrode was used at the bottom of the string.	Stainless steel braids encircling the main cable and exposed at selected depths along the electrode string. An old WRPS rod electrode was used at the bottom of the string.	Stainless steel braids encircling the main cable and exposed at selected depths along the electrode string. An old WRPS rod electrode was used at the bottom of the string.
Fill Material	Sand (20-40) and diatomite surround moisture probe, water added through tremie. Fill of bentonite, sand and diatomaceous earth.	Sand (20-40) and diatomite surround moisture probe, water added through tremie. Fill of bentonite, sand and diatomaceous earth.	Sand (20-40) and diatomite surround moisture probe, water added through tremie. Fill of bentonite, sand and diatomaceous earth.	Sand (20-40) and diatomite surround moisture probe, water added through tremie. Fill of bentonite, sand and diatomaceous earth.	Sand (20-40) and diatomite surround moisture probe, water added through tremie. Fill of bentonite, sand and diatomaceous earth.

Source: RPP-RPT-49650, 2011, *Completion Report for 241-BY East Tank Farm Direct Push Characterization*, Revision 0, Washington Rover Protection Solutions, LLC, Richland, Washington.

Table 7. Construction Details for BY Depth Electrodes.

Electrode Name	*C7813*	*C7819*
Construction Type	Multi-Probe	Multi-Probe
Date of Construction	7/10	7/10
Depth of Probes (feet)	36, 56, 76, 96, 136, 155	7, 47, 67, 84, 107, 127, 147
Construction Details	Stainless steel braids encircling the main cable and exposed at selected depths along the electrode string. An old WRPS rod electrode was used at the bottom of the string.	Stainless steel braids encircling the main cable and exposed at selected depths along the electrode string. An old WRPS rod electrode was used at the bottom of the string.
Fill Material	Sand (20-40) and diatomite surround moisture probe, water added through tremie. Fill of bentonite, sand and diatomaceous earth.	Sand (20-40) and diatomite surround moisture probe, water added through tremie. Fill of bentonite, sand and diatomaceous earth.

Source: RPP-RPT-48253, 2010, *Completion Report for 241-BY West Tank Farm Direct Push Characterization*, Revision 0, Washington Rover Protection Solutions, LLC, Richland, Washington.

The performance from the different types of electrodes can be explored through output current, repeat error, reciprocal error, and percent negative V/I values. Table 8 lists the summary statistics from each of these electrodes. All of the depth electrodes displayed positive and significant transmitting currents indicating good contact between the electrodes and surrounding material. Both the average repeat error and average reciprocal error for all electrodes are quite low indicating very consistent measurements. The percentage of negative V/I values was negligible for all depth electrodes.

Table 8. Depth Electrode Statistics for BY East. (3 sheets)

Electrode Name	Location	Probe Depths (ft)	Moisture Content (vf%)	Average Transmitting Current (mA)	Average Repeat Error (as Rx) (%)	Percentage of Negative V/I Values	Average Reciprocal Error (% difference)	Percentage of Data Below 5% Error Cutoff
C8131	BY-Farm	27	10	407	0.2	0	1	100
		47	5	410	0.2	0	1	100
		67	4	376	0.2	0	1	100
		107	5	383	0.1	0	1	100
		127	3	297	0.1	0	1	100
		147	3	358	0.1	0	2	99

Table 8. Depth Electrode Statistics for BY East. (3 sheets)

Electrode Name	Location	Probe Depths (ft)	Moisture Content (vf%)	Average Transmitting Current (mA)	Average Repeat Error (as Rx) (%)	Percentage of Negative V/I Values	Average Reciprocal Error (% difference)	Percentage of Data Below 5% Error Cutoff
		167	3	351	0.2	0	2	99
		186	24	431	0.1	0	4	99
C8133	BY-Farm	27	8	398	0.2	0	1	99
		47	8	430	0.2	0	1	100
		67	3	359	0.2	0	1	100
		87	4	424	0.1	0	2	99
		107	4	426	0.2	0	1	99
		127	5	414	0.1	0	1	100
		147	5	419	0.1	0	1	100
		167	11	392	0.1	0	1	100
C8135	BY-Farm	27	7	395	0.2	0	1	99
		47	10	413	0.2	0	1	100
		67	3	410	0.2	0	1	99
		87	4	364	0.2	0	1	100
		107	3	364	0.2	0	1	99
		127	4	365	0.2	0	1	100
		147	5	379	0.1	0	1	99
		167	7	387	0.1	0	2	98
		187	38	399	0.1	0	1	99
C8137	BY-Farm	27	5	389	0.2	0	1	100
		47	18	393	0.2	0	1	100
		67	4	348	0.1	0	1	100
		87	5	379	0.1	0	1	100
		127	4	340	0.1	0	1	99
		147	5	357	0.1	0	1	99
		167	9	401	0.1	0	1	99
		186	6	361	0.1	0	1	99
C8139	BY-Farm	27	5	368	0.2	0	1	99
		47	8	358	0.2	0	1	100
		67	5	360	0.2	0	1	100
		87	5	361	0.2	0	1	100
		107	4	332	0.1	0	1	99
		127	3	340	0.1	0	1	99
		147	3	345	0.1	0	1	99

Table 8. Depth Electrode Statistics for BY East. (3 sheets)

Electrode Name	Location	Probe Depths (ft)	Moisture Content (vf%)	Average Transmitting Current (mA)	Average Repeat Error (as Rx) (%)	Percentage of Negative V/I Values	Average Reciprocal Error (% difference)	Percentage of Data Below 5% Error Cutoff
		167	3	353	0.2	0	1	99
		186	4	365	0.1	0	2	99
C7813	BY-Farm	36	6	388	0.2	0	1	97
		56	4	381	0.3	0	1	99
		76	4	355	0.2	0	1	98
		96	6	374	0.2	0	1	99
		116	6	368	0.2	0	1	99
		136	5	362	0.2	0	1	98
		155	6	366	0.1	0	1	100
C7819	BY-Farm	7	8	356	0.2	0	1	100
		27	7	357	0.2	0	1	99
		47	7	351	0.2	0	1	99
		67	3	347	0.1	0	1	99
		87	4	350	0.2	0	1	100
		107	6	345	0.2	0	1	100
		127	4	344	0.2	0	1	100
		147	5	339	0.1	0	1	100

Source: RPP-RPT-48253, 2010, *Completion Report for 241-BY West Tank Farm Direct Push Characterization*, Revision 0, Washington Rover Protection Solutions, LLC, Richland, Washington.

Source: RPP-RPT-49650, 2011, *Completion Report for 241-BY East Tank Farm Direct Push Characterization*, Revision 0, Washington Rover Protection Solutions, LLC, Richland, Washington.

A performance measure can be computed for each individual depth electrode by summing the number of times each electrode passes the cut-off measure for the four statistics highlighted above in Table 8. Figure 23 shows the performance measure for all of the electrodes, which can take on values of {0, 1, 2, 3, 4}. It would be reasonable to assess good performance with a 3 or 4, marginal performance with a 2, and poor performance with a 0 or 1. For this survey the depth electrodes performed extremely well, with all receiving an assessment value of 4.

Figure 23. Performance Measure for Each of the Depth Electrodes.

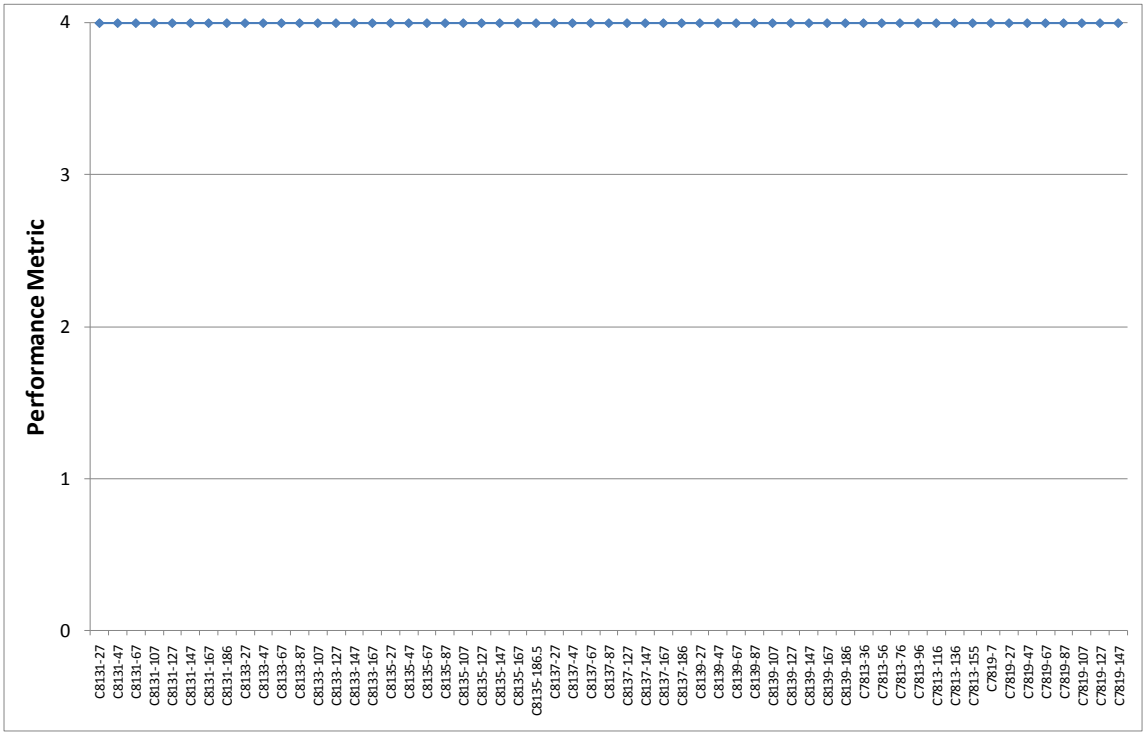

NOTE: Performance of 0 or 1 = Poor, Performance of 2 = Marginal, and Performance of 3 or 4 = Good

3.4.3 Time Lapse Performance of Well-To-Well Data

The re-evaluation of well (long electrodes) data for well-to-well (WTW) acquisition between 2006 and 2011 offers an opportunity to understand the temporal behavior of the waste plumes in the southwestern BY tank farm. Unfortunately, the comparison cannot be directly applied as the remote locations for each survey were different (see Figure 20). The remotes for the 2011 survey were closer to the BY tank farm, thereby changing the electrical field compared to the 2006 survey. This change would be unrelated to any changes occurring in the subsurface waste plumes. To demonstrate, Figure 24 shows the 2006 and 2011 WTW transfer resistance data. The 2011 data at larger distances appear to be generally higher than 2006, whereas the smaller distances appear to be similar.

Figure 24. Transfer Resistance Comparison for 2006 and 2011 WTW Data.

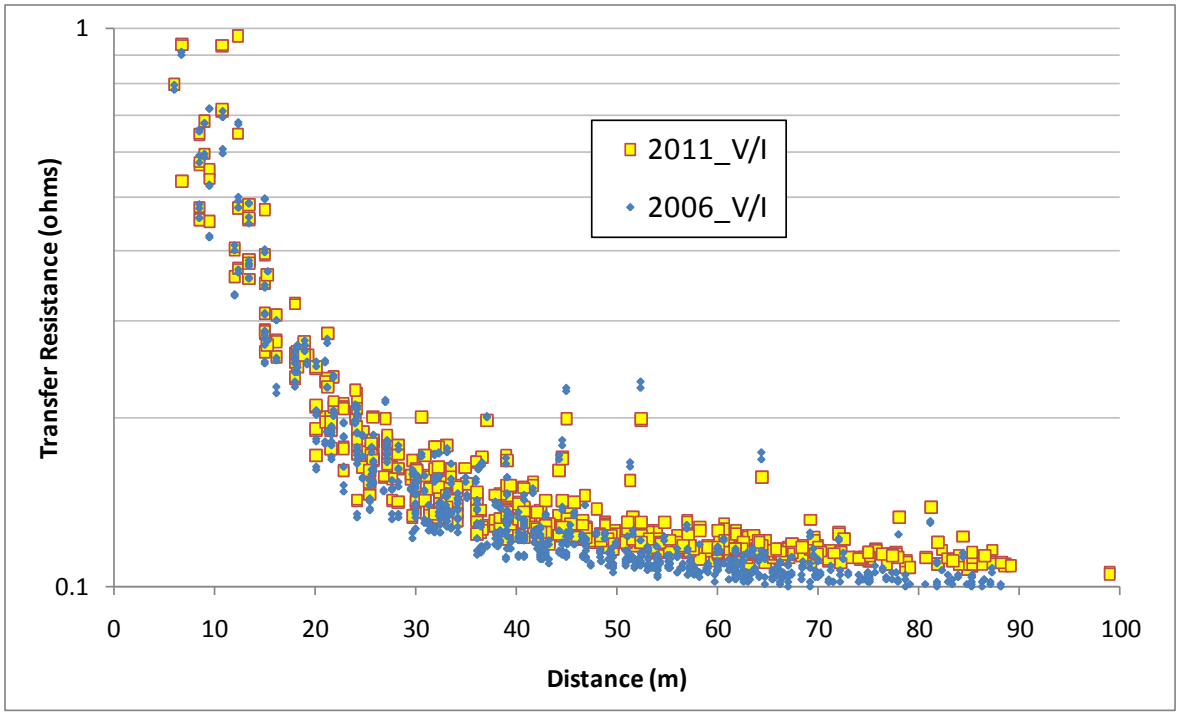

3.4.4 3D Inverse Modeling

Popular use of the RES3DINV series of resistivity inversion codes has led both professional and academic users to regard these codes as industry standard software. The BY East tank farm modeling effort used RES3DINVx64, a 64-bit multi-threaded version developed specifically for a large number of electrodes.

In general, inverse modeling can be summarized in the following five steps.

1. The study site's voltage data has been measured and is discretized into grid nodes using a finite difference or finite element mesh. The meshing parameters used in either case, to design the computational grids, are dependent on electrode spacing used in site-specific data acquisition.
2. The inversion will set out to estimate the true resistivity at every grid node. An initial estimate of the subsurface properties is made based on the literal translation of the pseudo-section to a true resistivity, a constant value, or some other distribution from *a-priori* information. A forward model run with these initial estimates is made to obtain the distribution of voltages in the subsurface. The root-mean-square (RMS) error is calculated between the measured voltage and the calculated voltage resulting from the forward run.
3. Based on the degree of model fit to field measurements, the initial estimate of resistivity is changed to improve the overall model fit and the forward model with the updated estimates is rerun. The iterative method linearizes a highly nonlinear problem using Newton's method. Using this method, the inverse modeling code essentially solves the linearized problem to obtain the change in modeled resistivity (Δm) for the next iteration.
4. The resistivity model is updated using the general formula $m_{i+1} = m_i + \Delta m$, where $_{mi+1}$ is the resistivity in a model cell at the next iteration, and m_i is the current value.
5. Steps 3 and 4 are repeated until the RMS error change between successive iterations reaches an acceptable level.

4.0 MODELING RESULTS

Upon completion of data editing, measured apparent resistivity data from the BY tank farm site were inverse modeled using the RES3DINVx64 software package. For specific details of the SGE resistivity method and theoretical basis applied to inverse modeling, the reader is referred to discussions provided in RPP-34690.

To accomplish the 3D inversion, every surface, depth, and long electrode were geo-referenced (using the Washington State Plane – Meters coordinate system) to allow absolute placement of an electrode within the inversion algorithm. The model was then run with a set of input parameters that have been demonstrated to work well in tank farm environments.
After inversion, the final 3D inversion results were interpolated to a regular grid and visualized

using the RockWorks® visualization software package and Surfer® surface contouring package. The visualization allows discrimination of low resistivity targets that could be associated with increased moisture, increased ionic strength of the pore water, infrastructure, or a combination of these items.

Two sets of model results are presented below that include 1) using point electrodes on the surface and within boreholes, and 2) long electrodes in a WTW inversion.

4.1 POINT ELECTRODE MODELING

Point electrode data from the Stage 1 and 2 (2010 and 2011 respectively) efforts for the BY tank farm surveys were combined for the current numerical inverse modeling. The initial starting points for the modeling initially included measurements on 212 surface electrodes and 53 depth electrodes for BY-West (Stage 1) and 185 surface electrodes and 57 depth electrodes for BY-East (Stage 2). However, not all of these data were of acceptable quality and some data and entire electrodes were dropped from the model data set. Typically to create the final dataset for inversion, two types of data reduction occurred between the data acquisition and final plotting phases. First, data quality was inspected to eliminate unacceptable data that may have resulted from instrumentation error or electrical interference. High data misfit with respect to neighboring points is also evaluated. The process of removing spurious data points is referred to as editing and is performed prior to the first inversion run. Second, data were filtered after each inverse model was completed to remove data points that contributed to a high model RMS error. This process is referred to as a filter run, and the objective of a filter run was to get the final RMS to an acceptable level, usually below 10 percent. Each trial model run was assigned a model number which designated a specific data set or set of modeling parameters and each filter run was assigned a number. An example label for a model with a filter run is “Model_001i.”

The initial model for point electrode data focused on the 3D data set using only the highest quality measured point electrode resistivity data, with no long electrodes. The high quality dataset for inversion was obtained by removing those data with repeat errors greater than 2 percent, reciprocal errors greater than 5 percent, and anomalously low current and resistance (V/I) values. After noisy data removal from the BY-West and BY-East surveys, 58,495 measurements remained for inclusion in the model, approximately 95% of the original data. Data quality was such that the model chosen as our final version did not require any filter runs. Table 9 lists the statistics for the final model.

Table 9. Inverse Modeling Data Statistics.

Model	Surface to Surface	Depth to Surface	Depth to Depth	Sum
Data file (BY3D_043)	37,532	18,753	2,210	58,495

A model mesh was created, as with any numerical modeling, whereby the subsurface was discretized into cells and nodes. The equations that describe the potential field during electrical current transmission are then solved at every node, with the appropriate boundary conditions. The RES3DINVx64 software automatically generates the model mesh for this forward model

® RockWorks is a registered trademark of Rockware, Inc.
® Surfer is a registered trademark of Golden Software, Inc.

calculation by placing grid lines at the intersection of electrodes. Additional requirements of the numerical model include explicitly assigning every block an initial resistivity value and every node a current source (if any).

For the inverse model calculations, where the resistivity values are changed in the model domain until the measured and modeled voltages are nearly equal, a separate model mesh was created that did not align with the forward model mesh. The arbitrary gridding for the inverse model mesh prevented the creation of very small cells due to the depth electrode locations not being aligned to the surface electrode grid. A 6 by 6 meter grid cell was selected for the inverse model (Figure 25), which created 23 cells in the x-direction and 19 cells in the y-direction. In some inverse model cells up to two electrodes would be placed. There are a number of cells which contain no electrodes within the model grid, either due to the differing survey geometry between the Stage 1 and Stage 2 layout or infrastructure affecting surface electrode placement. For the z-direction, 28 layers were used to accommodate all of the unique depth positions for the depth electrodes. The model mesh extended to a depth of 56 meters below ground surface.

Figure 25. Size And Position of the Inverse Model Grid Used To Model the BY3D Point Electrode Data.

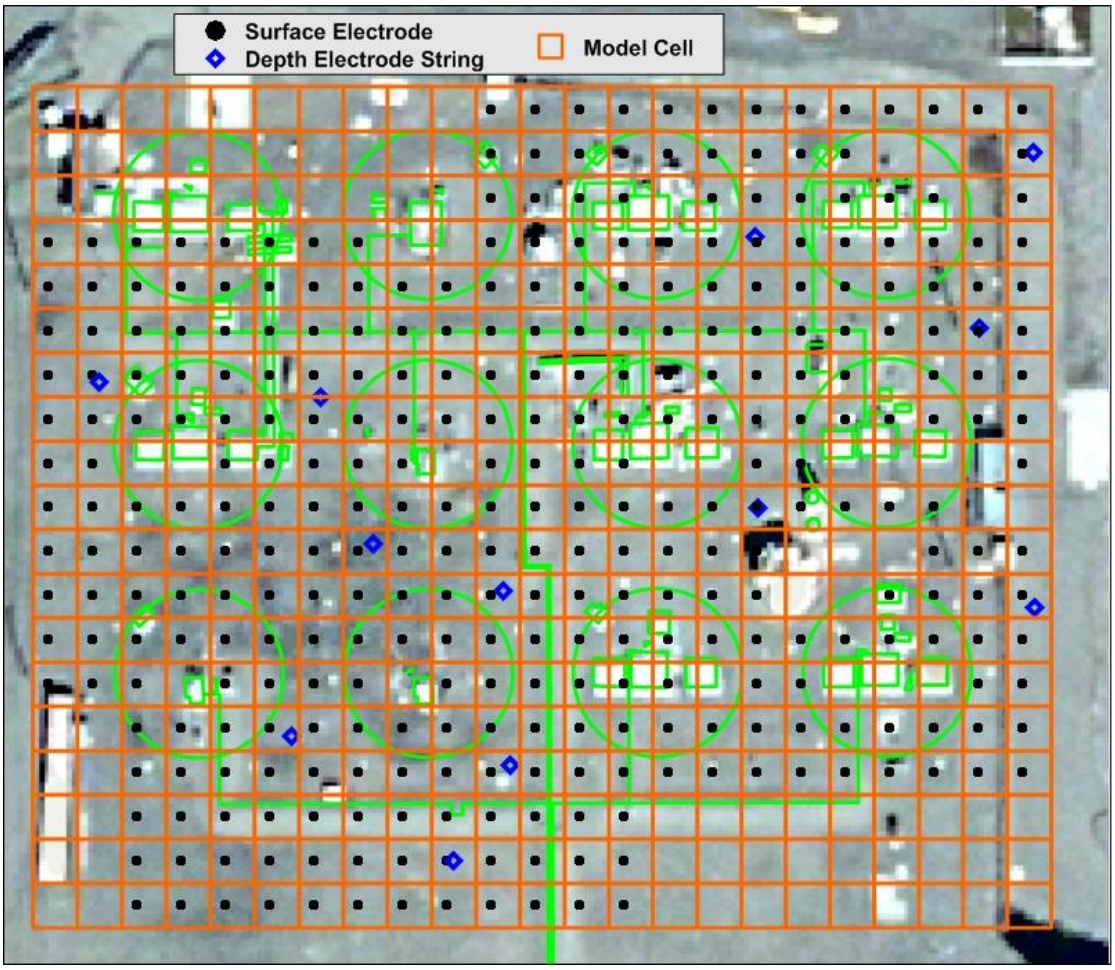

The locations of the storage tanks within the BY tank farm were incorporated into the inverse model input file as *a priori* information, due to their known conductive effects. The storage

tanks, with the exception of BY-109 and BY-112, were approximated by rectilinear blocks of dimensions 17 by 17 meters, extending between a depth of 2.5 and 14 meters beneath the surface. Each block was assigned a resistivity value of 0.1 ohm-m. Storage tanks BY-109 and BY-112 were approximated using the same properties, but the spatial dimensions were changed to 17 by 4 meters. Figure 26 displays the *a priori* blocks added to the model (It should be noted that the depth electrodes labeled underperforming in this figure originate from the 2010 - BY West survey installation).

Figure 26. *A Priori* Model Blocks Added to the Inverse Modeling Domain (Isometric View From The Southwest).

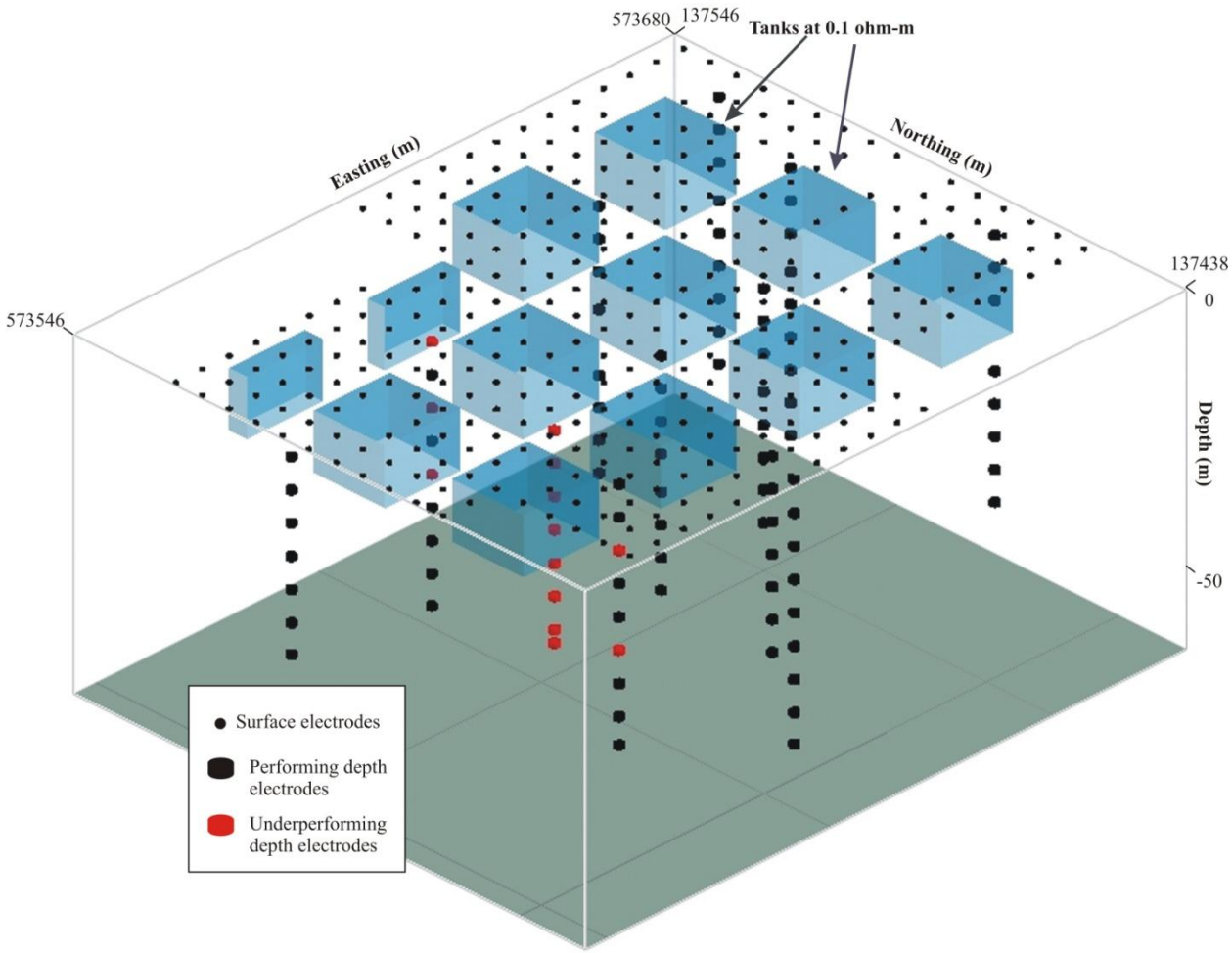

The results of the inverse modeling are displayed in Figure 27. The figure was constructed from the output file for the second iteration of the model run (with a final root mean square error of 10.18 %) and displays slices at select depths within the model domain. The depths are indicated in the lower left corner of each subplot within the mosaic of different slices. Those layers with *a priori* tank information include a black outline indicating the modeled position of the tanks.

Upon entering *a priori* information in the RES3DINVx64 software, the user is given the option for stating the confidence of the chosen resistivity value given to the model to account for the presence of the storage tanks (confidence level of 1 - 10). A low value is indicative of low confidence, and allows the model to change *a priori* information to fit with the measured data. A high confidence would not allow the model to change the *a priori* information. For this model, a confidence value of 2 was selected, thereby giving the model some flexibility to change the exact values of the tanks to some degree. In addition, the confidence value of 2 allows flexibility in the final overall shape and volume of the *a priori* tanks. Furthermore, the true outlines of the tanks are traced by black and red circles (the latter to denote tanks that are classified as historically leaking tanks) and pipelines are traced in green to show their effects on the final resistivity distribution.

Within Figure 27, the slice at 4 meters, just below the level of the top of the storage tanks, displays a resistive background with conductive tanks, and no signs of the piping infrastructure. The footprint of the tanks in the inverse model results are slightly smaller than that initially modeled in the input file, but they all appear to be consistent in size and shape. A slightly more conductive feature is observed located between storage tanks BY-101 and BY-102. This is probably an artifact of the modeling induced by the lack of surface electrode coverage in this region due to surface infrastructure obstructions.

The slice at 7 meters is about midway between the top and bottom of the storage tanks; the footprint of the storage tanks in the inverse model now agree well with the a priori information included in the input file. In this slice, we see that, with the exception of storage tank BY-110, the regions between the storage tanks are becoming more conductive. The most significant changes are observed in the regions between storage tanks BY-101 and BY-102; BY-102 and BY-103; and to the northeast of storage tank BY-108. This trend continues in the depth slices at 9.5, 12, 13.5, and 15.5 meters. The region around storage tank BY-110 becomes conductive in the depth slices at 12, 13.5, and 15.5 meters. Regions of enhanced conductivity are located between storage tanks BY-107 and BY-108; BY-102 and BY-103; and to the north of storage tank BY-108 for the depth slice at 9.5 meters. These enhanced regions remain in the depth slices at 12 and 13.5 meters, while the region to the southwest of borehole C7821 also becomes more conductive in these slices. In the depth slice at 15.5 meters the effects of the storage tanks in the modeled resistivity are gone, but the majority of the model domain remains conductive. The conductive region to the southwest of borehole C7821 remains dominant, while the model regions around storage tanks BY-101, BY-102, and BY-106 are becoming resistive again. The majority of the model domain is more resistive in the depth slice at 18 meters, with only the region surrounding storage tank BY-108 and to the southwest of borehole C7821 displaying lower resistivity values. In the depth slices below 18 meters, the domain is again resistive indicating that the waste plumes from past spills likely reside within the top 18 meters of the BY tank farm.

The main targets for this modeling effort are located in the region of storage tank BY-108, between storage tanks BY-102 and BY-103, and in the region of and to the southwest of borehole C7821. The target around storage tank BY-108 appears to extend to the north and northwest of the tank in the near-surface depth slices (between 4 and 7 meters). Deeper depth slices display a target between this storage tank and storage tank BY-107, which extends to the east towards storage

tanks BY-104 and BY-105. The second target between storage tanks BY-102 and BY-103 displays low resistivity values between 7 and 15.5 meters beneath the surface.

The target around borehole C7821 is a smaller feature that was not explicitly highlighted in the WTW inversion model. The source of this target is unknown. Figure 16 shows the moisture logs from the boreholes in proximity to C7821; there does not appear to be an explicit moisture anomaly localized at C7821 causing the target. Gamma logging data, and in particular the Cs-137 logging, shows high values from C7821 in the top 10 to 11 meters of soil (RPP-RPT-48253). In addition, C7819 displays an elevated gamma signature, with the remaining boreholes relatively low in gamma signature. Although not directly related to the resistivity data, the gamma logging can qualitatively indicate regions of past releases for ionic constituents.

Figure 27. Plan View Depth Slices of Calculated Resistivity for Point Electrode Dataset. (2 sheets)

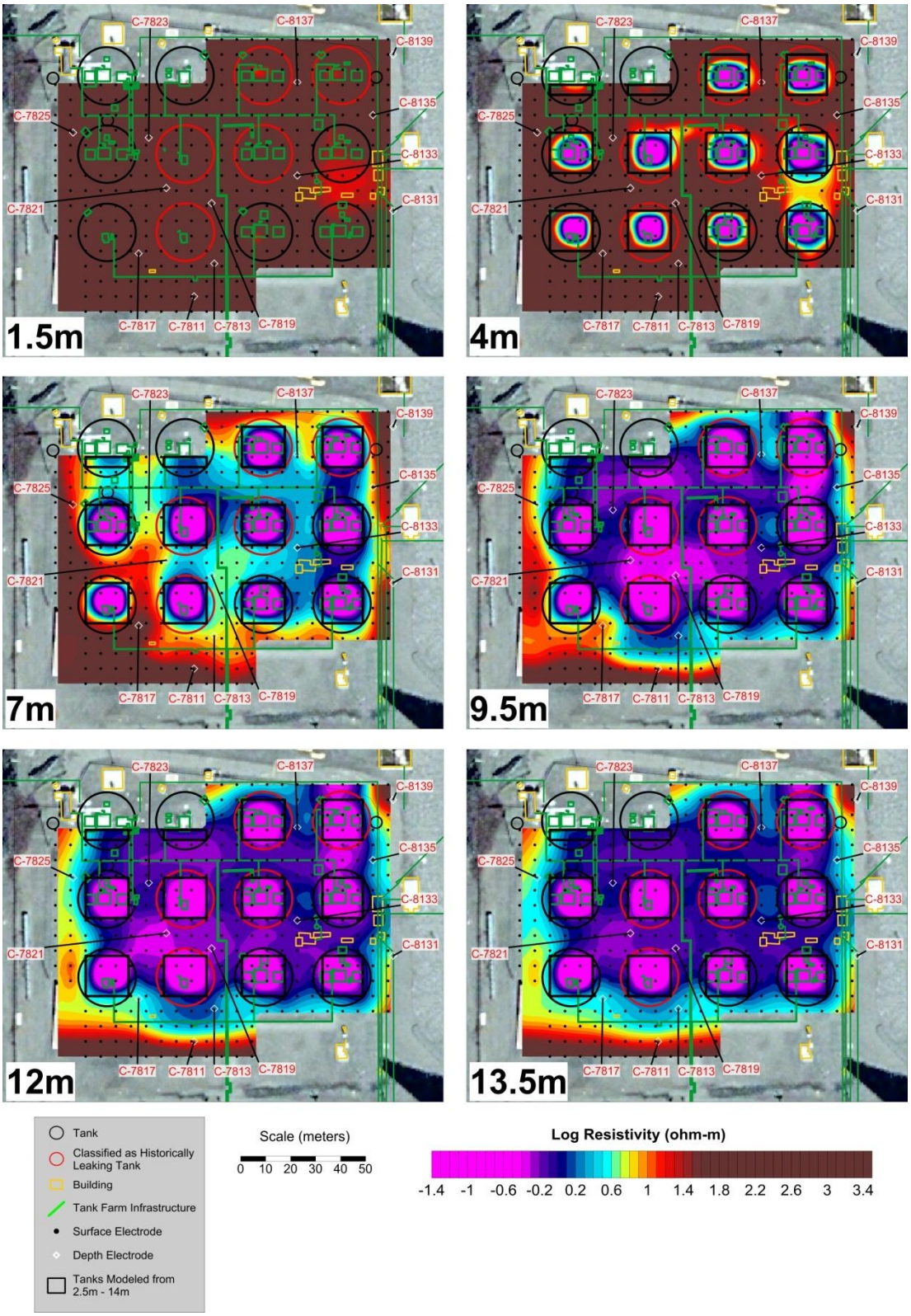

Figure 27. Plan View Depth Slices of Calculated Resistivity for Point Electrode Dataset. (2 sheets)

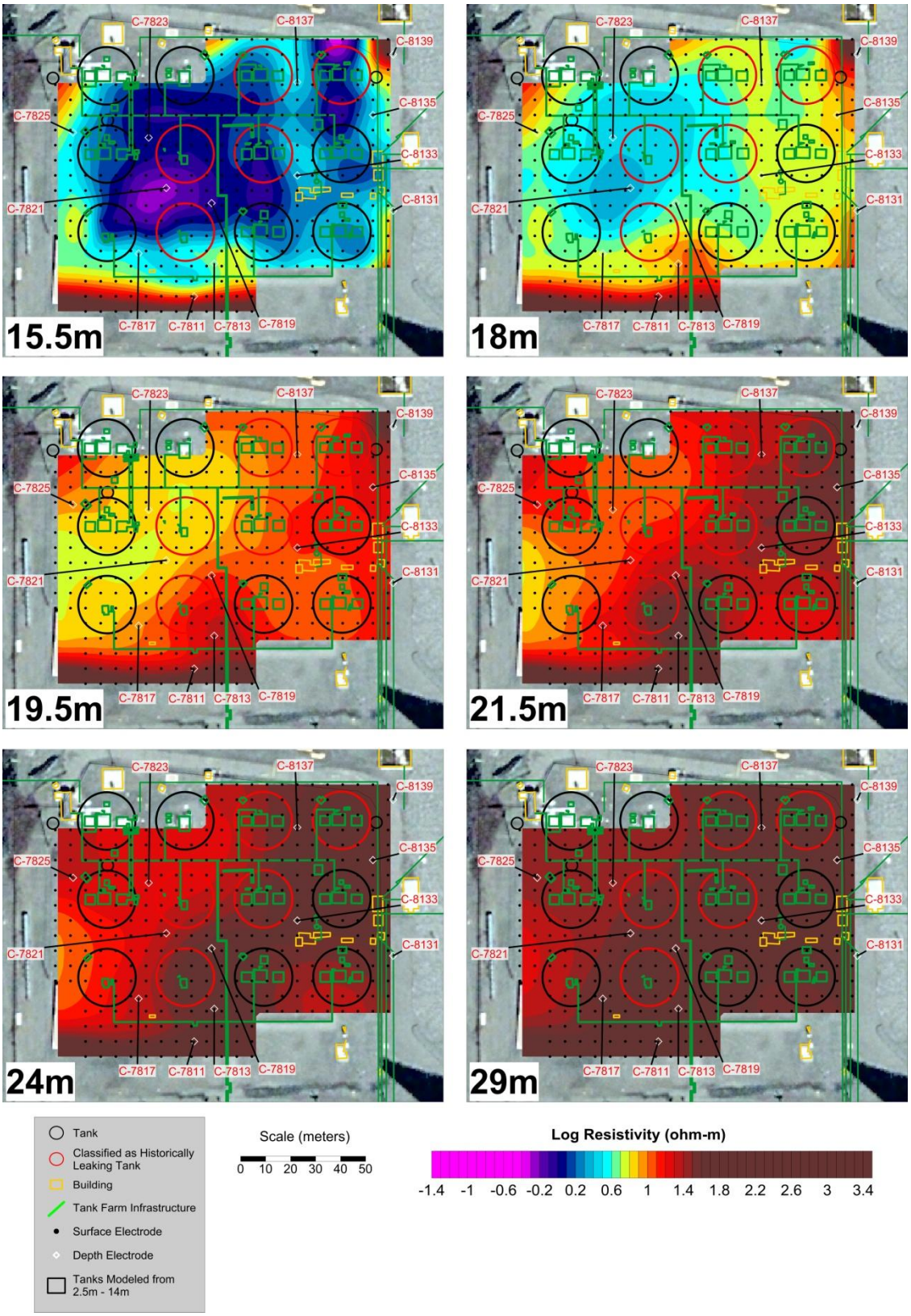

Figures 28 through 30 display three-dimensional renderings of the low resistivity features around the storage tanks in the BY tank farm. Figure 28 shows the isometric view of the tank farm, as viewed from the southwest (looking towards the northeast). Figure 29 shows the view from the northeast (looking southwest) and Figure 30 shows the view looking west. Two levels of resistivity values are presented, with the small opaque resistivity body in blue (resistivity value of 0.5 ohm-m) and the larger transparent higher resistivity body in green (resistivity value of 0.7 ohm-m). The main regions of interest in the figure are the low resistivity features between storage tanks BY-104, BY-105, BY-107, and BY-108; BY-102 and BY-103; and to the north of storage tank BY-103. These features appear to represent significant low resistivity anomalies within the BY tank farm. However, these features, as modeled by RES3DINVx64, are likely represented larger than actual extent due to the smoothing process smearing information from the *a priori* tanks with any waste plume feature. The smaller, isolated low resistivity area essentially associated with the representative outlines of adjacent storage tanks may be representative of the smoothing process mentioned previously. Other regions of the model did not have the same level of smearing between tanks, giving more confidence in the results of the low resistivity features

Figure 28. Three-Dimensional Rendered Bodies of the Low Resistivity Targets in the BY Tank Farm (Isometric View From The Southwest).

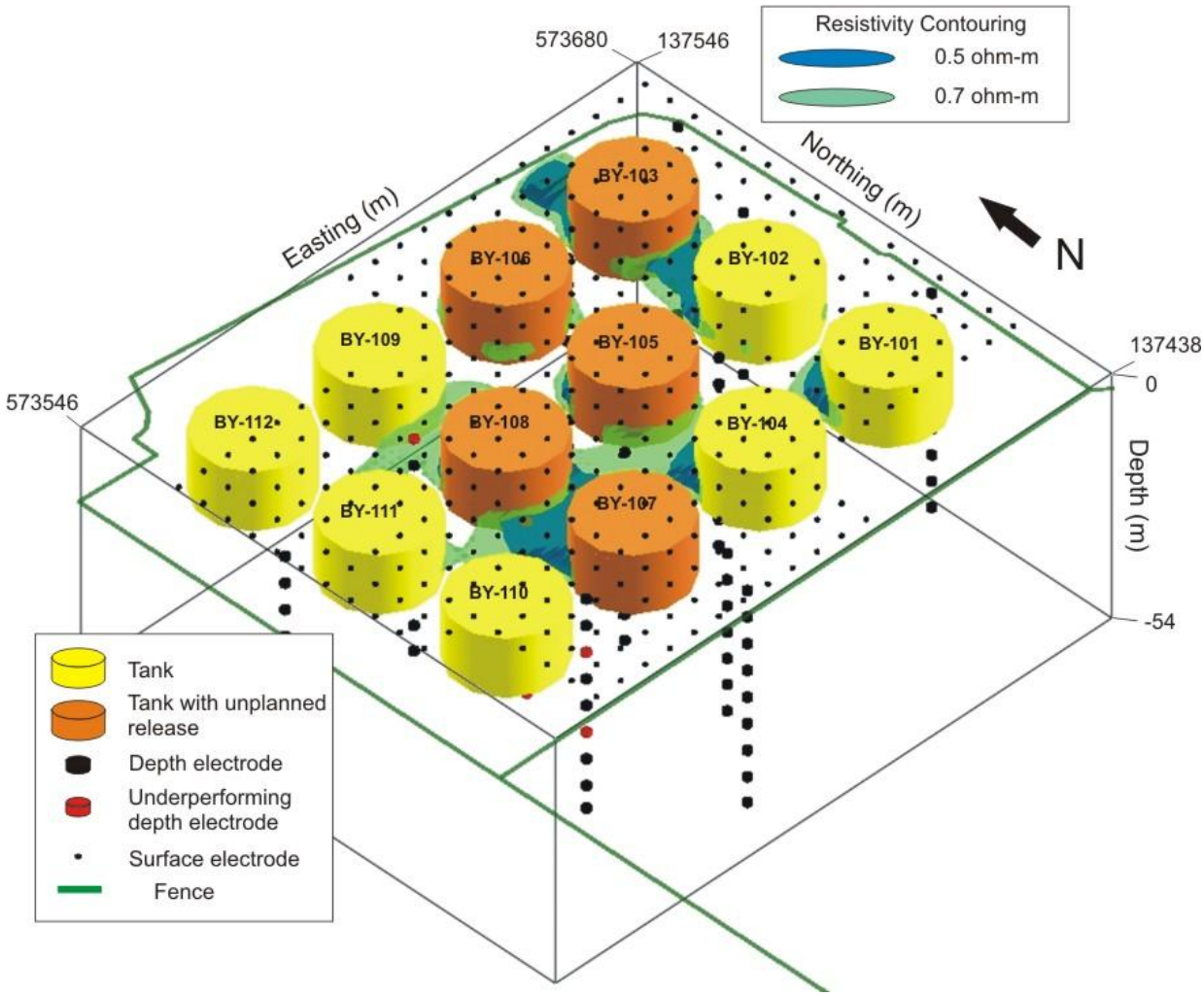

Figure 29. Three-Dimensional Rendered Bodies Of The Low Resistivity Targets in the BY Tank Farm (Isometric View From The Northeast).

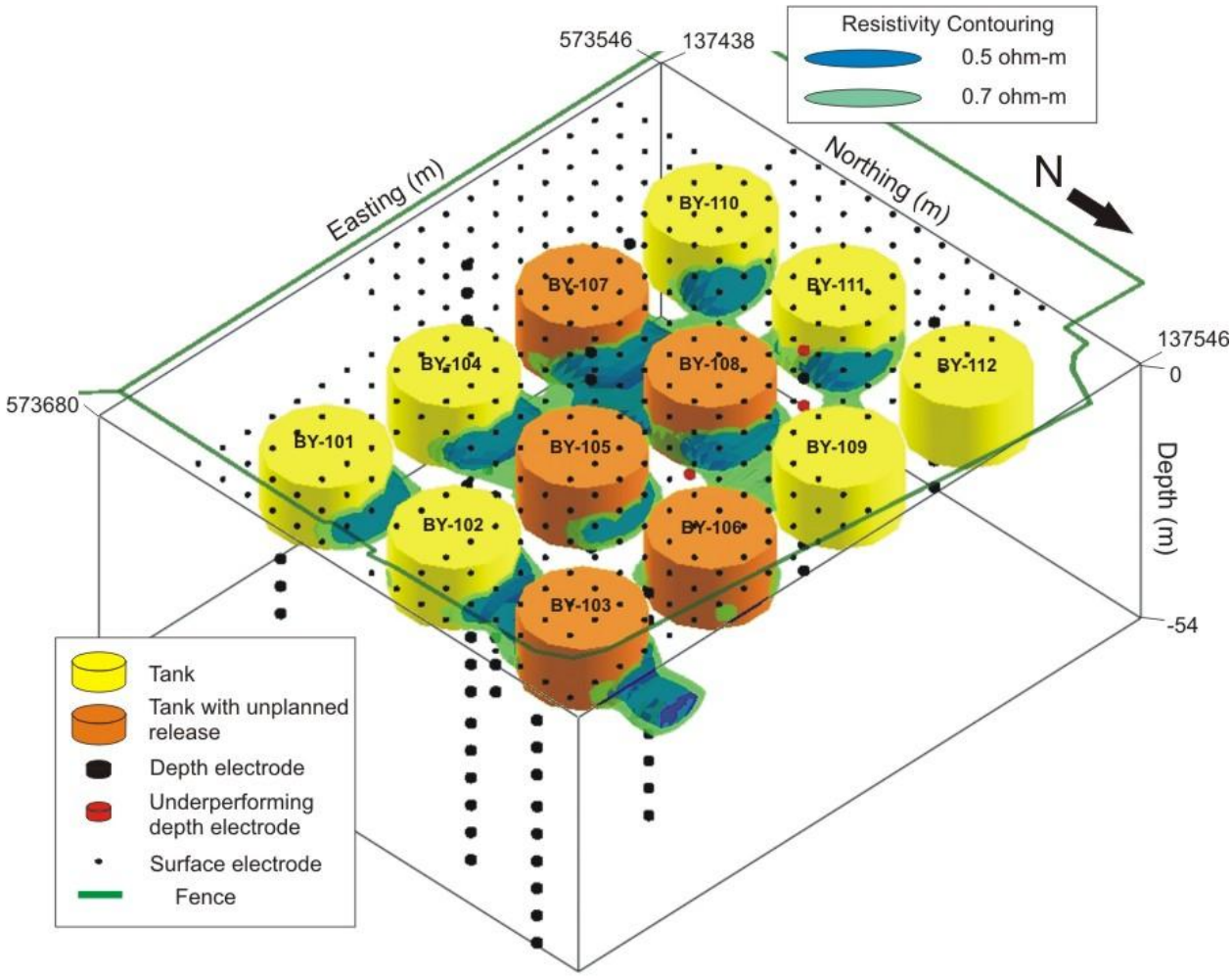

Figure 30. Three-Dimensional Rendered Bodies of the Low Resistivity Targets in the BY Tank Farm, View From the East.

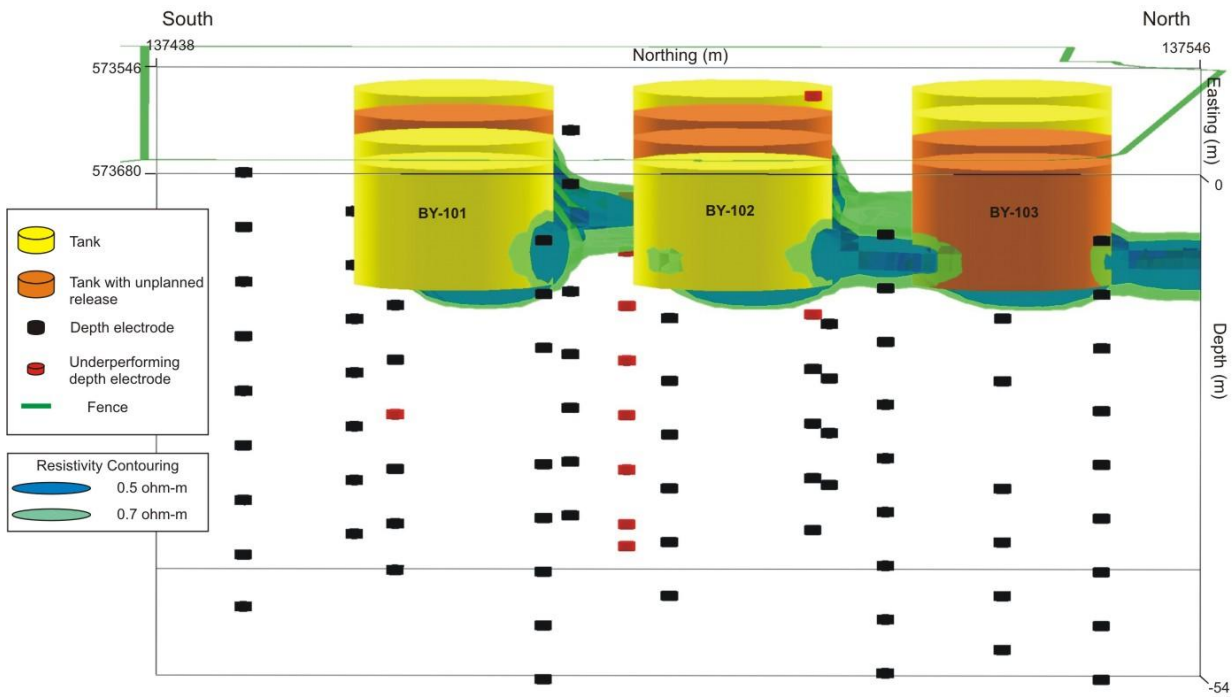

4.2 LONG ELECTRODE MODELING (WELL-TO-WELL INVERSION)

Well-to-well data from the Stage 1 and 2 (2010 and 2011) efforts for the BY tank farm surveys were combined for current numerical inverse modeling. A combined total of 57 wells were used as long electrodes; 31 of which were used in acquiring the 2010 survey and 33 were used in the 2011 survey. The results from the large scale 2006 survey are also presented for comparison. Further details of the 2006 and 2010 surveys can be found in RPP-RPT-49129, *Three-Dimensional Surface Geophysical Exploration of the BY Tank Farm*. The data were modeled independently and not part of a time-lapse modeling effort due to differences in survey geometry and locations between the three surveys. For example, the positions of the remote electrodes were different for the 2006-2010 and 2006-2011 surveys, and while the 2010 and 2011 survey shared the same remote electrode positions the areas being surveyed differed. Normally, data collected on the same set of electrodes at two different times could be used to assess temporal changes using a time lapse modeling strategy, where the results from the first snapshot would be used as an initial condition of the second snapshot to help further constrain the temporal changes between models.

Figure 31 displays the results of the WTW inversion modeling for the 2006, 2010, and combined 2010 and 2011 data. The combined 2010 and 2011 model (Figure 31C) has a different color scale to the remaining two subplots within the figure. This difference can be attributed to the differences in survey geometry and size, and resulting effect on the inverse model dimensions, between the three surveys. Figure 31A displays the 2006 data for the BY tank farm.
The location of the model grids for the 2010 and combined 2010 and 2011 models are shown for comparison with the other plots of Figures 31B and C. Figure 31A shows a low resistivity

feature mainly to the east of tanks BY-107 and BY-108, trending slightly to the northeast. This feature is consistent with the expected releases from the various tanks. Figure 31B displays the results for the 2010 dataset using the 31 available wells. There is a good agreement in the location of the low resistivity targets for the 2006 and 2010 model results. However, the intensity in resistivity of both targets and background (i.e., the amplitude of low and high resistivity representing the target and background, respectively) differs between these models. The low resistivity target on the east side of the 2010 model domain (i.e. east of tank BY-108) displays a much lower resistivity than the 2006 model. Furthermore, the background around the tanks displays a higher resistivity in the 2010 model compared to the 2006 model. The differences in these snapshots from 2006 to 2010 are likely the result of remote electrode location differences and not subsurface changes. Tank BY-111 stands out as a possible area of interest.

Figure 31C displays the results for the combined 2010 and 2011 data set using the 57 available wells. Again, there is good agreement in the location of the low resistivity targets between all the models presented. The combined 2010 and 2011 model displays a low resistivity feature to the east of tanks BY-107 and BY-108, which trends both slightly to the northeast and north. The intensity of the resistivity values for the low resistivity feature and the background differ as compared to the two previous models. We have previously discussed how the difference in remote electrode location may explain these intensity variations. In addition, refinements in the inverse model grid between the three surveys may also be affecting the intensity of the resistivity values observed, based on optimization due to differing survey geometries and spatial area. The latter affect is illustrated in an example in the Stage 1 report (RPP-RPT-49129) with the differences observed between Figures 31A and B in that report being due to the spatial extent of each model grid. Tank BY-111 again appears to stand out as a target of interest in the combined 2010 and 2011 model.

Remembering that geophysical tools are most reliable as target recognition tools, the three snapshots agree quite well. They also appear to agree well with the point electrode model, with the exception of the target in proximity to borehole C7821. The combined 2010 and 2011 model places the target further east, closer to borehole C7819. These variations are likely due to differences in the geometry of electrode coverage.

Figure 31. Well-to-Well Inversion Model Results for the BY Tank Farm (Resistivity Units: ohm-m).

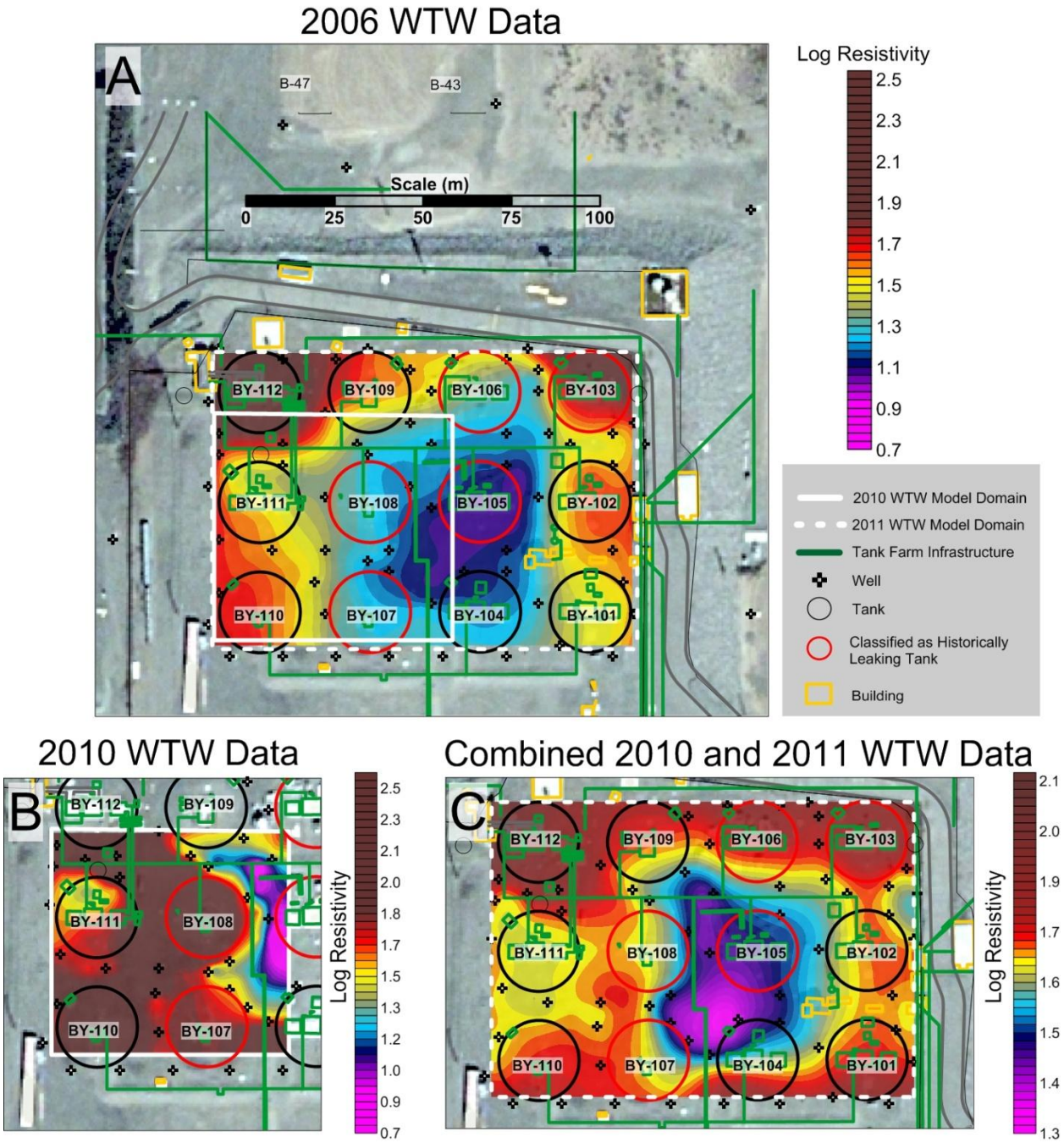

A) Complete BY tank farm inversion model of the 2006 data set.
B) Inversion model of the 2010 data set.
C) Inversion model of the combined 2010 and 2011 data set.

5.0 CONCLUSIONS

A two-part SGE survey was conducted within the BY tank farm on the Hanford Site in FY 2010 (Stage 1) and 2011 (Stage 2). The Stage 1 survey focused on the southwest corner of the tank farm. The Stage 2 survey focused on the eastern area of the tank farm, covering the area around tanks BY-101, BY-102, BY-103, BY-104, BY-105, and BY-106 and portions of tanks BY-107, BY-108, and BY-109. The survey included measurements on 185 surface electrodes placed within a grid, 57 depth electrodes in seven boreholes, and 33 wells acting as long electrodes. Data collection began on July 6, 2011, and was completed on July 10, 2011. After the data editing stage the data sets from the Stage 1 and Stage 2 BY tank farm surveys were concatenated to allow a combined inverse model to be produced.

Two inverse models were presented for the geophysical study that included: 1) point electrodes on the surface and within boreholes (i.e., surface and depth electrodes), and 2) long electrodes (i.e., wells). The combined point electrode inverse model included approximately 58,000 voltage measurements. The model run completed after four iterations with a root mean square error of 10.18 percent. The results of the model showed a continuous distribution of resistivity data within the BY tank farm, with modeled resistivities spanning from 0.04 to 2510 ohm-m, or approximately 4.5 orders of magnitude difference between the lowest and highest resistivities. The lowest resistivity values, not associated with the underground storage tanks, were observed; to the north and northeast of storage tank BY-108; in between and to the east of storage tanks BY-107 and BY-108; and in between storage tanks BY-102 and BY-103. Another smaller low resistivity feature was observed between the BY-107, BY-108, BY-110, and BY-111 storage tanks, where the C7821 borehole is located. Apart from the latter target, the low resistivity targets can be verified by similar modeling using the long electrode measurements. The validity of the smaller target between the tanks was qualitatively verified by gamma logging data from eight boreholes in proximity to this target installed within the study area. The adjacent wells of C7819 and C7821 (located between BY-107 and BY-108) showed the largest concentrations of Cs-137 compared to the other wells, with C7821 having the deepest and largest concentrations (RPP-RPT-48253). Although not directly comparable to the resistivity data, the gamma information provides an indication of past releases. The other boreholes that were installed in the study area showed very low gamma activity (RPP-RPT-48253, RPP-RPT-49650).

The second modeling effort used wells as long electrodes in a WTW inversion, and included approximately 1,500 voltage measurements. The results of the combined Stage 1 and Stage 2 modeling for the BY tank farm showed a low resistivity target to the east of storage tanks BY-107 and BY-108, trending towards the north east. The footprint of the low resistivity target coincided with expectations based on knowledge of past releases in the tank farm. These results correspond well to similar target locations observed in the 2006 SGE of the entire BY tank farm and the truncated 2010 survey of the western half of the tank farm, although different resistivity ranges are observed between the full and truncated data sets. Additional smaller low resistivity targets are observed around storage tank BY-111 and between and to the east of storage tanks BY-102 and BY-103.

In summary, the different inverse modeling conducted on the BY tank farm data agreed on the low resistivity targets in the vicinity of storage tanks BY-107 and BY-108 (to the north and northeast of the latter tank, and to the east of both tanks) and BY-102 and BY-103 (in-between

the two tanks). These targets were shallow, extending a minimal distance below the bottom of the storage tanks. The point electrode model, with significantly more electrodes and data, honed in on an additional target between the BY-107, BY-108, BY-110, and BY-111 storage tanks. The low resistivity targets appear to agree with what is known about past releases in the tank farm. The regions of interest were shallow, typically within the depth range of the storage tanks, but generally no deeper than 18 meters below ground surface. Overall, the shallow nature of these resistivity targets would likely support the value of an interim barrier should the targets prove to be waste related.

The greatest success of the SGE survey came from the extensive network of depth electrodes in the tank farm as well as the high density of surface electrodes. Preliminary models without the depth electrodes (not presented in this report) showed a more diffuse resistivity target at depths much greater than the bottom of the tanks. Additionally, improvements in modeling strategy came by incorporation of the storage tanks as *a priori* information and a separate inverse model grid from the forward model grid. For future work, it is recommended that whole tank farms be imaged at once as to not split conductive targets between two adjacent models.

6.0 REFERENCES

40 CFR 141, "National Primary Drinking Water Regulations," *Code of Federal Regulations*, as amended.

42 USC 2011, *Atomic Energy Act of 1954*, et seq., as amended.

CEES-0360, 2007, *Surface Geophysical Exploration System Design Description*, Revision 0, Columbia Energy and Environmental Services, Inc., Richland, Washington.

DOE/RL-88-30, 2010, *Hanford Site Waste Management Units Report*, Revision 19, U.S. Department of Energy, Richland Operations Office, Richland, Washington.

DOE/RL-2011-01, 2011, *Hanford Site Groundwater Monitoring Report for 2010*, Revision 0, U.S. Department of Energy, Richland Operations Office, Richland, Washington.

GJO-96-2-TAR, 1997, *Vadose Zone Characterization Project at the Hanford Tank Farms: BY Tank Farm Report*, GJO HAN 6, U.S. Department of Energy, Grand Junction Office, Grand Junction, Colorado.

GJO-98-40-TAR, 1998, *Hanford Tank Farms Vadose Zone: BX Tank Farm Report*, GJO HAN 19, U.S. Department of Energy, Grand Junction Office, Grand Junction, Colorado.

GJO-99-113-TAR, 2000, *Hanford Tank Farms Vadose Zone: B Tank Farm Report*, GJO HAN 28, U.S. Department of Energy, Grand Junction Office, Grand Junction, Colorado.

HNF-5231, 1999, *Historical Vadose Zone Contamination from B, BX, and BY Tank Farm Operations*, Revision 0, Fluor Hanford, Inc., Richland, Washington.

HNF-5507, 2000, *Subsurface Conditions Description of the B-BX-BY Waste Management Area*, Revision 0A, CH2M HILL Hanford Group, Inc., Richland, Washington.

HNF-EP-0182, 2010, *Waste Tank Summary Report for Month Ending July 31, 2011*, Revision 280, Washington River Protection Solutions, LLC, Richland, Washington.

PNNL-12128, 1999, *Borehole Data Package for Well 299-E-33-44 at Single-Shell tank Waste Management Area B-BX-BY*, Pacific Northwest National Laboratory, Richland, Washington.

PNNL-13022, 2000, *RCRA Assessment Plan for Single-Shell Tabnk Waste Management Area B-BX-BY at the Hanford Site*, Revision 1, Pacific Northwest National Laboratory, Richland, Washington.

PNNL-14119, 2002, *Characterization of Vadose Zone Sediment: Borehole 299-E33-46 Near B 110 in the B BX-BY Waste Management Area*, Pacific Northwest National Laboratory, Richland, Washington.

PNNL-14121, 2003, *Characterization of Vadose Zone Sediment: RCRA Borehole 299-E33-338 Located Near the B-BX-BY Waste Management Area*, Revision 0, Pacific Northwest National Laboratory, Richland, Washington.

PNNL-14128, 2002, *Characterization of Vadose Zone Sediment: Borehole C3103 Located in the 216-B-7A Crib and Selected Samples from Borehole C3104 Located in the 216-B-38 Trench Near the BX Tank Farm*, Pacific Northwest National Laboratory, Richland, Washington.

PNNL-16346, 2007, *Hanford Site Groundwater Monitoring for Fiscal Year 2006*, Pacific Northwest National Laboratory, Richland, Washington.

PNNL-19277, 2010, *Conceptual Models for Migration of Key Groundwater Contaminants Through the Vadose Zone and into the Unconfined Aquifer Below the B-Complex*, Pacific Northwest National Laboratory, Richland, Washington.

RCW 70.105, "Public Health and Safety," "Hazardous Waste Management Act," *Revised Code of Washington*, Washington State Department of Ecology, Olympia, Washington.

RCRA, *Resource Conservation and Recovery Act of 1976* (41 U.S.C., Sec. 6901, et seq.), as amended.

RHO-ST-23, 1979, *Geology of the Separation Areas, Hanford Site, South-Central Washington*, Revision 0, Rockwell Hanford Operations, Richland, Washington.

RPP-10098, 2002, *Field Investigation Report for Waste Management Area B-BX-BY*, Revision 0, CH2M HILL Hanford Group, Inc., Richland, Washington.

RPP-23405, 2008, *Tank Farm Vadose Zone Contamination Volume Estimates*, Revision 3, CH2M HILL Hanford Group, Inc., Richland, Washington.

RPP-23748, 2006, *Geology, Hydrogeology, Geochemistry, and Mineralogy Data Package for the Single-Shell Tank Waste Management Areas at the Hanford Site*, Revision 0, CH2M HILL Hanford Group, Inc., Richland, Washington.

RPP-34690, 2007, *Surface Geophysical Exploration of the B, BX, and BY Tank Farms at the Hanford Site*, Revision 0, CH2M HILL Hanford Group, Inc., Richland, Washington.

RPP-PLAN-47487, 2010, *Work Plan for Supplemental Surface Geophysical Exploration in the 241-BY Tank Farm*, Revision 0, Washington River Protection Solutions, LLC, Richland, Washington.

RPP-RPT-43704, 2011, *Hanford BY-Farm Leak Assessments Report*, Revision 0A, Washington River Protection Solutions, LLC, Richland, Washington.

RPP-RPT-47562, 2011, *Hanford BX-Farm Leak Assessments Report*, Revision 0, Washington River Protection Solutions, LLC, Richland, Washington.

RPP-RPT-48253, 2010, *Completion Report for 241-BY West Tank Farm Direct Push Characterization*, Revision 0, Washington Rover Protection Solutions, LLC, Richland, Washington.

RPP-RPT-49129, 2011, *Three-Dimensional Surface Geophysical Exploration of the BY Tank Farm*, Revision 0, Washington River Protection Solutions, LLC, Richland, Washington.

RPP-RPT-49650, 2011, *Completion Report for 241-BY East Tank Farm Direct Push Characterization*, Revision 0, Washington Rover Protection Solutions, LLC, Richland, Washington.

WAC 173-303, "Dangerous Waste Regulations," *Washington Administrative Code*, as amended.

Washington "Hazardous Waste Management Act," Chapter 70.105, *Revised Code of Washington*, as amended.

WHC-SD-WM-ER-575, 1996, *Liquid Radioactive Waste Discharges from B-Plant to Crib*, Revision 0, Westinghouse Hanford Company, Richland, Washington.

Womack, J.C. and D.J. Larkin, 1971, *Investigation and Evaluation of 102-BX Tank Leak*, ARH-2035, Atlantic Richfield Hanford Company, Richland, Washington.

APPENDIX A

QUALITY ASSURANCE

A1.0 QUALITY ASSURANCE

Collection and analysis of surface geophysical exploration (SGE) data are performed under a project-specific quality assurance plan using a graded approach that conforms to applicable requirements from Columbia Energy and Environmental Services, Inc. (Columbia Energy) quality assurance procedures (CEES-0333, *Quality Assurance Plan for Surface Geophysical Exploration Projects*). These procedures implement the requirements of ASME NQA-1, *Quality Assurance Requirements for Nuclear Facility Applications* and DOE O 414.1C, *Quality Assurance*. Work not covered in the quality assurance plan will conform to accepted industry standards for SGE and sound engineering principles.

This quality assurance plan implements the criteria of DOE O 414.1C and the following requirements from ASME NQA-1:

- Requirement 1 Organization
- Requirement 2 Quality Assurance Program
- Requirement 5 Instructions, Procedures, and Drawings
- Requirement 6 Document Control
- Requirement 16 Corrective Action
- Requirement 17 Quality Assurance Records.

Columbia Energy and hydroGEOPHYSICS, Inc. (HGI) collected data using designed systems or off-the-shelf commercially available hardware. Designed systems conform to applicable requirements in approved procedures that address design, design analysis, design verification, and engineering drawing.

A project specific software management plan, CEES-0338, *Software Management Plan for Surface Geophysical Exploration Projects*, was prepared to implement a graded approach to software management in accordance with the following requirements documents:

- ASME NQA-1, Subpart 2.7 , "Quality Assurance Requirements for Computer Software for Nuclear Facility Applications"
- CEES-0333
- CE-ES-3.5, *Software Engineering*
- Contract 28090, *High Resolution Resistivity Characterization of Single Shell Tank Farm Waste Management Areas*
- DOE O 414.1C.

A1.1 CALIBRATION AND MAINTENANCE OF EQUIPMENT AND INSTRUMENTS

Calibration and maintenance of equipment used for data collection is addressed in CEES-0360, *Surface Geophysical Exploration System Design Description*. Where periodic calibration and/or maintenance of instruments used to collect quality affecting data is recommended those instruments were current on calibration at the time the instrument was used for data collection and the calibration certificate is maintained in the project files.

Field notes are used to document the specific instruments used. Electronic logs are utilized to provide traceable documentation for each data set collected. Information recorded in the electronic field log includes date, instrument identification, operator, and applicable settings for each data set collected. All instruments have current calibration certificates and documentation is maintained in the project files. Instrument calibration frequency and calibration tests performed in the field are documented in the system design description (CEES-0360).

A1.2 DATA COLLECTION

The setup, operation, and maintenance of the SGE equipment used in collecting and analyzing resistivity data is described in CEES-0360. This document identifies the requirements for the hardware/software used for data collection and analysis and provides a rationale for the hardware/software selected for use.

Calibration requirements are described for hardware used to collect geophysical data. As an example, the manufacturer (Advanced Geosciences, Inc.) of the resistivity data acquisition instrument (SuperSting R8) recommends a yearly calibration of internal calibration resistors. The calibration is performed at the manufacturer's facility and a certificate of calibration is provided. A copy of the calibration documentation, serial numbers, and expiration dates are maintained in project files.

In addition, daily inspection of the receiver calibration is performed onsite using the manufacturer-supplied calibration resistor test box. The supplied test box is connected to the SuperSting R8 before commencing the daily survey. A specific calibration test firmware is provided within the SuperSting and provides the operator with a pass/fail indication for each of the eight receiver channels. If any of the channels fail, a recalibration or repair is required.

In addition to calibration checks, data accuracy will be evaluated by performing reciprocal data collection. Reciprocal collection is used as a tool to assure the data collected is accurate and repeatable. The transfer, storage, and management of data collected in the field are described in the system design description (CEES-0360).

A1.3 ELECTRICAL INTERFERENCE MONITORING

Electrical interference can affect resistivity measurements in two ways:

1. Grounded conductive infrastructure (pipes, tanks, fences) may provide a preferential current pathway that distorts predictable current flow paths within the earth
2. Electrical noise (voltage/current) sources from electrical systems (cathodic protection, pumps, motors, earth grounding arrays, etc.) may inject a competing signal.

Electrical noise interference can be minimized by identifying noise sources and then turning off electrical sources where possible for the duration of the resistivity surveying.

A passive monitoring detection system, developed for field use by HGI, was used to detect and map possible electrical noise interference prior to the start of resistivity measurements at the BY Farm. The electrical interference survey consists of temporarily wiring several electrodes or steel-cased monitoring wells, distributed over a tank farm (inside and outside of the farm fence), to a distribution panel. A digital recording oscilloscope is connected at the electrode measuring

points (two at a time) and the background electrical field is digitally recorded via a laptop computer. The oscilloscope operates via the universal serial bus (USB) port on the laptop computer and does not transmit signal into the ground. Data is recorded before and after electrical systems are turned off to verify the reduction in electrical interference. The data is then assessed at an offsite location and recommendations to minimize electrical interference are made. The electrical interference survey is designed to identify the magnitude, frequency, and cycle time of possible interference. A suitable electrode distribution (as shown in Figure A1) may allow an assessment of the location (directionality) of possible localized noise sources such as pumps and motors. The actual location and quantity of electrodes are determined as part of the project survey design. For this survey, the wells selected were used as sampling points for the electrical interference testing.

Figure A1. Example of Electrical Interference Monitoring.

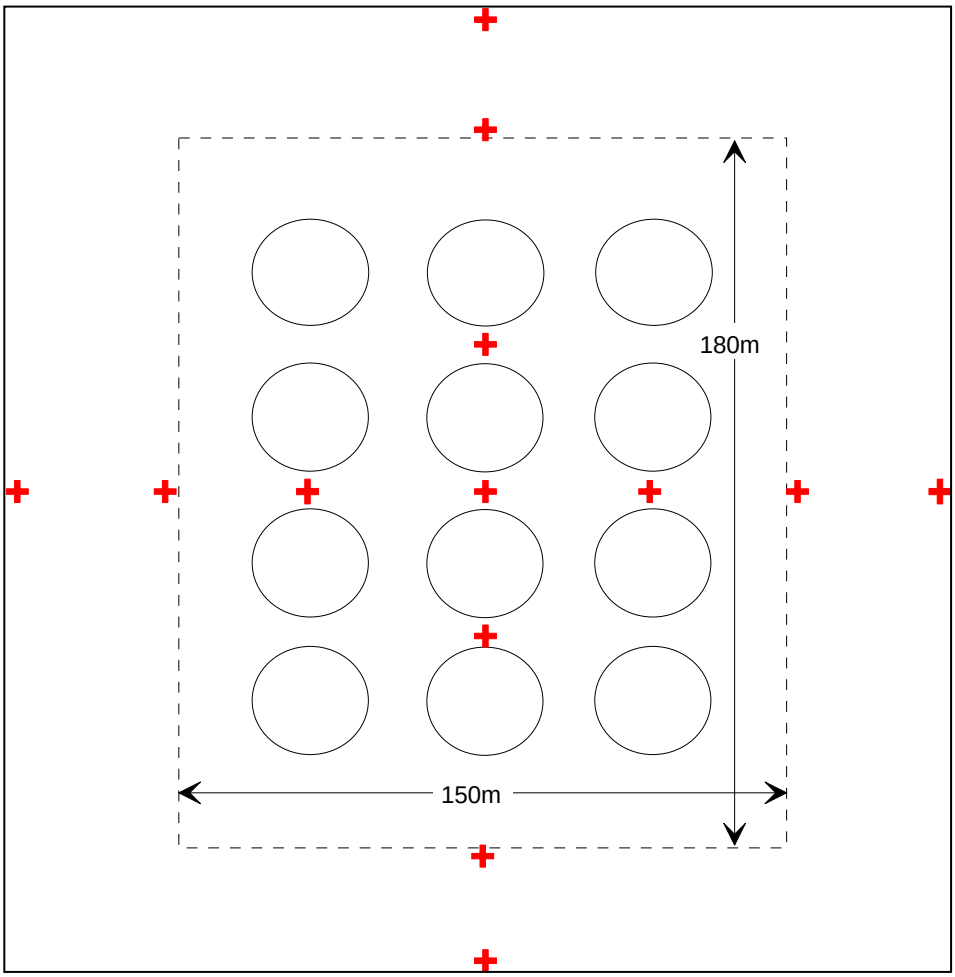

Electrode arrangement for a generalized tank farm, electrodes are shown as red +.
m = meter(s)

A1.4 EQUIPMENT TESTING

A1.4.1 SuperSting

Daily inspection of the receiver calibration was performed onsite using the manufacturer-supplied calibration resistor test box. The supplied test box is connected to the SuperSting R8 before commencing the daily survey. A specific calibration test firmware is provided within the SuperSting and provides the operator with a pass/fail indication for each of the eight receiver channels. If any of the channels fail, a recalibration or repair is required.

A1.4.2 SwitchBoxes

A relay test was performed on a daily basis. For the relay test the operator connects a switchbox or switchboxes to the SuperSting R8 and performs the relay test that is incorporated into the SuperSting R8 firmware. This test sends a signal to each switchbox electrode to assess the functionality of the relays on each switchbox electrode channel. The SuperSting reports the success or failure of each relay (switchbox electrode channel) as a pass or fail. The relay test only inspects the operability of each relay.

As part of field equipment testing on all resistivity surface exploration geophysics deployments at the Hanford site, it is necessary to provide equipment evaluation specifically with regard to the functionality of the Advanced Geosciences Inc. Super Sting R8 Resistivity meter ("Sting") electrode multiplexors (switchboxes). The switchboxes come in three standard capacities, all in increments of 28 switches, e.g., 28, 56, and 84 switches. Any combination of these switchboxes may be used on a Hanford Site deployment of SGE.

A Switchbox test was performed on all switchboxes used on a weekly, and as needed basis. For the Switchbox test, the operator connects a switchbox to the SuperSting R8 and to a switchbox diagnostic tester (SBDT) (HGI, Tucson, Arizona). The SBDT simulates an actual resistivity survey using a network of resistors of known resistance. The measured data is compared to the known resistances for the SBDT and success or failure is reported for each switchbox electrode channel as a pass or fail. The switchbox test evaluates the operability of each relay and in addition evaluates any possible shorting, lack of isolation or failures of internal electronics that control the relays. If a relay fails in the opened or closed state during typical testing, relatively high measurement errors, sometimes exceeding 100 percent relative to the standard baseline results recorded for the SBDT by the High Resolution Resistivity™ Leak Detection and Monitoring™ Data Acquisition System (DAS), can be expected.

The selection of an appropriate error threshold for passing or failing needs to be consistent with the type of survey being performed and environmental conditions that could be encountered during testing. A 5 percent error threshold is typical for industry use in bench-scale testing of equipment and this level could be very appropriate for some applications. Under a bench testing setting, where environmental conditions are generally controlled, our own experience shows that recorded Sting measurements for operational relays within a switchbox can be much less than 5 percent of standard baseline values for the SBDT. The 5 percent level is also supported by the

---

™ High Resolution Resistivity HRR is a trademark of hydroGEOPHYSICS, Inc.
™ Leak Detection and Monitoring LDM is a trademark of hydroGEOPHYSICS, Inc.

manufacturer, Advanced Geosciences, Inc. in bench-scale evaluation of switchbox relays in their facilities.

However, under field conditions, where changes in ambient temperature, wind conditions, and electrical interference can potentially affect measurement error during data acquisition, it is possible that this 5 percent pass/fail threshold may not be adequate and could potentially result in apparent relay failures in a fully operational switchbox. Geophysical resistivity data taken in less than ideal environment conditions can often exceed a 5 percent error in repeatability, but can still be used to produce usable results. Therefore, to account the additional effects of field conditions, our professional judgment is that a 10 percent threshold would be a more appropriate level to use and this level was initially used in switchbox testing for this project. As we gain additional experience with SBDT field testing, we will reevaluate this value as an effective pass/fail threshold.

A1.5 DATA PROCESSING

The process used to filter the raw data is described in the system design description (CEES-0360). Data are downloaded from the resistivity instrument and parsed into a usable format. Data filtering techniques are then used to remove data spikes or anomalous data caused by data acquisition card instabilities, or extraneous current sources.

Data filtering is performed by copying the parsed raw data into an Excel data filtering template that contains a series of graphs that show the various data parameters. The process of filtering eliminates data points, but no data modification (rounding, averaging, smoothing, or splining) is permitted. The rationale is to seek out and remove spurious points that do not conform to the data population or points that violate potential theory.

The final step is to inverse model the measured data to obtain the spatio-temporal distribution of electrical resistivity. Inverse modeling is accomplished using either EarthImager3DCL (EI3DCL) or RES3DINVx64 (RES3D). Verification and testing of the inversion software was performed and documented in RPP-34974, *Verification and Testing of the EarthImager Series of Electrical Resistivity Inversion Codes – A Benchmark Comparison*. Verification and testing was performed on the existing two-dimensional (2D) and three-dimensional (3D) versions of the software as well as the upgraded 64-bit, multi-threaded versions developed for tank farm projects.

The objective of the verification and testing study was to demonstrate that the resistivity inversion codes were comparable to known conditions from a pilot-scale field resistivity experiment. The pilot-scale field experiment was used to test the WTW inversion methodology by establishing a known conductive target in the subsurface and making measurements with a set of 27 simulated wells. To date, there is no industry standard for the WTW resistivity imaging technique, which necessitated the field experiment. The field experiment was designed to test the inversion code's ability to replicate a target of known geometry. The subsurface geophysical target was an amended, electrically conductive soil, buried approximately 1.6 feet (0.5 meters) below ground surface. The 27 wells were distributed around the target in a pattern similar to tank B-105 in the B tank farm.

Data processing is performed using a number of software packages. The requirements and responsibilities for the identification, evaluation, development, testing, and maintenance of

quality-affecting software acquired, developed, or modified in support of the SGE efforts are defined in the CEES-0338.

A2.0 REFERENCES

ASME NQA-1, 2004, *Quality Assurance Requirements for Nuclear Facility Applications*, American Society of Mechanical Engineers, New York, New York.

CEES-0333, 2006, *Quality Assurance Plan for Surface Geophysical Exploration Projects*, as revised, Columbia Energy and Environmental Services Inc., Richland, Washington.

CEES-0338, 2006, *Software Management Plan for Surface Geophysical Exploration Projects*, Revision 0, Columbia Energy and Environmental Services Inc., Richland, Washington.

CEES-0360, 2007, *Surface Geophysical Exploration System Design Description*, Revision 0, Columbia Energy and Environmental Services, Inc., Richland, Washington.

CE-ES-3.5, *Software Engineering*, as revised, Columbia Energy and Environmental Services, Inc., Richland, Washington.

Contract 28090, Requisition 123974, *High Resolution Resistivity Characterization of Single Shell Tank Farm Waste Management Areas*, Revision 3, CH2M HILL Hanford Group, Inc.

DOE O 414.1C, *Quality Assurance*, U.S. Department of Energy, Washington, D.C.

RPP-34974, *Verification and Testing of the EarthImager Series of Electrical Resistivity Inversion Codes – A Benchmark Comparison*, Revision 0, CH2M HILL Hanford Group, Inc., Richland, Washington.